Cretaceous dyke swarms and brittle deformation structures in the upper continental crust flanking the Atlantic and Indian margins of Southern Africa, and their relationship to Gondwana break-up

By

Thomas Tshifhiwa Muedi

Thesis submitted to Nelson Mandela Metropolitan University in partial fulfilment of the requirements for the degree of Master in Geology.

August 2013

Supervisor/ Promoter: Prof. Maarten de Wit (AEON-African Earth Observatory Network, Nelson Mandela Metropolitan University, South Africa)

Co-supervisors: Prof. R.O Greiling (Karlsruhe Institute of Technology, Germany)

Dr. R.B Trumbull (GFZ, German Research Centre for Geosciences, Germany)

Cretaceous dyke swarms and brittle deformation structures in the upper continental crust flanking the Atlantic and Indian margins of Southern Africa, and their relationship to Gondwana break-up

By

Thomas Muedi

Thesis submitted to Nelson Mandela Metropolitan University in partial fulfilment of the requirements for the degree of Master in Geology.

August 2013

Supervisor/ Promoter: Prof. Maarten de Wit (AEON-African Earth Observatory Network, Nelson Mandela Metropolitan University, South Africa)

Co-supervisors: Prof. R.O Greiling (Karlsruhe Institute of Technology, Germany)

Dr. R.B Trumbull (GFZ, German Research Centre for Geosciences, Germany)

Certificate of Originality

I, Thomas Muedi (s211266973), hereby declare that this submission is my own work and to the best of my knowledge and belief, it contains no material previously published or written by another person nor material which to a substantial extent has been accepted for the award of any other degree or diploma of a university or higher learning, except where due to acknowledgement was made in the text.

(Signed)……

Thomas Muedi

List of Acronyms

HOD	Henties Bay-Outjo Dyke Swarms
PG	Ponta Grossa Dyke Swarms
KLIP	Karoo Large Igneous Province
GVS	Golden Valley Sill
CFB	Cape Fold Belt
TMG	Table Mountain Group
MSS	Multispectral Scanner Imagery
LIP	Large Igneous Province
DRS	Dabbahu Ridge Segment
D_f	Fractal dimension

List of definitions used in this thesis

En-echelon array	Refers to an array of mutually parallel fracture segments that are all inclined relative to the overall orientation of the array.
Brittle deformation	The failure of stressed material that leads to the formation of fractures when the elastic limit is exceeded.
Dykes	Discordant sheet like bodies of magma that cut at a high angle through and across strata or igneous bodies.
Faults	A fracture or fracture zone in a rock along which movement has occurred.
Pure shear deformation	Deformation that takes place with no rotation of the principal strain axis.
Simple shear deformation	Deformation that involves rotation of the principal strain axis.
Columnar joints	Joints that form as results of thermal-contraction during cooling in the basaltic flow and other extrusive rocks such as sills, dykes, and other shallow level intrusions.
Gorge	A narrow valley or canyon between hills or mountains, typically with steep rocky walls.
Fractals	Infinite complex patterns that are self-similar across different scales where small object represent the whole object.

Epeirogeny	Vertical elevation of the Earth surface in response to natural causes such as changes of lithosphere movement or mantle convection that may bend the crust into an arc or dome.
Failed Arm	Branch of the triple junction not developed into an ocean basin.
Denudation	The sum of the process that results in the wearing away or the progressive lowering of the Earth's surface by various natural agencies which includes weathering, erosion, mass wasting and transportation.
Exhumation	Gradual exposure of subsurface rocks by stripping off surface layers.
Uplift	A process that raises topography.
Lineament	A straight line or gently curving feature on the Earth's surface that are commonly expressed topographically as ridges or elongated depressions.
Mantle plume	A rising mass of hot mantle material that can create an area of volcanic activities in the center of lithospheric plate.

LIST OF FIGURES

LIST OF TABLES

TABLE OF CONTENTS

ACKNOWLEDGEMENT

I would like to thank all individuals and organization (Inkaba yeAfrica) that funded this project, and all people who have supported and encouraged me during my MSc studies at NMMU. I will also like to thank the German-South African Government for allowing me to pursue my research technical work and data collection at the Karlsruhe Institute of Technology (KIT), Germany.

I would like to express my gratitude and thanks to my principal supervisor Prof. Maarten de Wit, for his guidance, full support, encouragement and caring during my studies. I am also gratitude for my second supervisor Prof. Reinhard.O Greiling (KIT, Germany) for his scientific criticism and helpful suggestions. I am also thankful for the opportunities he gave me to attend all helpful conferences, seminars, fieldwork and workshops. I would like to express my sincere thankful to my third supervisor Dr. Robert Trumbull for all the arrangements in Germany, recruiting me to come for my MSc, and his fine comments during the course of this project. My sincere gratitude to Ms. Miriam Wiegand (KIT) for the technical and moral support during my stay in Karlsruhe.

I would like to thanks Mr. R.D. Almanza (NMMU) and Mr. J. Mullins (Birmingham University) for accompanying and helping me in the field. My sincere gratitude to Ms. Taryn Scharf and Mr. Scott MacLennan (UCT) for their invaluable assistance: without them this research would not be the same. I would also like to express thanks to my classmates in Geology at NMMU, for the moral support: Dr. Bastien Linol, Mr. Jean-Luc Mendon, Ms. Claire Geel, Ms. Megan Dejager, Ms. Vhuhwavhohau Nengovhela, Ms. Thakhane Ntholi, Dr. Gaathier Mahed, I would also like to express my gratitude to all 2009 classmates at UNIVEN, especially my honours classmates Ms. Kone Maraga, Mrs. Mpho Mavhudzida-Mudimeli, Mr. Nkhetheni Tshivhandekano, and Mr. Nthambeleni Nendauni. I would also like to express thanks to my old friend Mr. Fhatuwani Mudau for their support during this study.

I would also extend my thanks:

- To my family especially Mrs Muedi-Mudau N.L, my brother Mr. Hulisani Muedi, sisters Ms. Tendani and Ntungufhadzeni Muedi, Uncle Abel Muedi and my Guardian Mrs. Ndou F.L for their words of encouragement and their support during the MSc progress.
- I would also like to thank Dr. Francis Amponsah-Dacosta (HOD, UNIVEN) for giving me courage and helping me, giving me inspiring words to pursue my research.
- To Dr. Selepe Catherine (UNIVEN) who has been a pillar and so inspiring to me in order to pursue this research project.
- To Dr. Jens Grimmer and Pr. Dr Kontny for allowing me to join their fieldwork group with honours students to see diversity of geology around Karlsruhe, Germany.

ABSTRACT

Permanent brittle deformation of rocks of the upper crust is often manifested in the growth of fractures, or sliding along fractures, which may subsequently be intruded by magma and other fluids. The brittle deformation structures described here include faults, joints and dykes. Brittle deformation structures along passive continental margins result from continental fragmentation and related uplift, as is seen around the southern African margins in response to Gondwana break-up. In many cases the fragmentation is accompanied by significant magmatic events, for example the Cretaceous mafic dyke swarms that form major components of the South Atlantic Large Igneous Province (LIP) and originated during the break-up of West Gondwana (Africa and South America).

The magmatic events accompanying the break-up of Gondwana resulted in crustal extension and the formation of joint systems and dyke swarms that exhibit distinct geometric features that appear to display fractal patterns. This work analyses the relationship between the Henties Bay-Outjo Dyke Swarm (HOD) on the west coast of Namibia, and the Ponta Grossa Dyke Swarm (PG) on the coast of Brazil, both of which formed ca. ~130 Ma, to test for their co-linearity and fractal geometry before and during West Gondwana break-up. This was achieved by reconstructing Gondwana's plates that contained the PG and HOD swarms, using ArcGIS and Gplates software. The dyke analyses was complemented with a comparative study of joints of the Table Mountain Group quartzites (TMG, ca. 400 Ma) in the Western Cape Province and Golden Valley Sill (GVS, ca. 180 Ma) in the Eastern Cape Province, to compare their fractal patterns and possible relationship. Mapping of joints was carried out in the field with the use of a compass and GPS.

The HOD trend is positioned largely NNE > NE, but a NW dyke trend is also common. The dominant joints in the TMG trend NNW > WSW and the GVS joints trend WNW > NNE and others. The GVS and HOD orientations appear strongly correlated, while TMG shows no simple orientation correlation with GVS and HOD. The lack of correlation is attributed to the TMG's formation in different host-rocks with variable anisotropy and/or the presence of different mechanical processes acting at a different time in geological history.

All mapped dykes and joints were analysed to test for fractal geometry. The fractal dimension results of about 18605 HOD dykes from microscopic to mega scale (0.1 mm – 100 km) shows fractal patterns that range between D_f = 1.1 to 1.9; and the fractal dimension of about 1716 joints in the TMG and about 1026 joints in the GVS at all scales range between ca. D_f = 1.6 to 1.9. The similarity of the fractal patterns indicates that joints and dykes may have formed in response to similar tectonic stress events; and similar orientations may indicate that joints pre-dated the dyke intrusions. However, the data also indicate that dykes are not always related to pre-existing joints.

Chapter 1. Introduction

Mafic dyke swarms are major components of the South Atlantic Large Igneous Province that originated when South America and Africa broke away from one another during the Cretaceous rifting and break-up of West Gondwana. This study presents data on the geometry and spatial distribution of dykes within the major Henties Bay-Outjo dyke swarm (HOD), flanking the coastal margin of NW Namibia.

Numerous studies have been conducted on the Henties Bay-Outjo dyke swarm including paleo-magnetic, aeromagnetic, geophysical, geochronological, and geochemical studies (Frindt *et al*., 2004; Trumbull *et al*., 2004; Thompson *et al*., 2007). Despite these numerous studies, little detailed mapping of the HOD Cretaceous dykes has been carried out. This research addresses the lack of map-data by providing detailed remote sensing maps of the HOD dykes. Reconstructing the dykes along the African-South American plates will aid our understanding of the emplacement history of these dykes during Gondwana break-up, and provide insight as to why dykes follow systematic patterns along with joints systems during fracturing and rifting of the upper crust.

Joints are fractures near the Earth's surface that form during brittle deformation of crustal rocks due to uplift and release of stored elastic stress (Ramsay *et al*., 1983; Engelder, 1987; Gehle and Kutter, 2003). Joints or fractures form when the cohesion of the materials is lost leading to brittle failure of a rock without relative movement across the fracture (Pollard and Aydin, 1988; Twiss and Moore, 1992; Mamtani *et al*., 2004). There are also two types of special joints: columnar and sheeting joints. Columnar joints form in igneous rocks when magma cools; sheet joints form in all rocks when uplift and exhumation/denudation removes overlying rocks thus reducing lithostatic stresses (Engelder and Geiser, 1980; Ladeira and Price, 1981; Roberts, 1995; Bai *et al*., 2002). Joints that form in sedimentary rocks typically follow systematic uplift (Hancock and Engelder, 1989 Bahat, 1991). Brittle joint systems around the margins of southern Africa are not well studied and this study investigates joints in two different rock types: Karoo dolerites (sills) and Table Mountain Group (TMG) quartzites flanking the margins of southern Africa, to investigate their possible origin related to Gondwana break-up and isostatic uplift along these rift margins.

This dissertation is structured into 6 chapters. **Chapter 1** highlights the aim of the research related to the brittle deformation structures, fractal geometry and provides a brief introduction to the HOD dykes, and their emplacement related to Gondwana break-up. **Chapter 2** explores the theoretical background of the deformation and emplacement history of the HOD dyke swarm, and the geometry of the dykes and joints. **Chapter 3** collates the digital data sources, methods and analysis. Gathered data from digital, aerial and satellite image-based mapping was used to analyse the geological structures formed during Gondwana break-up. **Chapter 4** introduces laboratory data and analysis of the HOD, field data of the joint systems in the mafic GVS, and field data of the joints systems in the TMG quartzites. **Chapter 5** gives a brief description of West Gondwana reconstructions and how brittle structures may

relate to break-up and **Chapter 6** provides conclusion remarks and recommendations for future work.

1.1. Aim of the research

- Document and analyse brittle deformation structures such as joints, faults and dykes along the continental margins of southernmost Africa, to test if they have fractal pattern and if they can be related to the processes of Gondwana break-up.

- The HOD, GVS, TMG geometrical patterns flanking the coastal region were analysed to test for systematic and consistent relationships (Figure 1.1).

- Comparing brittle structures such as joints formed in two different rock types (1) Table Mountain Group (TMG) quartzites from the Tsitsikamma area, Western Cape Province and (2) dolerite of the Golden Valley Sill (GVS), Karoo basin, Eastern Cape Province, in order to test for their variability related to Gondwana break-up and continental marginal uplift (Figure 1.1).

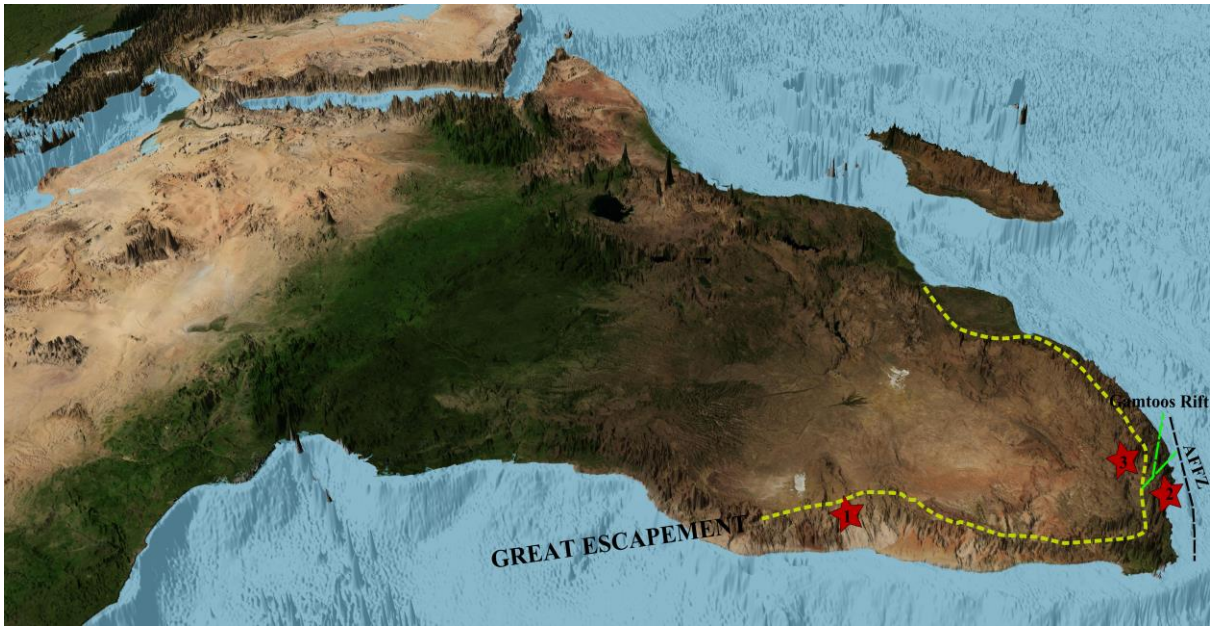

Figure 1.1: The topographic map showing the southern African great escapement (Yellow broken line), Agulhas- Falkland Fracture Zone (AFFZ) (Black broken line), Gamtoos Rift (Lime broken line) and the locations of the areas studied (red numbered stars). (1) HOD=Henties Bay-Outjo dyke swarms, Namibia, (2) TMG=Table Mountain Group quartzite in the Tsitsikamma area, Western Cape Province and (3) GVS=Golden Valley Sill, Tarkastad in the Karoo basin, Eastern Cape Province both (1) and (2) in South Africa (Modified 3D diagram from F. Eckardt, unpublished; see also http://aeon.org.za/activities/kalahari_drilling_project).

1.2. Geodynamic history of Western Gondwana

The high topography of southern Africa has been linked to dynamic uplift related to hot lower mantle upwelling, known as the African super plume which is seismically detected to be deep below southern Africa and may have contributed to Great Escapement uplift and subsidence along the continental margins (Lithgow-Bertelloni and Silver, 1998; Conrad and Gurnis, 2003; Behn *et al*., 2004; de Wit, 2007). The southern Africa uplift from ~130 Ma onwards, is suggested to have been associated also with relative motion of the African plate (Flament *et al*., 2013).

1.2.1. Horizontal motions and opening of South Atlantic Ocean

The Pan-African Orogeny resulted from the closure of the Adamastor and Mozambique Oceans during late Precambrian-early Palaeozoic times and caused the formation of Gondwana (Reeves, 1999; Kröner and Stern, 2005; Watkeys, 2006; Gray *et al*, 2008; de Wit *et al*., 2008; Moulin *et al*., 2010).

Subsequently, the Gondwana break-up took place in several steps: first, break-up of East Gondwana was initiated in the Jurassic at ca. 183-180 Ma when South America-Africa separated from Antarctica, India, New Zealand and Australia (Storey, 1995; Encarnación *et al*., 1996). This break-up period was thought to be associated with a series of deep-seated mantle plumes, continental flood basalts and emplacement of dykes such as seen in the Karoo Large Igneous Province (LIP) (Coffin and Eldholm, 1994; Mahoney and Coffin, 1997; Le Gall *et al*., 2002; Fairhead and Wilson, 2002; Reeves, 2009).

Second, break-up of West Gondwana in the early Cretaceous occurred at ca. 130 Ma when Africa separated from South America, accompanied by the Parana-Etendeka Large Igneous Province (LIP), and which resulted in the emplacement of dyke swarms along the margins of the two continents, these include the Henties Bay-Outjo dyke swarms (HOD) on the west coast of Namibia, and the Ponta Grossa dyke swarm (PG) on the east coast of Brazil (O'Connor and Duncan, 1990; Raposo and Ernesto, 1995; Hefferan *et al*., 2000; Ewart *et al*., 2004; Torsvik *et al*., 2004; Gray *et al*., 2008).

The initial opening of the South Atlantic and the formation of the earliest oceanic crust, as suggested by magnetic anomalies-based models started at ca. 132-134 Ma, progressing from south to north during the early Cretaceous (Figure 1.2, Torsvik *et al*., 2004). Whilst (Austin and Uchupi (1982) dated the seafloor spreading in the southern Atlantic Ocean at ca. 130 Ma, this has since been modified using newly identified magnetic anomalies to show that the spreading started at ca. 127-120 Ma (Torsvik and Cocks, 2011). The Cretaceous continental break-up and seafloor spreading in the South Atlantic Ocean was also preceded at ca. 134-128 Ma along both sides of the Atlantic Ocean, by the formation of the Parana-Etendeka Large Igneous Province (LIP) and the emplacement of mafic dyke swarms (Nürnberg and Müller, 1991; Peate, 1997).

Figure 1.2: Map showing the opening of the South Atlantic Ocean and emplacement of the Lebombo Dyke Swarms (LDS), Save Limpopo Dyke Swarm (SLDS), Okavango Dyke Swarms (OKDS), Henties Bay-Outjo Dyke Swarms (HOD), False Bay Dyke Swarm (FBDS) and Ponta Grossa Dyke Swarms (PG) during Gondwana break-up (modified after: de Wit *et al*., 2008; magnetic anomalies from: www.gplates.org).

1.2.2. West and East Gondwana Large Igneous Provinces (LIP)

East Gondwana break-up resulted in magmatism that took place close to the margin of the SW Indian Ocean (Figure 1.3a), in the Karoo Large Igneous Province (KLIP), which is related to the Bouvet hotspot and Karoo lavas (Reeves, 1983; Cox, 1992; Elburg and Goldberg, 2000; White and Mckenzie, 2000; Torsvik *et al*., 2010; Flowers and Stanley, 2013). The KLIP covers part of Antarctica, India, Madagascar, the Falkland Islands,

Mozambique, and is the largest continental flood basalt in the world (Storey, 1995; Manninen *et al.*, 2008). Originally the Etendeka volcanic rocks in Namibia were described as part of the Karoo LIP. However, differences in age and composition separate the Karoo from the Parana-Etendeka Province even though they are geographically adjacent to each other (Cox, 1988; Renne *et al*., 1992; Renne *et al*., 1996; Duncan and Marsh, 2006).

A mantle plume underlying the Tristan da Cuhna hotspot appears to have been closely related to the Paraná-Etendeka magmatic event (see Figure 1.3b), which gave rise to extrusive and intrusive igneous rocks in an extensive area of the Parana-Etendeka Large Igneous Province (Gibson *et al*., 2006). The Parana-Etendeka flood basalt occurred shortly before continental rifting of the South Atlantic in the early Cretaceous ca. 132 Ma (Lord *et al*., 1996; Gibson *et al.*, 2006; Glen *et al.*, 1997; Peate, 1997; Ustrino *et al.*, 2010). The age of the Parana-Etendeka flood basalt suggests its magmatism preceded crust rupture, and that major magma eruption occurred prior to the first formation of the seafloor magnetic anomalies on the Atlantic Ocean (Kirstein *et al*., 2001; Torsvik *et al.*, 2004).

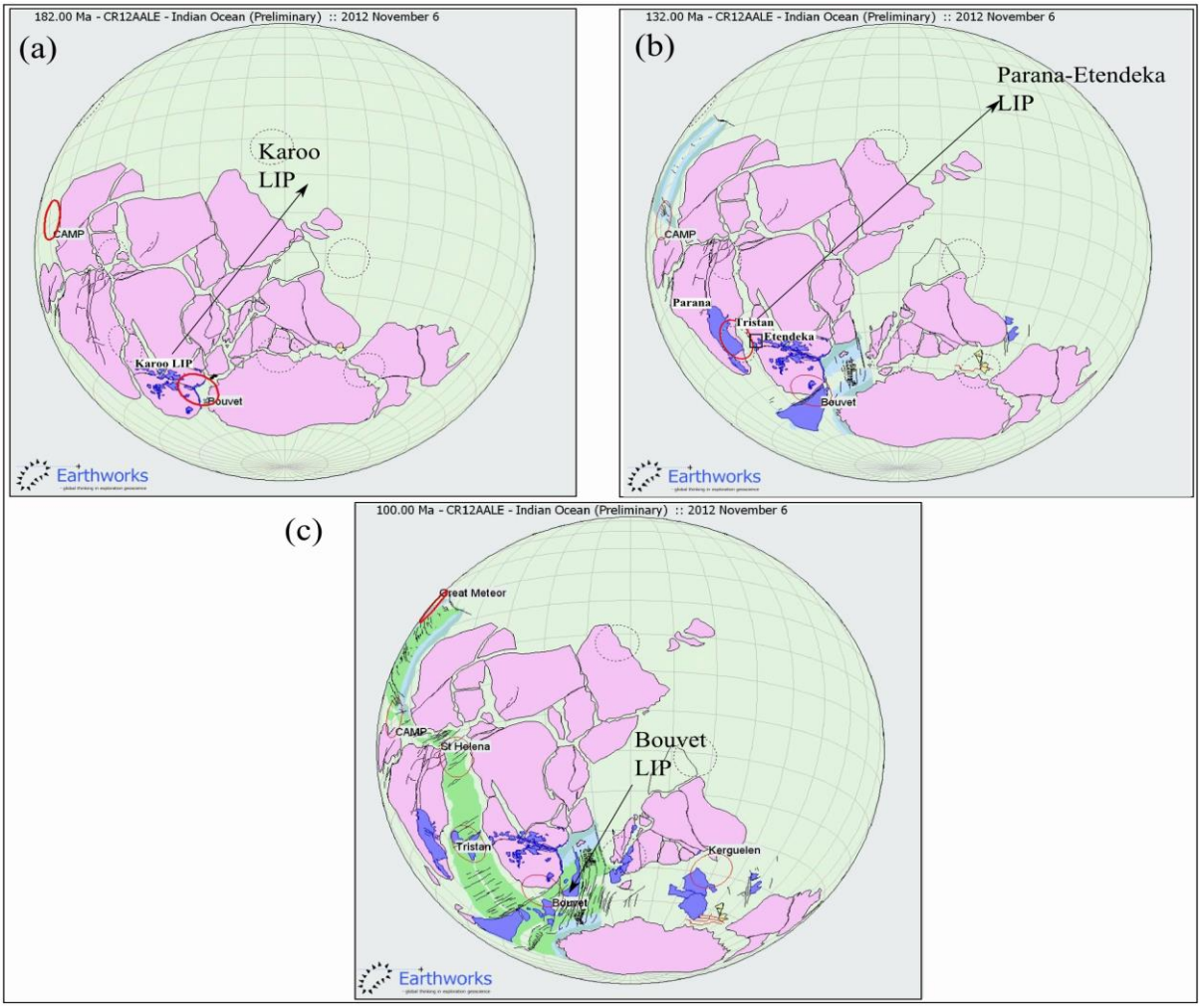

Figure 1.3: (a-c) Maps to show the opening of Indian-Atlantic Ocean between 182 and 100 Ma and the position of the Large Igneous Provinces (Dark blue) during Gondwana break-up and formation of oceanic crust (Pale blue) (Reconstructed from: www.reeves.nl/gondwana, 2012).

The following table describes Gondwana break-up events in chronology order.

Table 1.1: Summary of chronological events during the break-up of Gondwana. Only events documented discussed in this research work are listed.

Period	Events	References
183-180 Ma	Karoo large igneous province (LIP) that initiated separation of east Gondwana. The Karoo continental basalt, sills and dykes occurring in this period.	(Renne *et al*., 1996)
134-128 Ma	Mafic igneous event in southern Africa and formation of the Parana-Etendeka LIP. Cretaceous dyke emplacement in Gondwana, including the Henties Bay-Dyke Swarms, Namibia.	(Reid *et al*., 1991;(Nürnberg, and Müller, 1991); Renne, *et al*., 1996; (Peate, 1997); Gohl, *et al*., 2012)
127-120 Ma	Ocean-floor magnetic anomalies indicate the onset of spreading along the Mid-Atlantic spreading ridge, in the south Atlantic	(Torsvik *et al*., 2004)
120-80 Ma	Uplift of southern Africa during the Cretaceous (1-7 km denudation); formation of the Agulhus plateau and Bouvet LIP.	(Tinker *et al*., 2008; Decker *et al*., 2013; Flament *et al*., 2013); (Viola *et al*., 2012)
50-40 Ma	Uplift of southern Africa in the Cenozoic period. (< 1 km denudation)	(Partridge and Maud, 1987; Burke, 1996; Tinker *et al*., 2008; de Wit, 2007)

1.2.3. Dyke swarms and triple junctions flanking southern Africa

A triple junction is formed during continental break-up by three tectonic rifts junction (Dewey and Burke, 1974; Burke, 1977). A sterling example of a rift triple junction is the Benue trough that is assumed to have been active before and during continental break-up and is situated in the gulf of Guinea (Dewey and Burke, 1974; Petters, 1978; Nürnberg and Müller, 1991).

Numerous models have been proposed to explain the mechanism by which the intrusion of magma into the upper crust may have initiated a triple junction e.g. rifts joined at ca. 120° angles. The Mogi model (Mogi, 1958) suggests that successive injection of magma can deform and uplift the volcanic edifice (Figure 1.4). The systematic testing of this model revealed that the volcanic edifice may build up when the magma is thick and results in fracturing and formation of a triple junction (Delaney and McTigue, 1994; Rymer and Williams-jones, 2000; White and Mckenzie, 2000; Annen *et al*., 2001; Manninen *et al*., 2008). Mogi's model has been adapted by many workers (e.g. Burke, 1977; Gates, 2003).

Dewey and Burke (1974) elaborated on how a hotspot can form the tectonic rift junctions. Triple junction dykes may reflect the variation in the stress field during their emplacement and the associated deformation of the crust. The increase in domal uplift and rifting caused by a mantle plume may result in fracturing of the crust and the consequent formation of radiant dykes (Ernst and Buchan, 1997; Ernst *et al*., 2001; Hou, 2012).

One of the dyke swarm of the 120° apart triple junction in the Karoo was interpreted as a failed Gondwana spreading axis forming the Okavango dyke swarm (failed arm), whilst two others are parallel to spreading axis in Indian Ocean; Save Limpopo dyke swarm and the Lebombo dyke swarm (Reeves, 1978; Cox, 1989; Moore and Blenkinsop, 2002). The triple junction was initiated by uplift due to a mantle plume that resulted to bulging and cracking of the upper crust (Cox, 1989; Koppers, 2011). Similarly, the Ponta Grossa dyke swarm (PG) has also been interpreted as the failed rift arm on the South American margin of a triple junction formed during the opening of the South Atlantic ca. 130 Ma (Renne *et al*., 1992; Renne *et al*., 1996; Heine *et al*., 2013). The HOD was interpreted also as failed arm on the African margins that was once a part of the south Atlantic rift, and is also assumed to mark the initiation of the extension and magmatism across the failed rift (Trumbull *et al*., 2004; Heine *et al*., 2013).

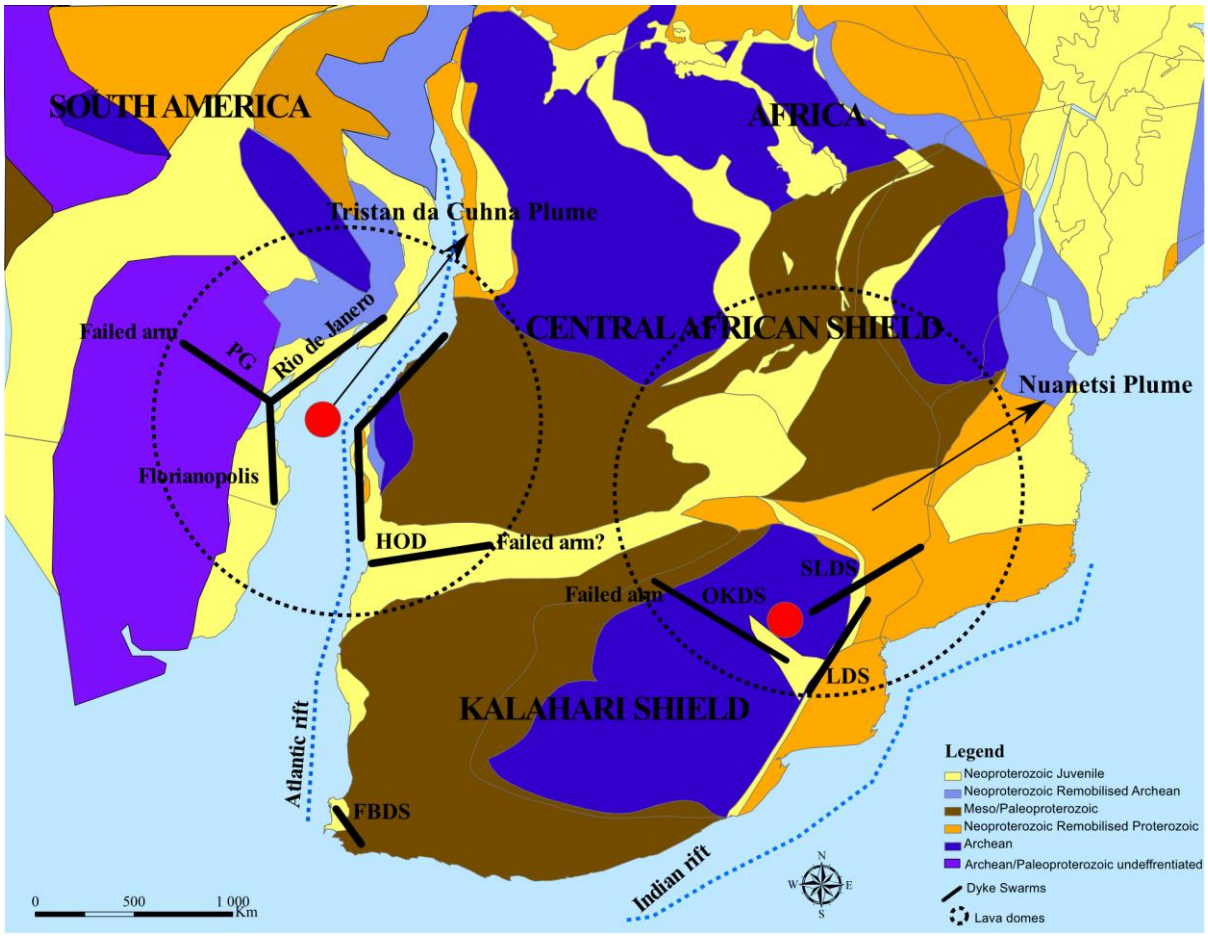

Figure 1.4: Location of triple junctions represented by: (1) the Okavango Dyke Swarm (OKDS), the Lebombo Dyke Swarm (LDS) and the Save Limpopo Dyke Swarm (SLDS) during opening of Indian

Ocean); (2) the Florianopolis, Rio de Janeiro and Ponta Grossa Dyke Swarm (PGDS) in Brazil, South Atlantic along South American margin; (3) the False Bay dyke swarms (FBDS) and, (4) the Henties Bay-Outjo Dyke Swarms (HOD) which appear to be part of triple junction along the African margin of the South Atlantic (Renne *et al*., 1996; Trumbull *et al*., 2004; Jourdan *et al*., 2006; Geology from: de Wit *et al*., 2008).

1.2.4. Vertical motions: Epeirogeny and Isostacy of southern Africa

There are 3 types of uplift: orogenic (collisional) uplift, mantle dynamic uplift (extensional) associated with large igneous provinces (Saunders *et al.*, 2007) and isostatic uplift (Figure 1.5a) Epeirogeny refers to the vertical movements of the lithosphere (de Wit, 2007); Orogenic uplift involves horizontal plate collisions that result in mountain ranges over a large region such as the Himalaya, Tibet and Andes Mountains (England and Molnar, 1990; Bonnet and Crave, 2003). Isostatic uplift also known as Wegener type uplift involves gradual vertical uplift of the surface that results from compensation during erosion (exhumation) and removal of materials (denudation) from continents such as exemplified by the southern African Great Escapement (see Figure 1.5b) (Brandt, *et al*., 2003; Tinker *et al*., 2008; Parsiegla *et al*., 2007; de Wit, 2007; Decker *et al*., 2013; Flowers and Stanley, 2013).

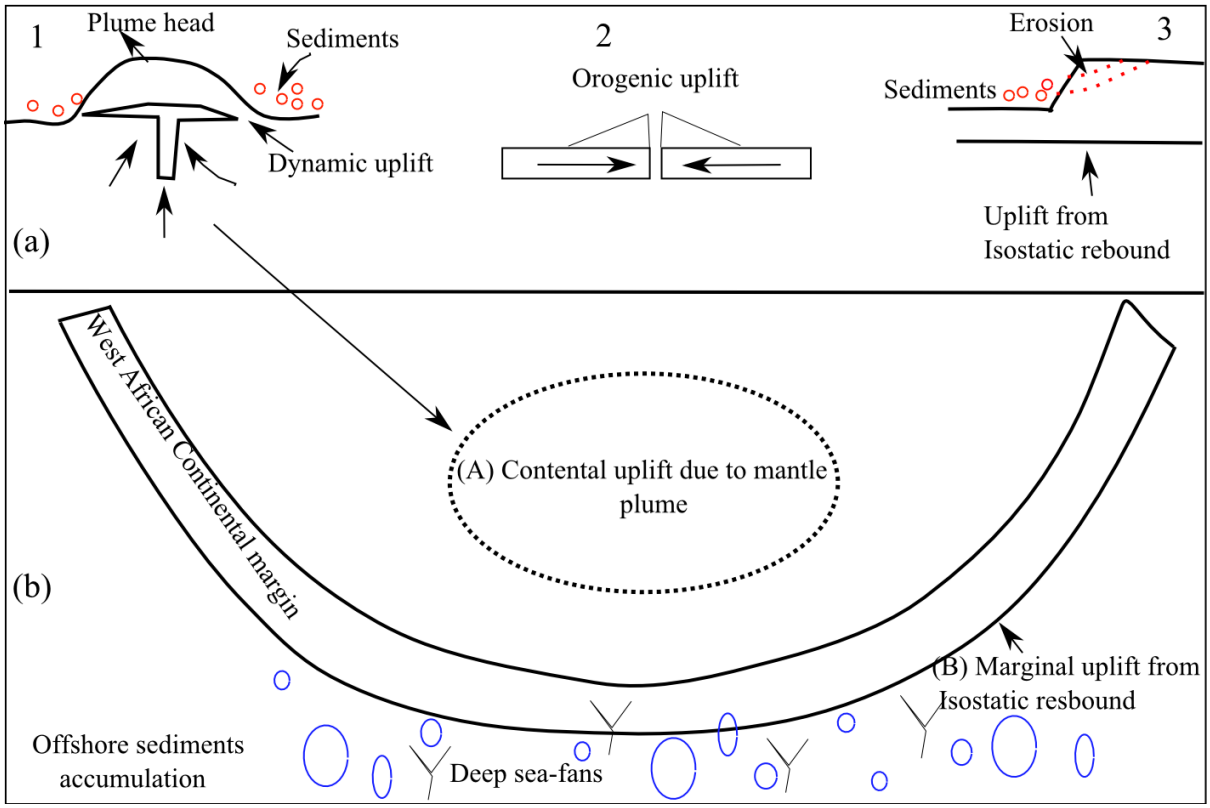

Figure 1.5 (a) Uplift formations and processes and (b) simplified sketch showing the occurrence of uplift due to a mantle plume with dynamic uplift and marginal uplift due to erosion from the marginal continental surface of southern Africa (modified after: Burov and Guillou-Frottier, 2005; Séranne and Zahie, 2005).

Timing of the uplift

The timing involved the uplift remains controversial (Doucouré and de Wit, 2003; Stecker *et al*., 2005; Viola *et al*., 2005; de Wit, 2007; Tinker *et al*., 2008; Viola *et al*., 2012). The occurrence of erosion on the southern Africa margins appears to have influenced the uplift on the southern Africa that resulted in the formation of the Great Escapement after continental separation at about 100 Ma (Tinker *et al*., 2008; Flowers and Schoene, 2010; Stanley and Flowers, 2011; Flowers and Stanley, 2013). However, some workers argue that the uplift on the southern Africa margins was initiated before continental break-up (Buck, 1986; Behn *et al*., 2006; Esedo *et al*., 2012) whilst other workers dispute that the uplift on the southern Africa margins is Mesozoic in age and some workers advocate sediments dated to the Cenozoic age ca. 30-25 Ma (Partridge and Maud, 1987; Sahagian, 1988; van Balen *et al*., 1995; Burke, 1996; Séranne and Zahie, 2005; de Wit, 2007; Rowberry *et al*., 2010; Dominique *et al*., 2013). The younger events could have happened during the Cenozoic, when Africa moved north-eastward over the mantle upwelling beneath Eastern Africa (e.g. Conrad, 2003; Wichura *et al.*, 2010; Esedo *et al.*, 2012). Either way the uplift may have contributed to fracture and joints development in the southern African upper crust.

1.2.5. Brittle deformation and joint formation

Brittle deformation is the rupture of stressed rock that takes place when the stress exceeds the strength of the rock (Griffith, 1924). It generally occurs in the upper crust up to ca. 10-15 km deep (Scholz, 2002; Fossen, 2010).

Rocks deform in response to different stresses such as extensional, compressional and shearing stresses. An extensional stress leads to thinning of the Earth crust and can trigger the rifting of the crust. The brittle deformation of the rock is recorded by structures such as faults, joints and folds (Van der Pluijm and Marshak, 2004; Booth, 2009; Fossen, 2010) which together with dykes were observed and mapped in the study areas.

Models concerning the initiation of fracture systems initiations have emerged and they describe the relationship between joints and stress directions (Viola *et al*., 2012). Three principle stresses are used $б_2$, $б_1$ and $б_3$. Fossen (2010) suggested $б_1 > б_2 = б_3$ and the principal ($б_2$) and least ($б_3$) stress directions are horizontal or sub-horizontal while the medium ($б_1$) stress direction is vertical (see Figure 1.6), joints may develop parallel to the medium stress direction and parallel with $б_2$-direction (Chapman and Wingard, 1958; Suryanarayana and Anjanappa, 1975; Scholz, 2002).

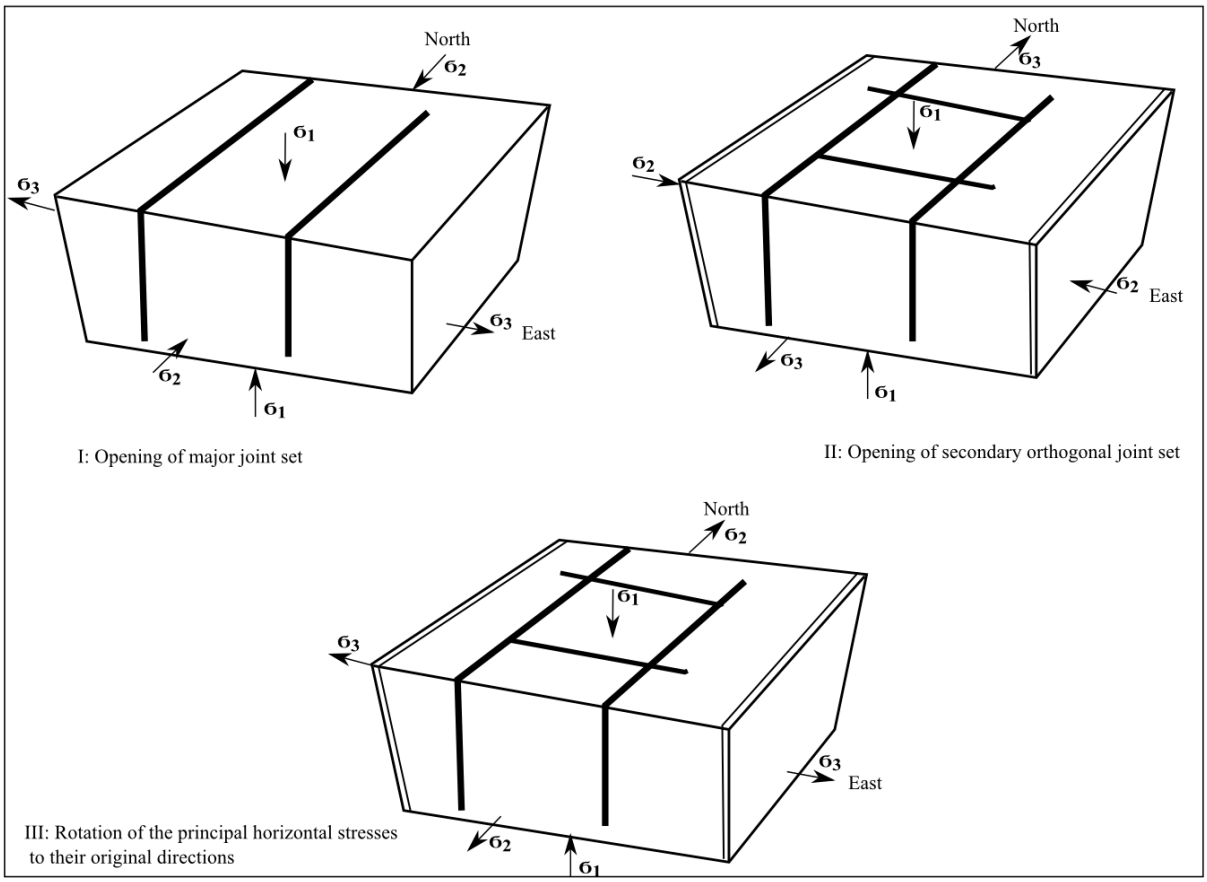

Figure 1.6: Stress distributions in the upper crust that can result in brittle deformation (Dershowitz, and Einstein, 1988; Dershowitz *et al.*, 1997; Van der Pluijm and Marshak, 2004; Bird *et al.*, 2006; Viola *et al.*, 2012; Fossen, 2010).

Joint systems of southern Africa were likely initiated when overburden was removed during Gondwana break-up and the vertical pressure consequently decreased (Bench *et al.*,1977). The brittle structures of the western margin of Southern Africa may have been associated with the opening of the Atlantic Ocean during the mid-Cretaceous (130-90 Ma) (Raab, 2001; Crider *et al.*, 2004).

In summary, the triple junction arrangement of HOD and PG is thought to be inherited from the geometry of the Pan-African fold belt (Trumbull *et al.*, 2004). The South Atlantic triple junction that includes the HOD failed arm were also explained by the same model (Dewey and Burke, 1974; Jourdan *et al.*, 2004; Almeida *et al.*, 2005). The uplift is speculated to have initiated horizontal joint system whilst horizontal stresses in the upper crust during rifting and spreading act as the controlling factors of various orientations of vertical dykes and joint systems (e.g. Figure 1.6, Cruikshank and Aydin, 1995).

Chapter 2. Stress system, geometry of dykes, and natural joint systems, and geological settings of the study areas

Dykes are a common expressions of crustal extension in both oceanic and continental environments (Figure 2.1), and their study may lead to a better understanding of the tectonic history of continents and paleocontinent reconstruction and past tectonic regime (Halls and Fahrig, 1987; Hald and Tegner, 2000; Rao *et al*., 2005). They are not generally as well exposed on the ocean floor as they are on the continents (Wilson, 1965). Dyke swarms have been used to reconstruct paleocontinents based on paleo-magnetic data due to their magnetic properties (Halls and Fahrig, 1987; Srivastava and Oliveira, 2011). Over the past 25 years, studies of the oceanic dykes exposed in ophiolite complexes, such as Caribbean, Chilean, Ligurian, Macquarie, Mediterranean, Sierra and Franciscan and continental dykes have also increased significantly (Stern *et al*., 1976; Furnes *et al*., 2007; Robinson *et al*., 2008; Furnes *et al*., 2009). Using these example, the HOD dyke geometry can help us to understand the tectonic stress patterns and emplacement history during West Gondwana break-up ca. 132 ± 6 Ma (O'Connor and Duncan, 1990; Kirstein *et al*., 2001).

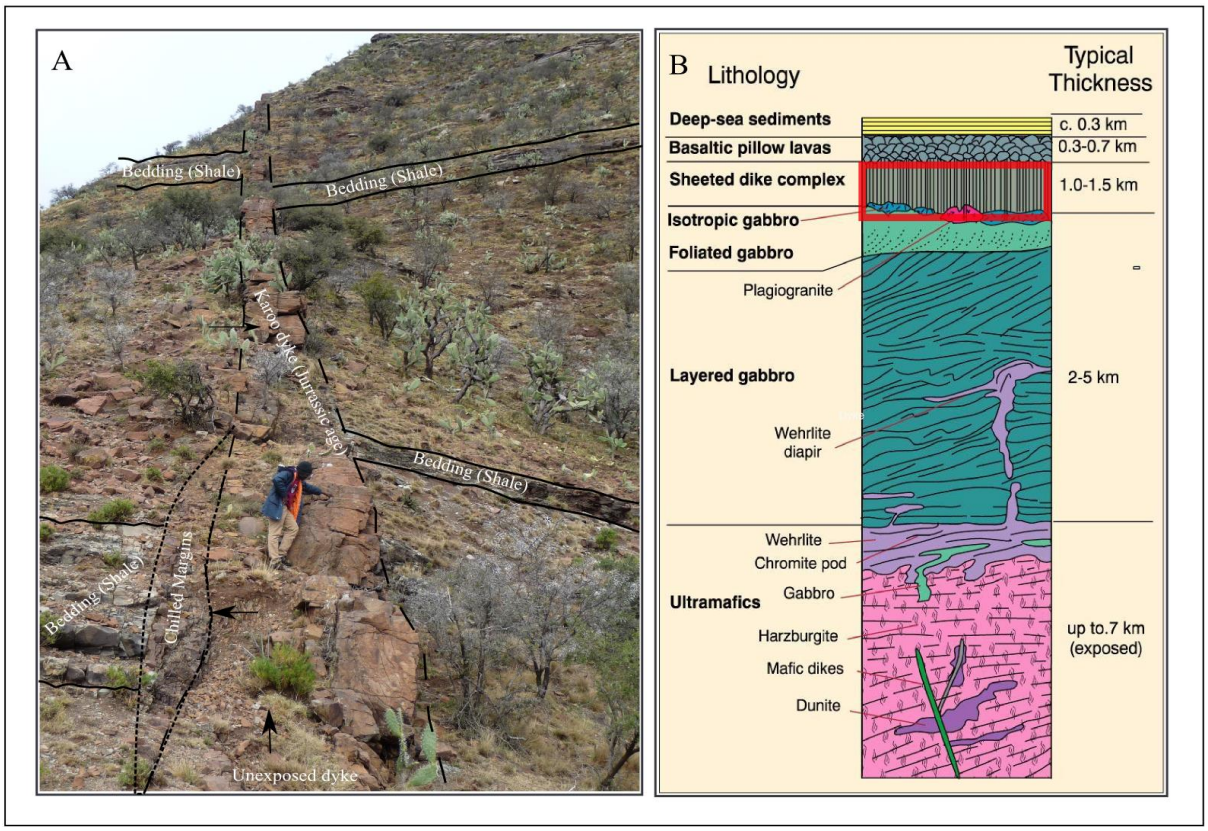

Figure 2.1: (A) An example of a continental dyke from the Karoo Basin, South Africa (West of Queenstown, Eastern Cape Province) and (B) schematic representation of the sheeted oceanic dykes from the Samial Ophiolite complex, Oman (Bouldier and Nicolas, 1985).

2.1. Emplacement propagation and geometry of dykes

Dykes transfer hot magma to the cold crustal host-rock. When magma migrates through the upper crust to a volcanic complex via dykes, it must overcome high compressive stress directed downwards from the weight of the above lying volcanic complex. Propagation of dykes is categorized by straight, curved and echelon path depending on the orientation and geometries between the shear stress and dyke walls (Cooke and Pollard, 1996; Pollard and Raymond, 2005; Clemente *et al.*, 2007). Dyke propagation is mostly along a straight path (see Figure 2.2) but also associated with both curved and echelon paths (Currie and Ferguson, 1970; Pollard, 1987).

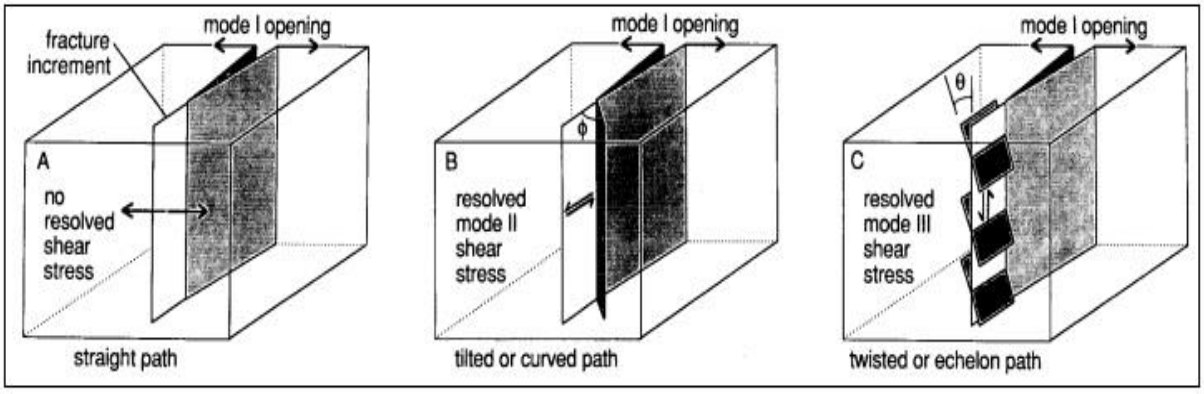

Figure 2.2: Illustration of dyke propagation and their geometries in response to (A) local least compressive (Extensional) stress, as well as B and C, the response on the shear stress against the wall rock (Modified after: Pollard and Aydin, 1988).

Dykes often intrudes through pre-existing fractures and into joints by exerting excess stress at the dyke tip on its way up to the surface (Anderson, 1936; Traversa and Grasso, 2009). The reason magma can reach the surface is that it propagates through brittle fractures towards areas of least stress (Cook and Gordon, 1964; Watanabe *et al*., 2002). The stress exerted on the Earth's crust by a volcano is the cause of multiple eruptions at large volcanic centers, while the surrounding areas do not experience major volcanic eruptions. The mechanisms of dyke emplacement likely took place the same way in the HOD during these Gondwana break-up.

The propagation process of dykes involves viscous flow of magma, elastic deformation of crust, heat loss from the flowing magma (Taisne and Tait, 2011). Mafic dykes generally propagate perpendicular to the direction of the least horizontal compressive stress (Emerman and Marrett, 1990; Morgan, 2004; Manconi *et al*., 2007). If the magma pressure exceeds the least horizontal compressive stress only cracks nearly perpendicular to the principal compressive horizontal stress can be dilated. Alternatively, when magma pressure exceeds the greatest compressive stress, cracks of any orientation can be dilated (Delaney *et al*., 1986).

As magma propagate towards a volcano, it forms level of neutral buoyancy (LNB) within the crust due to the maximum horizontal compressive stress (Pinkerton *et al*., 2002; Partiff and Wilson, 2008). When this level of neutral buoyancy is encountered by vertically propagating dykes the velocity of dyke injection decreases and the viscous flow drops causing dykes to widen (see Figure 2.3). Thereafter there is limited upward penetration beyond the LNB and, if this does not intersect the Earth's surface, the melt will be emplaced laterally along the LNB in the form of sills (Cook *et al*., 1964; Rubin, 1995). Propagation directions may also change due to changes in lithology, or variation in the structural fabric of the host-rock when dykes reach the surface (Rubin, 1995; Gudmundsson *et al*., 1999; Jolly and Lonergan, 2002; MaCcaferri *et al*., 2011).

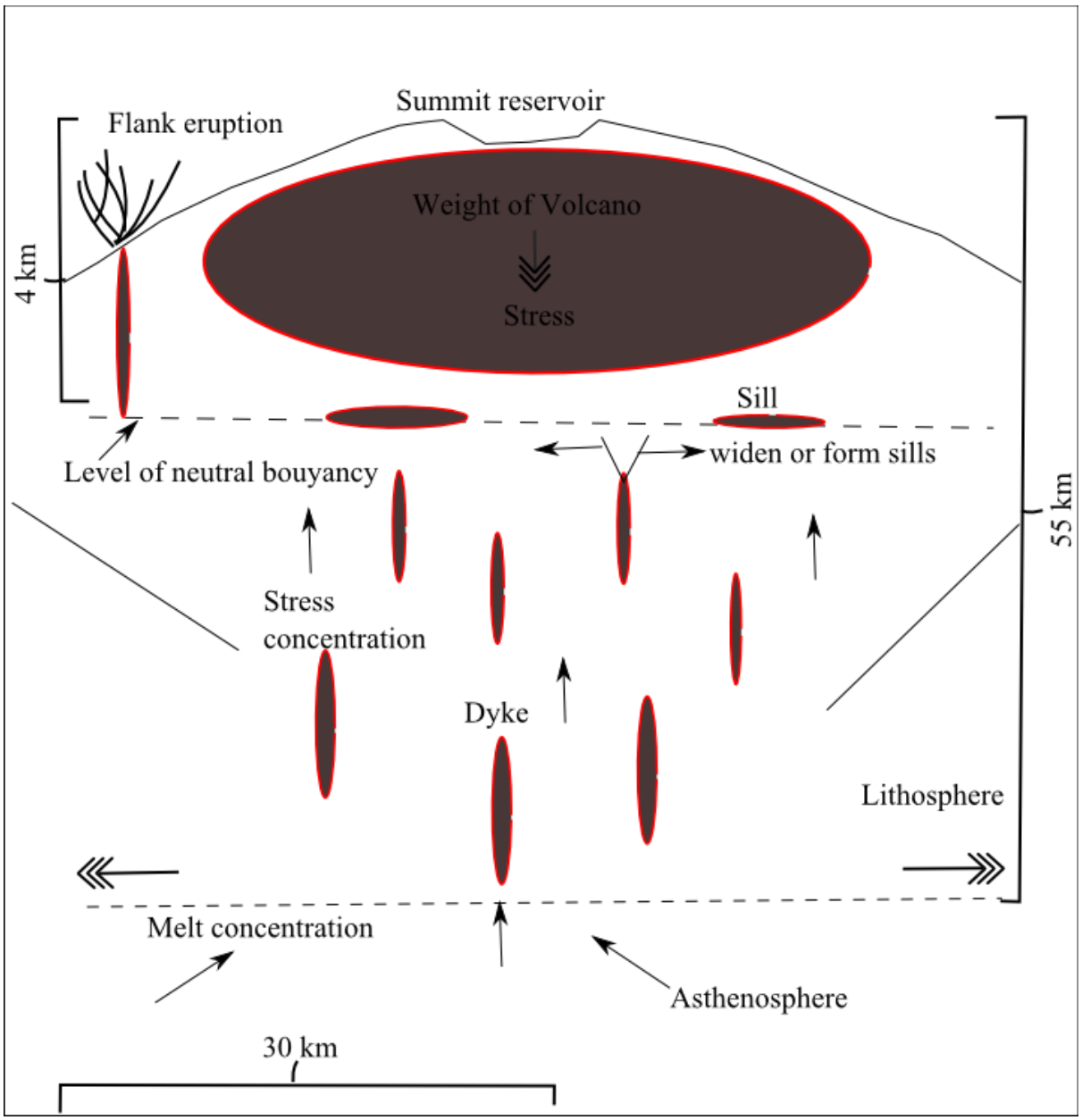

Figure 2.3: Sketch representing the directions of dyke propagation and emplacement relative to the failing stress towards the level of neutral buoyancy after which the dykes extend horizontally and or form sills (Modified after: Bahat and Engelder, 1984; Poland *et al*., 2007).

2.2. Geometry and relative age of dykes and joints

Common Structures of dykes

Dykes commonly preserve evidence of brittle structures that are found in the form of en-echelon dykes and bridge structures. En-echelon arrays are interpreted as discontinuous segments of planar parent dykes (see Figure 2.3 and Figure 2.4). An array typically consists of either continuous non-overlapping stepped segments, or overlapping connected segments (Olson and Pollard, 1991; Crider and Peacock, 2004; Hutton, 2009). It is postulated that the en-echelon arrays of dykes are formed as a result of shearing deformations and that they grow as straight propagating or curved propagating fractures (Pollard and Nicholson, 1985; Hoek, 1991; Clemente *et al*., 2007; Watkeys and Kattenhorn, 1995). Dykes can also be emplaced in pre-existing stepped fractures (Currie and Ferguson, 1970) and as a result, at times, can display a zigzag emplacement pattern (Marinoni, 2001). Straight propagating stepped dykes follow a net-like deformation patterns whereas the curved propagation stepped dykes appear to be fan-like deformation patterns (Figure 2.4; Pollard and Nicholson, 1985; Olson, 1993).

Bridges of host-rock may separate dykes: typically a bridge is a section of host-rock separating one dyke segment from its neighbour in an en-echelon array (Delaney and Pollard, 1981; Hutton, 2009). Bridges may form at local rock discontinuities in heterogeneous rocks (e.g. bedding, layers) or due to the microstructures in homogenous rock segments (Pollard and Nicholson, 1985; Crider and Peacock, 2004). Bridge structures and en-echelon arrays can be used to deduce the direction and magnitude of strike-slip movement relative to the crustal extension associated with dyke formation. During dilation the secondary host-rock bridges are formed (see Figure 2.4 A and B). A bridge structure in a dyke represents a change in level that results in a gap between two segments (see Figure 2.4. A and B) or stepping up between two vertical segments (Rickwood, 1990; Nicholson and Ejiofor, 1987).

Curved propagating dykes occurs due to mechanical interaction (heterogeneities) adjacent to crack tips which may also cause them to overlap (Nicholson and Pollard, 1985). The interaction of the propagating tips of en-echelon segments is controlled by the proportion of near field (magma pressure) and far field stresses (tectonics). The shear stresses in the interaction zone increase as crack ends approach each other and these can remain large as the ends overlap; crust in this zone may fracture (Hutton, 2009; Maccaferri *et al*., 2011). The tendency to curve is most pronounced if the rock properties and stress fields are isotropic and simple shear components dominate. Simple shear is the deformation that involves rotation of the principal strain axis (Pollard and Raymond, 2005). When cracks overlap each other, connecting tips rotate and the crack direction rotates with it (see Figure 2.4.A, Fender *et al*., 2010).

Straight propagating dykes are guided by strong anisotropic fabric (e.g. bedding or layering, (see Figure 2.4B). The dykes are either not displaced or they are emplaced across the discontinuity en-echelon separated by fractures. Two cracks may propagate along

approximately straight paths in response to pure shear until they pass each other, after which they curve and form a convex shape (Melissa *et al*., 2010). Straight propagation-path dykes are formed because of a failure of the intervening bridge of host-rock. By contrast, curved propagating paths occur when one dyke tip propagates into the near wall of the adjacent dyke (see Figure 2.4, Melissa *et al*., 2010).

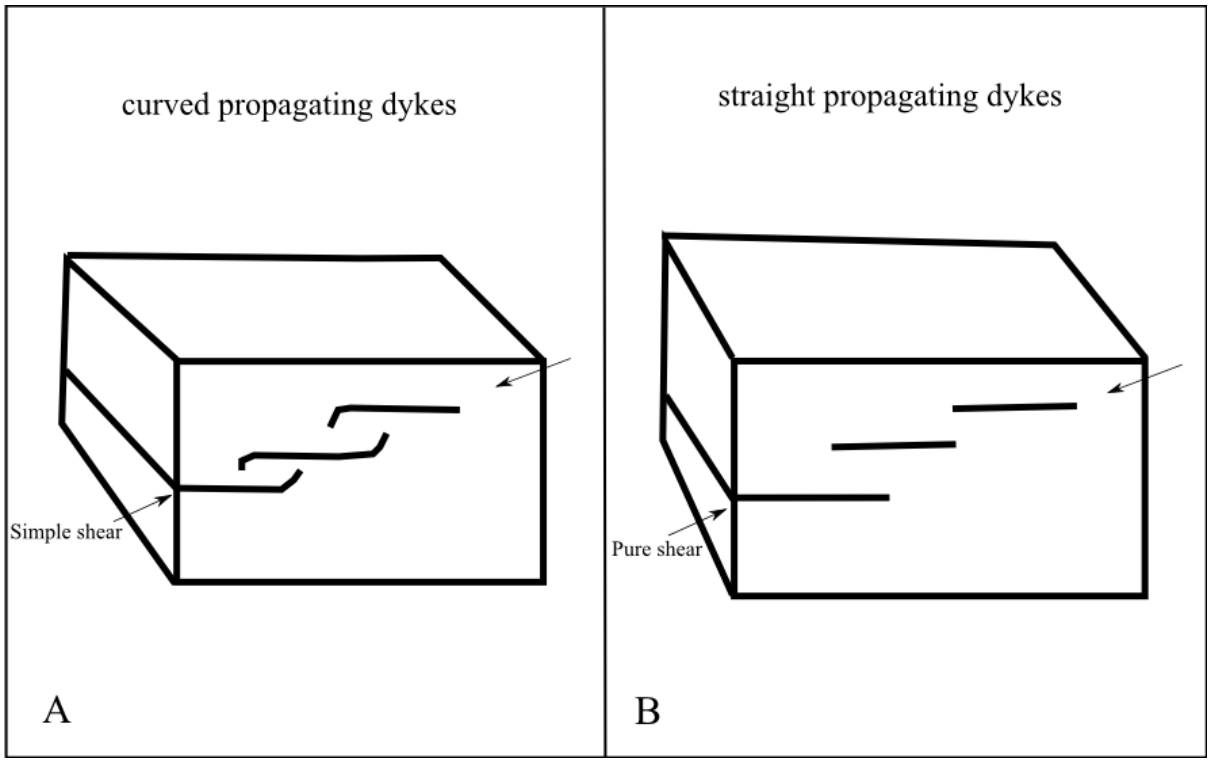

Figure 2.4: Simplified sketch illustrating (A) bridges separating en-echelon cracks that grow along curved projections and (B) bridges separating straight en-echelon dykes (Modified from: Hoek, 1991; Watkeys and Kattenhorn, 1995; Yoneyam*a et al*., 2007).

2.3. Joints and their relationship with dykes

Recent studies suggests that fractures initiate along bedding boundaries and along stress concentrations in brittle materials (Bahat and Engelder, 1984; Bahat, 1991; Helgeson and Aydin, 1991; Lacazzete and Engelder, 1992; Weinberger, 2001; Bahat *et al*., 2005). Once surface joints are created, tensile stresses decrease, which forces the joint propagation to decrease (Gross *et al*., 1995).

According to Secor (1965), the growth of joints is a slow and cumulative process of short episodes of crack propagation (Secor, 1965; Crider and Peacock, 2004). It is challenging to distinguish joints formed by the uplift of the crust from joints formed by horizontal neotectonic activities because both types of joints have similar characteristics such as joint spacing and apertures (Hancock and Engelder, 1989; Stecker *et al*., 2005). Joints are generally divided into three types or modes as follows: mode I, mode II and mode III as illustrated in Figure 2.5, (Mamtani *et al*., 2004; Pollard and Raymond, 2005).

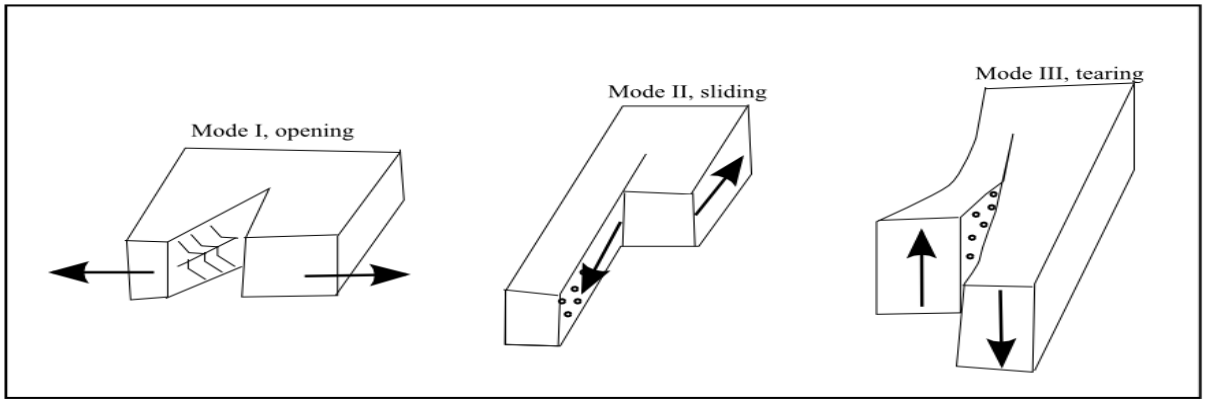

Figure 2.5: Simplified sketch of the three different joint modes (Modified after: Pollard and Raymond, 2005).

Skameta (1983) and Price and Cosgrove (1990) suggested that the orientations of dykes are generally influenced by pre-existing joints at the time of intrusion as joints run parallel to the dykes and as a corollary the orientations of joints can be used to construct the original relationship between intrusive rock and the surrounding country-rock. Due to increasing observations that joints trend parallel to dykes, it was postulated that joints were generated as a result of the dyke intrusion mechanism (Skameta, 1983). Where dykes kink it may indicate that the dyke was displaced or that they may follow pre-existing joints (see Figure 2.6). If displacement happened after dyke emplaced then there would be more fracturing than when the dyke follows pre-existing joints. Delaney and Gartner (1997) investigated how magma may have migrated through pre-existing structures to reach the surface. They, and others, have found that joints commonly formed by the stress caused by dyke intrusions (Delaney *et al*., 1986; Ransome, 1992; Grout and Verbeek, 1998).

Increasing evidence also indicates that joints do not occur at depth greater than 12 km in the Earth's crust, as below that depth ductile deformation (flow) occurs (Mandl, 2005). Secor (1965) also proposed this but he did not give a precise depth above which joints can initiate, since this depends on the aperture, and heat flow (e.g. the geothermal gradient). The example of Iceland dykes shows that joints can take place at depths of ca. 17.5-13.5 km (Mandl, 2005; White *et al.*, 2011). The relationships, if any, between joints and dykes are determined by the similarity of the orientations (Suryanarayana and Anjanappa, 1975; Rives *et al.*, 1994; Shang *et al*., 2009).

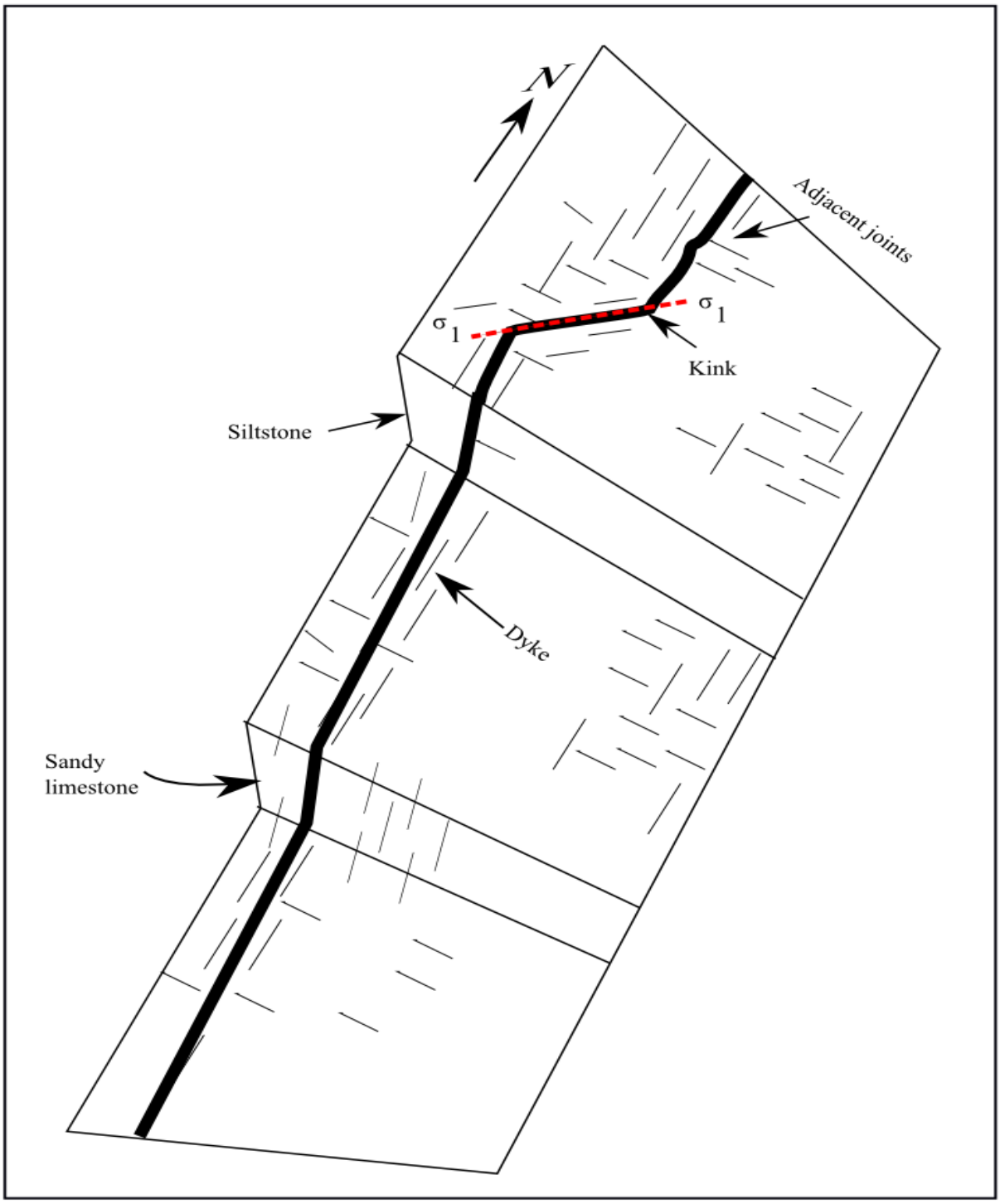

Figure 2.6: Schematic diagram showing possible relationship between dyke and joint systems (Modified: Delaney *et al*., 1986; Price and Cosgrove, 1990).

In summary, overlapping and kinking dykes are common and often are controlled by a change of the lithology; dykes also generally follow weak zones e.g. joints, bedding, foliation and schistosity. Although some studies have proven a close relationship of dykes and joints questions remain unanswered about those dykes that do not seem to follow pre-existing joints.

2.4 Geological settings and structures of the HOD, TMG and GVS

In this chapter I introduce the (1) geological settings of the HOD dykes in the North West of Namibia, (2) the geological settings of the Golden Valley Sill (GVS) in the Tarkastad area of the Eastern Cape Province and (3) the geological settings of the Table Mountain Group quartzites (TMG) in the Tsitsikamma area of the Western Cape Province, both in South Africa.

2.4.1 Geological settings and structures of the Henties Bay-Outjo dyke swarm (HOD) in Namibia

The HOD trends NE-SW, following the structural trends of the Damara Belt that extends to the Lufilian Arc (Passchier, 2002) along the coast of northwest Namibia (see Figure 2.7). The HOD is about 100 km wide and extends ca. 500 km inland from the coast along the Damara Belt in Namibia (Trumbull *et al.*, 2004). The Damara Belt and Lufilian Arc form part of a Pan-African Orogenic Belt (650-500 Ma) and the tectonic trends following the Damara Belt "coils" as they approach the Lufilian Arc in Zambian and Botswana (Prave, 1996; Kröner and Stern, 2005). The HOD was interpreted as a result of the Etendeka magmatism (Dewey and Burke, 1974; Thompson *et al*., 2007; Trumbull *et al*.,2007).

The HOD intrudes rocks of the Damara sequence such as basal Nosib, Otavi, Swakop and Mulden Groups, and parallels various geological features such as the Pan-African lineament, and faults (Germs and Gresse, 1991; Germs, 1995; Gray *et al.*, 2008).

Locally, dykes crosscut the basement foliations and lithological contacts and they do not preferentially exploit a specific lithology. The lithology of the area comprises of the late Cretaceous to Tertiary volcanic activities (Gray *et al*., 2008). The Kalahari Group which covers most of the eastern and northern part of Namibia, is about 300 m thick in south east Namibia and may be 600 m thick at the Angolan border (Miller, 2008). The Etendeka Group, north of the HOD in the NW of Namibia is made up of aeolian sandstone up to 100 m thick and at the base is overlain by successions of 132 Ma volcanic rocks up to 1000 m thick. The Etendeka volcanic succession makes up to 6% of the Parana-Etendeka Large Igneous Province (Miller, 2008). The Etendeka volcanic rocks and their inter-bedded aeolian sandstones are considered early Cretaceous (Milner *et al*., 2004; Miller, 2008).

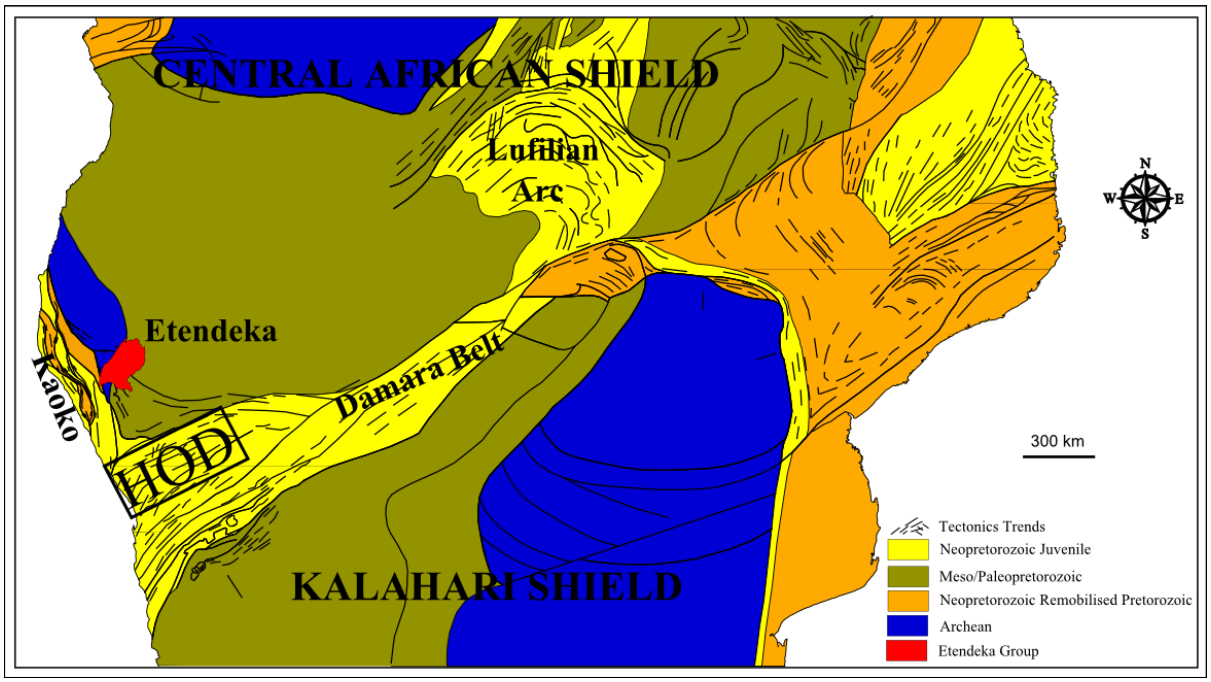

Figure 2.7: Regional geological map of part of South Central Africa representing the position of the Pan African Damara, Kaoko Belts and Etendeka lavas in Namibia and the Lufilian Arc in Zambia (Modified after: de Wit *et al.*, 2008). The location of the Henties Bay-Outjo dyke swarm is shown in box (HOD).

2.4.2 Regional occurrence of the HOD dykes

The HOD dyke swarm also extends into the southern part of the Kaoko Belt where the width of the swarm is greatest (Passchier, 2002; Zerfassl *et al*., 2005; Miller and Becker, 2008). It was shown that the HOD formed as part of the Cretaceous large igneous province ca. 132 Ma, linked to the Tristan mantle plume that caused magma to rise through crustal discontinuities (e.g. Figure 1.3, Valente *et al*., 2007; Tupinambá *et al*., 2012). The HOD was formed due to tectonic extension of the upper crust in the lower Cretaceous associated with the widespread emplacement of predominantly mafic dykes and intrusive ring complexes representing the remnants of volcanic centres (Hahne, 2004). The orientation and distribution of the HOD dykes suggest a strong influence of the Damara Belt basement structures that trend NE-SW (Jourdan *et al*., 2006).

2.4.3 Lineaments, Damaraland Complex and Faults

Lineaments are straight lines or gently curving features on the Earth's surface that are commonly expressed topographically as ridges or linear depressions (Shake and McHone, 1987). Lineaments are the result of weakness or displacements in the Earth's crust. These weaknesses can be easily seen on satellite images (Richards, 2000; Leech *et al*., 2003; Hung, *et al*., 2005) while faults are planar fractures or discontinuous rock volume where there has been measurable displacement and as a result of differential Earth movements (Girty, 2009; Fossen, 2010).

The Waterberg fault is connected along strike to the Omaruru lineament (see Figure 2.8) while the Autseib lineament is connected with the Otjohorongo fault. The surface expression of these faults follows a 65° strike orientation, but the geometry below surface has not been investigated geophysically. The Autseib and Waterberg faults appear to have a similar orientations as the Omaruru and Autseib lineaments (Figure 2.8, Clemson *et al*., 1997; Clemson *et al*. 1999; Corner, 2000; Dunlop, 2006). The Waterberg fault was reactivated as thrust with a vergence, that thrusts basement over early Cretaceous rocks (Viola *et al*., 2005; Viola *et al*., 2012).

The Cretaceous Omaruru lineament-Waterberg fault, and Autseib lineaments-Otjohorongo faults along the Henties Bay-Outjo Dyke Swarm (HOD), are believed to have formed as a result of collision of continents during the Pan-African Orogeny about 550 Ma (Corner, 2000; Kröner and Stern, 2005) and are thus fundamental lithospheric structures. The Omaruru lineament may have influenced dyke emplacement in the HOD (Wanke, 2000; Raab, 2001) giving the NE-SW trend of dykes in the HOD while dykes on the southern side of the lineament show no preferred orientation as they decrease in abundance (see Figure 2.8). Dykes to the north of the Autseib lineament shows less abundance (Figure 2.8) which means Autseib lineament might have no or little influence on the emplacement of Henties Bay Cretaceous dykes (Trumbull *et al*., 2004). The Autseib lineament lies south of the Brandberg igneous complex in the Damara Belt (Clemson *et al*., 1997; Clemson *et al*., 1999).

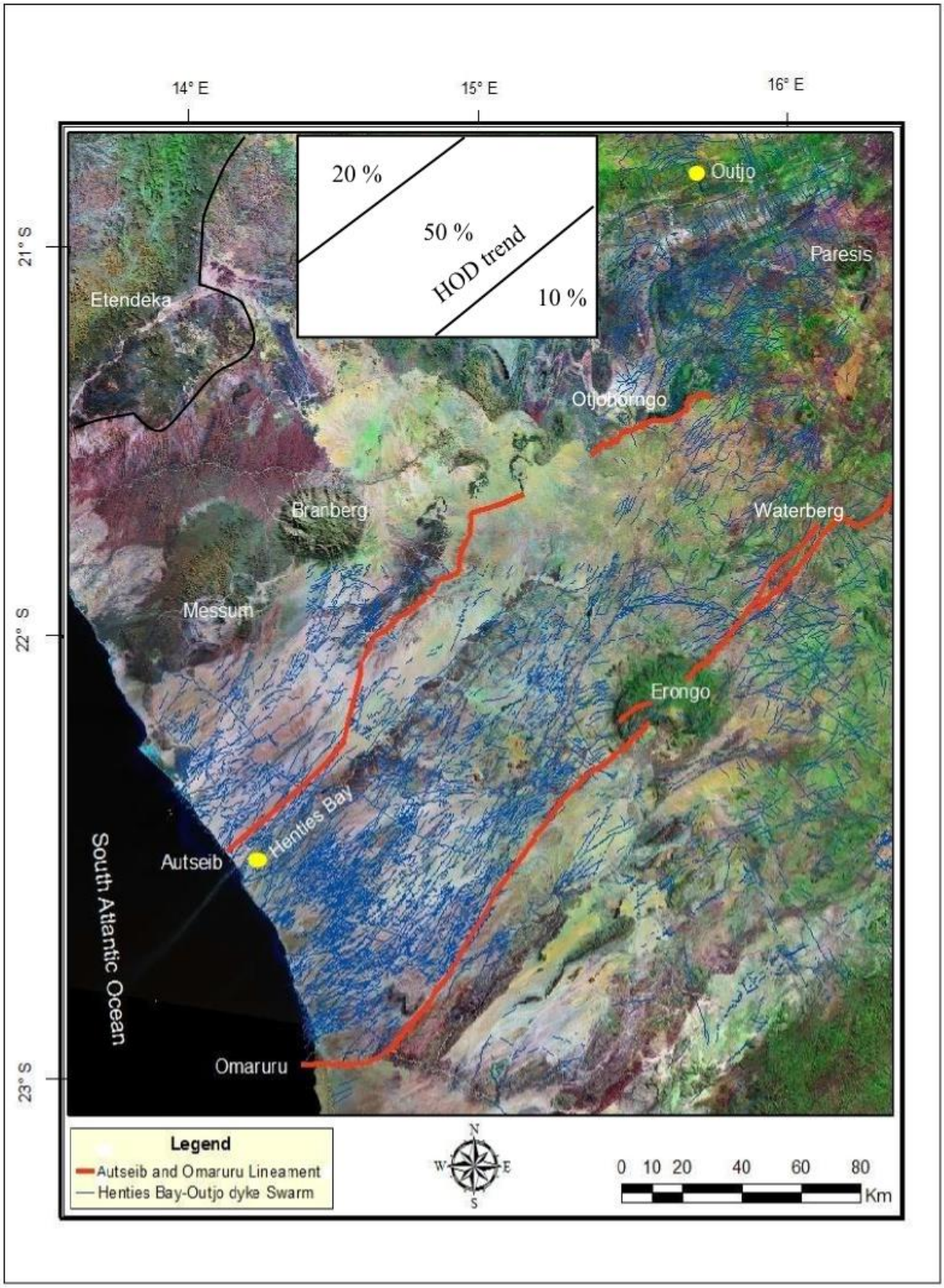

Figure 2.8: Satellite imagery showing dyke trends (blue) striking NE-SW between the Erongo, Messum, Omaruru and Autseib lineaments (red), extending inland from the coast. The percentage of dyke trends between the lineaments are shown in the inset (From: National Aeronautics and Space Administration (NASA), 2005).

2.5 Geological settings and structures of the GVS

The Golden Valley Sill (GVS) are situated in the Tarkastad area about 65 km west of Queenstown within the Eastern Cape Province, South Africa (Johnson *et al*., 1996).

The Karoo Supergroup in southern Africa occurs extensively in the main Karoo basin, Kalahari basin and associated basins in South Africa, Botswana, Mozambique, Zimbabwe, and Namibia (Mountain, 1968; Catuneanu *et al*., 2005). The Karoo Supergroup is economically significant since it hosts shale gas, uranium and almost all coal deposits of southern Africa (Mason and Christie, 1986; Segwade, 2008). It is also considered scientifically significant because it is composed of the non-marine fauna and flora that dated to Permian-Triassic times and tectonic events related to the formation of continental flood basalt (Johnson *et al*., 1996; Segwade, 2008; Bordy and Prevec, 2008). The Karoo Supergroup consists of the Dwyka, Ecca, Beaufort, Stormberg Groups and Drakensberg volcanics as shown in Figure 2.9 (Walker and Poldervaart, 1949; Botha *et al*., 1998; Polteau *et al*., 2008; Flint *et al*., 2011).

The sills occur as hundreds of saucer-shaped intrusions, amongst which is the GVS. They are of interest because they show excellent finger-like intrusion shape that may indicate the mechanism of emplacement (Schofield *et al*., 2010). Karoo linear dykes are also common, but lesser numbers compared to the sills and ring dykes (Rubin, 1995; Botha *et al*., 1998).

The studied dolerite sills are intruding the Burgersfort Formation (Figure 2.9). The GVS intruded the flat-lying and undeformed Triassic sediments of the upper Permian-lower Triassic Beaufort Group (Polteau *et al*., 2008; Schofield *et al*., 2010). The columnar joints are well exposed along erosional scarps and details are given in chapter 4, section 4.2. The sizes of the columnar joints occurs due to cooling and uplift (Toramaru and Matsumoto, 2004; Polteau *et al*., 2008; Fernandez *et al*., 2008).

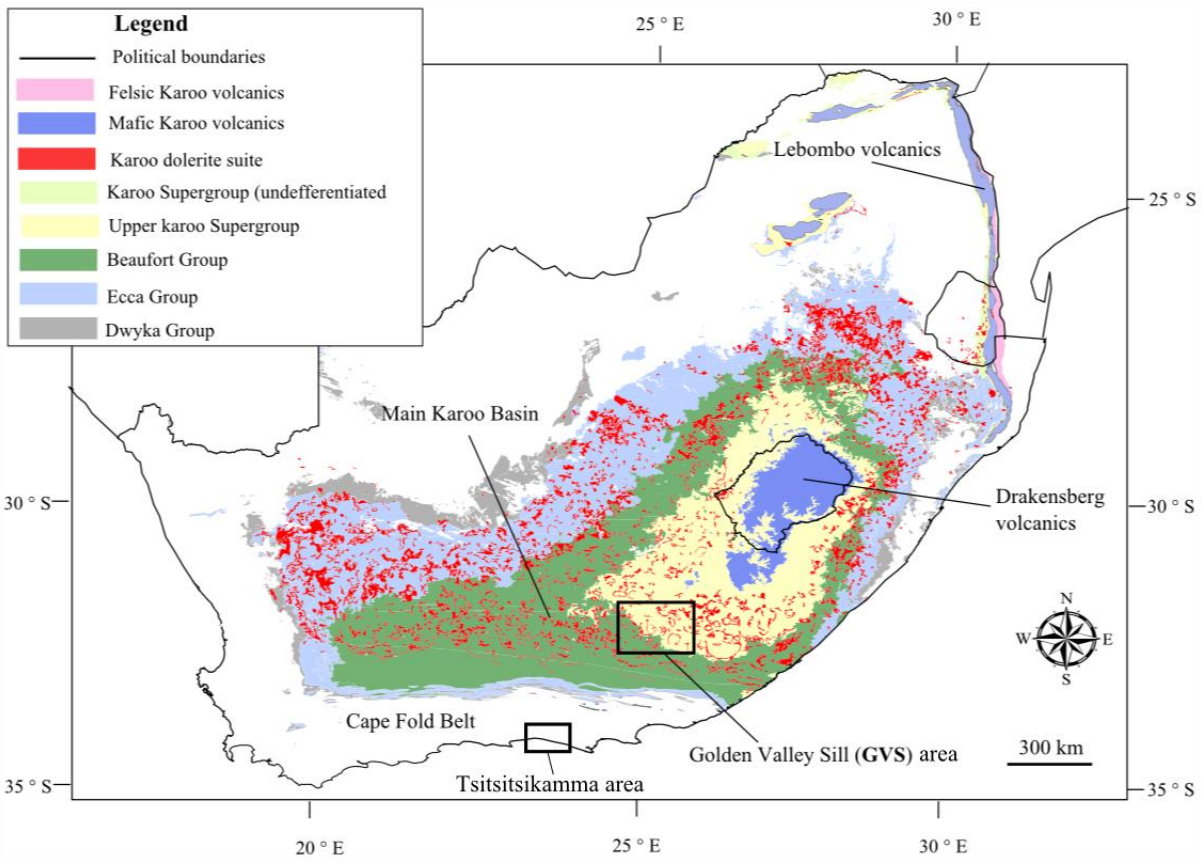

Figure 2.9: Simplified geological map of the South Africa showing the Golden Valley Sills (GVS) area (Modified from: Decker *et al.*, 2013).

2.6 Geological settings and structures of the TMG, Tsitsikamma

Joint systems of the TMG, Tsitsikamma area

The Tsitsikamma area is located 200 km west of Port Elizabeth and about 40 km from Plettenberg Bay, South Africa (Figure 2.9). The Cape Fold Belt was formed during the Permo-Triassic transition ca. 248-258 Ma (Gentle *et al.*, 1978; Hälbich *et al.*, 1983; Bordy *et al.*, 2005). Joints were mapped along the Bobbejaans and Groot River valleys in the Tsitsikamma area (Figure 2.10). It is suggested that the eastern margins of the Cape Fold Belt may have been uplifted after Gondwana break-up and structures such as joints may have resulted from Cretaceous-Tertiary uplift (Van Zyl, 1982; Compton, 2004).

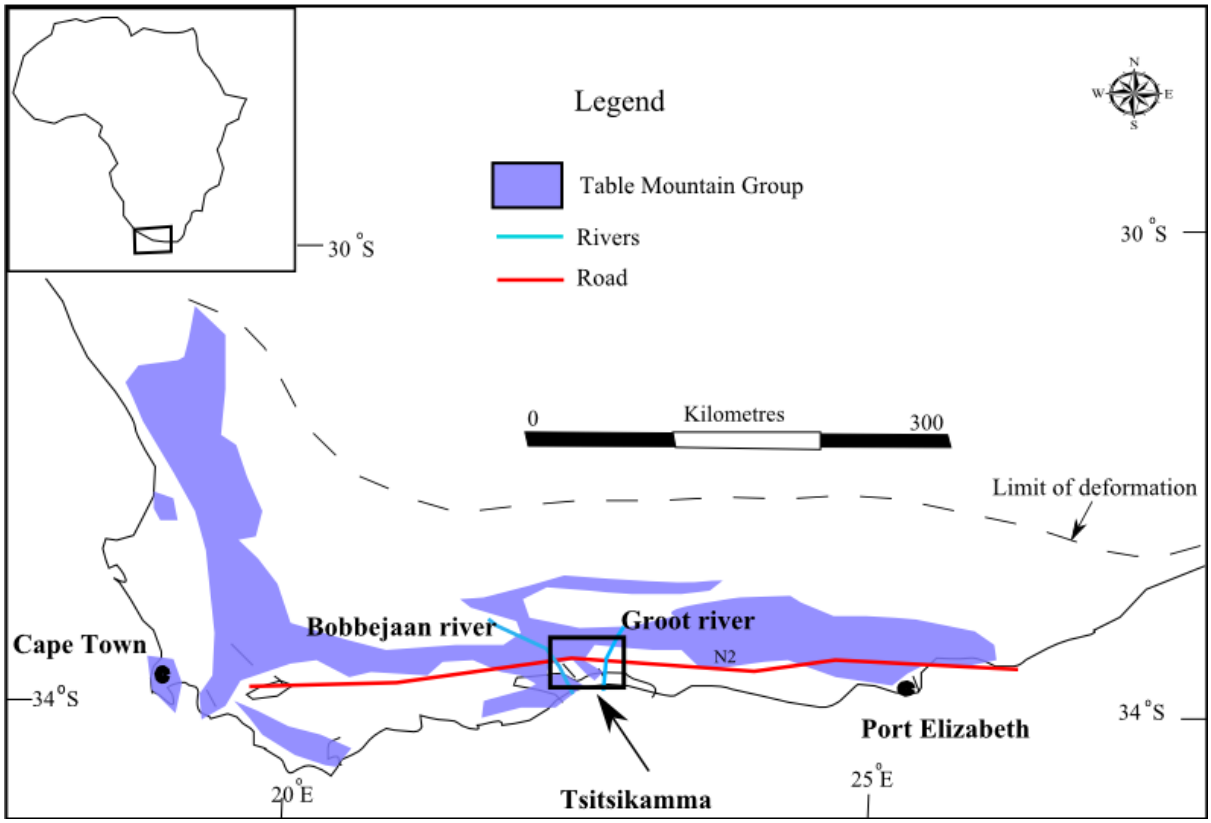

Figure 2.10: Geological map of the Cape Fold Belt (CFB) showing the location of the Tsitsikamma area shown in the black inset box (TMG) (Modified after: Bachtadse *et al*., 1987).

Structures of the TMG

The Cape Supergroup is composed of the Table Mountain Group (TMG) at its base Cape Supergroup, overlain by the Witteberg Group and followed by the Bokkeveld Group (Thamm and Johnson, 2006; Fourie *et al*., 2008). The TMG further comprises the Graafwater, Peninsula and Pakhuis Formations, where Graafwater consists of sandstones and mudstones, Peninsula consists of pale to white thick beds of quartzite that is believed to have stabilised the Table Mountain to resist deformations and denudation. The Pakhuis Formation is at the top of the TMG and comprises glacial sandstones pebbles and sandy diamictite (University of Cape Town, 2012; Scharf, 2012).

The Bobbejaan River in the Tsitsikamma area cuts the middle succession of the tightly folded quartzites of the TMG (see Figure 2.11). The Tsitsikamma comprise dominants quartzites of the Table Mountain Group which is one of the common structures in Tsitsikamma area. The most common structures in the Tsitsikamma area include folds, faults, lineaments, and joints (Johnston, 2000; Newton *et al*., 2006).

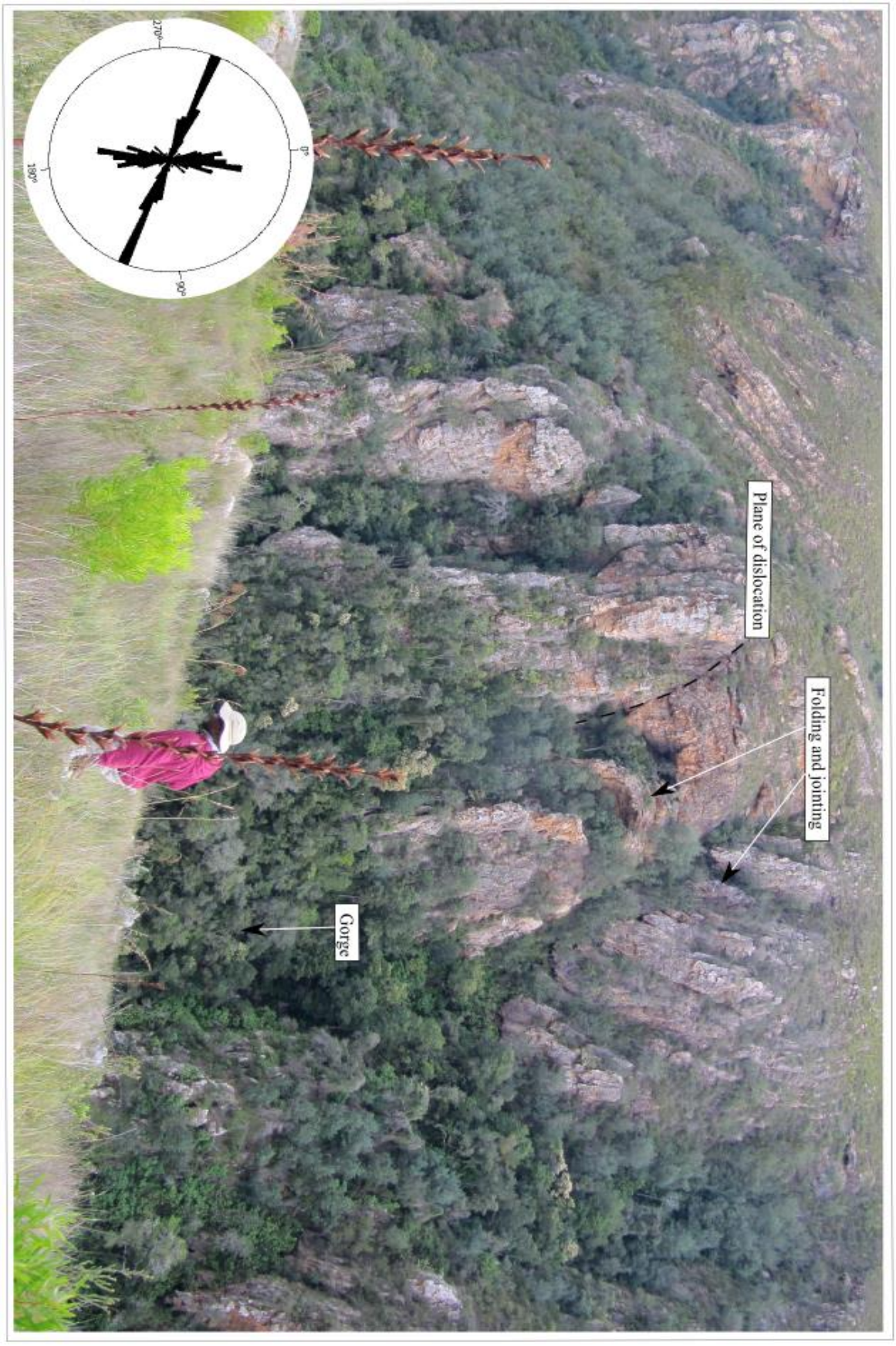

Figure 2.11: Photo showing folds, joints plotted on a rose diagram in TMG quartzite in a gorge at by Bobbejaans River, in the Tsitsikamma area (Thomas Muedi as a scale).

Chapter 3. Data sources, Methods and Analysis

Numerous authors have mapped dykes in southern Africa, including the HOD of Namibia.

(a) Mubu (1995) mapped dykes of southern Africa, including those of the HOD. Dykes were mapped using aeromagnetic data from the African Magnetic Mapping Project (AMMP) to visualize dyke trends related to Gondwana geology using GIS at a 1:1 000 000 scale. Mubu (1995) digitised dykes using data between 1976 and 1990, geological and geophysical maps including geological surveys from South Africa, Zimbabwe, Mozambique, Botswana and Namibian geological surveys. Mubu, (1995) found that Precambrian and Phanerozoic dykes have orientation relationships with major faults and used this to interpret the pre-breakup of Gondwana between the South America-Africa and Antarctica.

(b) Lord *et al*., (1996) used Multispectral Scanner (MSS) imagery data to map dykes in southern Africa. They recognised dykes as dark positive lineaments against a paler sandy background. They concluded that dykes were associated with the initial continental rifting processes, and that they were emplaced prior to rifting of Western Gondwana (e.g. separation of Africa and South America).

(c) Reeves (2000) geophysically compiled and mapped 14, 000 dykes of southern Africa and determine their geometry in relations to the plate movements during the break-up, and he also used GIS for the compilation and analyses of the data. Reeves (2000) results suggest that dyke injection can be a passive reaction along fracture line of brittle crust rather than upwelling magma.

(d) (Hahne, 2004) mapped dykes, lineaments and faults in Namibia, with emphasis on the HOD. Satellite and GIS software were used to acquire data for dykes in the HOD. It was deduced from this data that as intrusion of magma increases and the extensional rate of the crust increases as magma solidifies within the cracks.

All these authors have commonly used GIS techniques to capture data and create databases, but none included detailed geometrical analyses of dyke emplacement patterns. In this study, GIS is used to explore the geometry and emplacement history of dykes within the HOD.

3.1. Methods

Mapping and characterization of the dykes in the HOD was done using MapInfo applying to information from previous studies. The HOD database was designed in an appropriate GIS compatible format that can be manipulated in the GIS environment. The GIS database includes high-resolution aeromagnetic maps, satellite images and orthophotos to enhance the visibility of the dykes. Aeromagnetic data (maps) were used to visualize buried dykes

covered by vegetation. GIS and Gplates animation were used thereafter to improve understanding of geological processes related to Gondwana break-up.

3.2 Data Sources

(a) Aeromagnetic Data: the aeromagnetic data of Namibia (Geological Survey of Namibia, 1997) in this research was used to visualise buried dykes, particularly in cases where overlying vegetation cover and soil obscure the orientation of the dykes. The aeromagnetic data of Namibia offer comprehensive coverage of the HOD (Corner, 2002).

(b) Orthophotos and Google Earth Data: Orthophotos are aerial photographs that are geometrically corrected to a uniform scale. The orthophotos at a scale of 1:50 000 and Google Earth were used. Orthophotos indicate the precise locations of the dykes and helps to visualize geometric details of the dykes. Orthophotos have an image resolution >2.5m that increased the accuracy of mapping the length and thickness of the dykes.

3.3 Mapping and plate reconstruction

Gplates (www.gplates.org.), along with ArcGIS software, was used for plate reconstruction. Mapping of the dykes was carried out by remote sensing using digital aerial and satellite images. ArcGIS was used to manipulate the data and produce maps. Plate reconstruction refers to the digital rotation of tectonic plate together with their Cretaceous dyke swarms, to recreate the plate positions as they were before Gondwana break-up.

3.3.1 ArcGIS desktop for data preparation

GIS software was used for the visualization of images and vector data as well as the creation of shapefiles. The use of remote sensing data together with GIS software is one of the most effective techniques for mapping dykes and other geological features. Data for the dykes were collected and analysed within GIS software. GIS data could then be linked to software such as ImageJ and Gplates in the form of exported TIFF, PNG or JPEG files.

(a) Arc Desktop: desktop is composed of ArcMap, ArcCatalog (Figure 3.1) and ArcTools: **ArcMap** is the main application in the ArcGIS desktop package. ArcMap is used for all map based tasks including editing, mapping with the integration of the attribute tables. It can create digital maps within a data frame that contains elements such as a legend, scale bar and compass orientation. ArcMap thus assists in creating quality digital maps, and in many map based tasks.

(b) **ArcTools**: ArcTools provides a means of manipulating GIS data for conversion, analysis and processing.

(c) **ArcCatalog**: ArcCatalog helps to create layers and manage all the GIS data. When ArcCatalog is opened it displays a catalogue tree. One can add and remove folders from the

catalogue tree as required. A screenshot (see Figure 3.1) shows content, metadata, and preview. **Content** shows all the data captured. **Metadata** provides quality, creation and spatial information that make the data easy to read and, **Preview** shows data in many formats such as text file and spatial record (Figure 3.1).

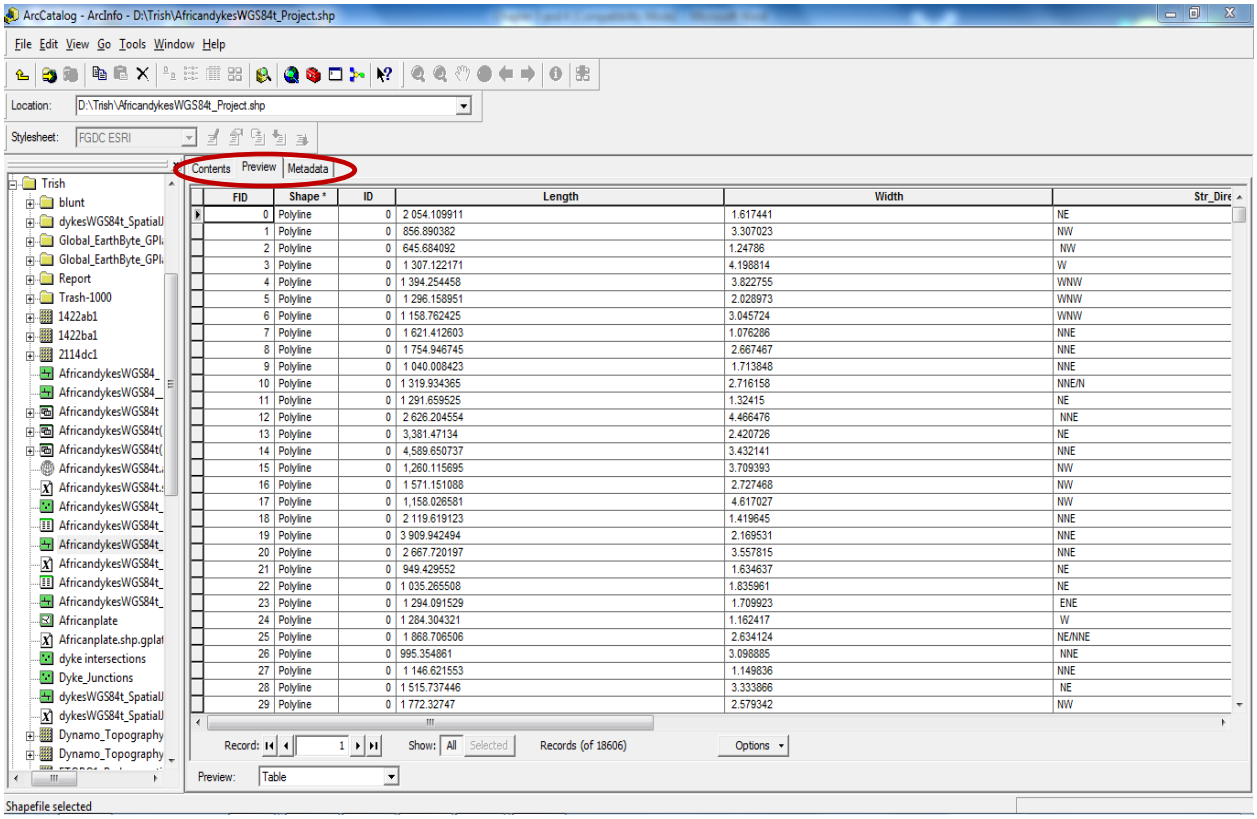

Figure 3.1: Example: ArcCatalog screenshot showing dyke length, width and orientations.

3.3.2 Data preparation in ArcGIS for Gplates use

Data had to be prepared in ArcGIS for viewing in Gplates (www.gplates.org). Gplates shapefiles can be exported to any GIS platform. Shapefiles of dyke swarms and plates were split, merged and spatially joined before being loaded into Gplates. It is necessary to combine a plate's ID in the same shapefiles. If dykes and plates are not linked they cannot be reconstructed and rotated.

The procedures to split shapefiles are as follows:

1. **SPLIT**: Arctools—analysis tools—extract—split (Input features>dyke swarms; split features> plates; and split field>Name).
2. **MERGE**: Arctools—Data Management tools—general—merge (contains input dataset that were split and need to be merged. Dataset created in shapefiles such as point, polygon and polyline).

3. **JOIN**: Arctools—analysis tools—overlay—spatial join (target features>dyke swarms; join plates in attributed table with different plate ID's>join operation> join one to one (see Figure 3.2).

The newly prepared Shape file can now be imported directly in Gplates and reconstructed to the desired position during Gondwana break-up.

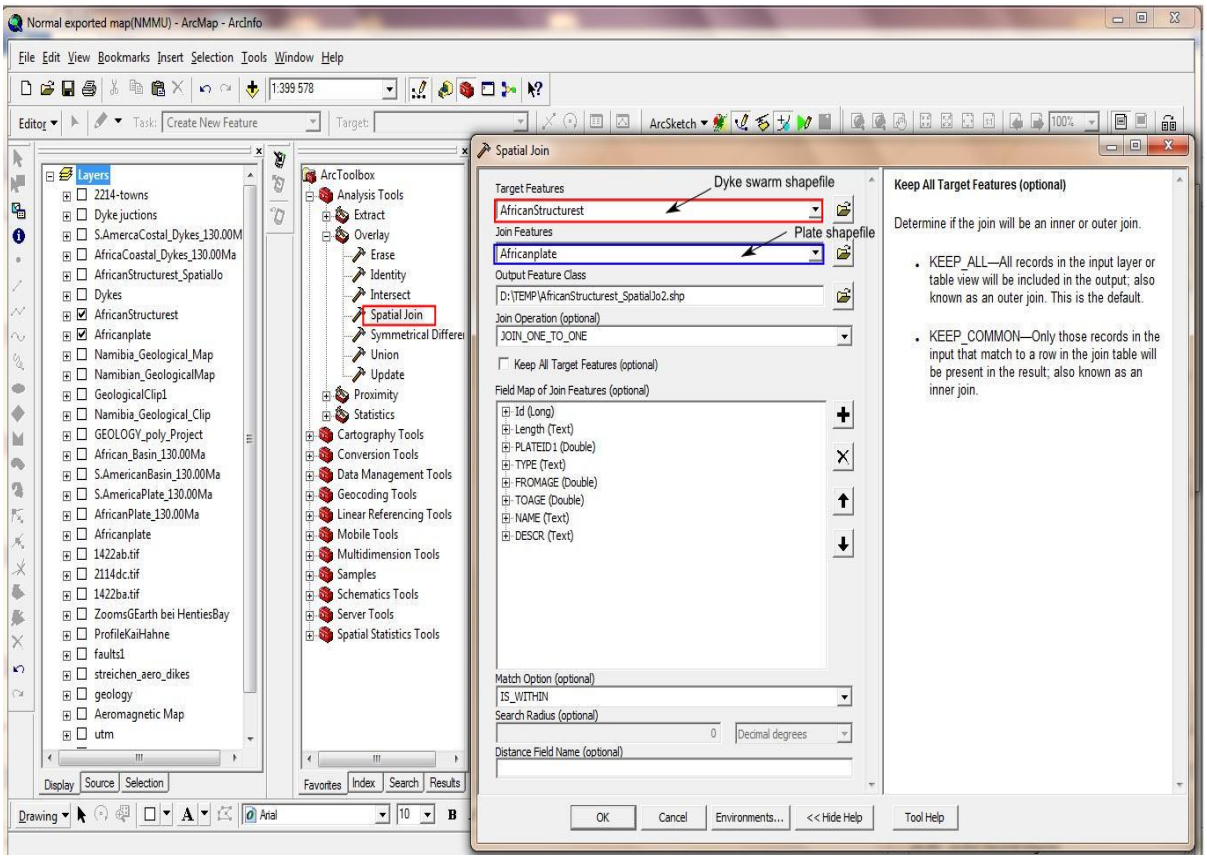

Figure 3.2: Example of ArcMap screenshot showing data; red rectangle = dyke swarm shape file and blue rectangle = African plate shape file being prepared for use in Gplates (Modified from: Dangermond and Dangermond, 1969).

3.4 Gplates for Gondwana plate reconstruction

In this research I used Gplates software (www.gplates.org) for plate reconstruction, the software that links my GIS data with a geodynamic model of Gondwana break-up. Gplates is desktop software for the interactive visualisation of plate-tectonics. It offers a good combination of interactive plate-tectonic reconstructions, geographic information system (GIS) functionality and raster data visualisation. It also enables both the visualisation and the manipulation of plate-tectonic reconstructions and associated data through geological time (Qin *et al.*, 2012).

The static polygon, ridge, dyke swarm and plate shapefiles (as described above), were loaded in the Gplates platform (Gurnis *et al.*,2012; Qin *et al.*, 2012). A 'Dyke Swarm Shape file' is linked (connected using the Plate ID) with the 'Static polygon' shape file of Gplates that is

connected with a rotation file (see Figure 3.3.). The same procedure is also possible with a raster file (e.g. jpeg). As plates are rotated all data that are spatially joined to the plates (e.g. faults and dykes) will likewise be rotated. The procedure for plate reconstruction in Gplates is as follows:

Reconstruction—export (export 130 Ma time instant)—add export type—choose data type to export (reconstructed geometry)—output file format and export option (shapefiles)—file option (export to a single file)—geometry shapefiles and export snapshots.

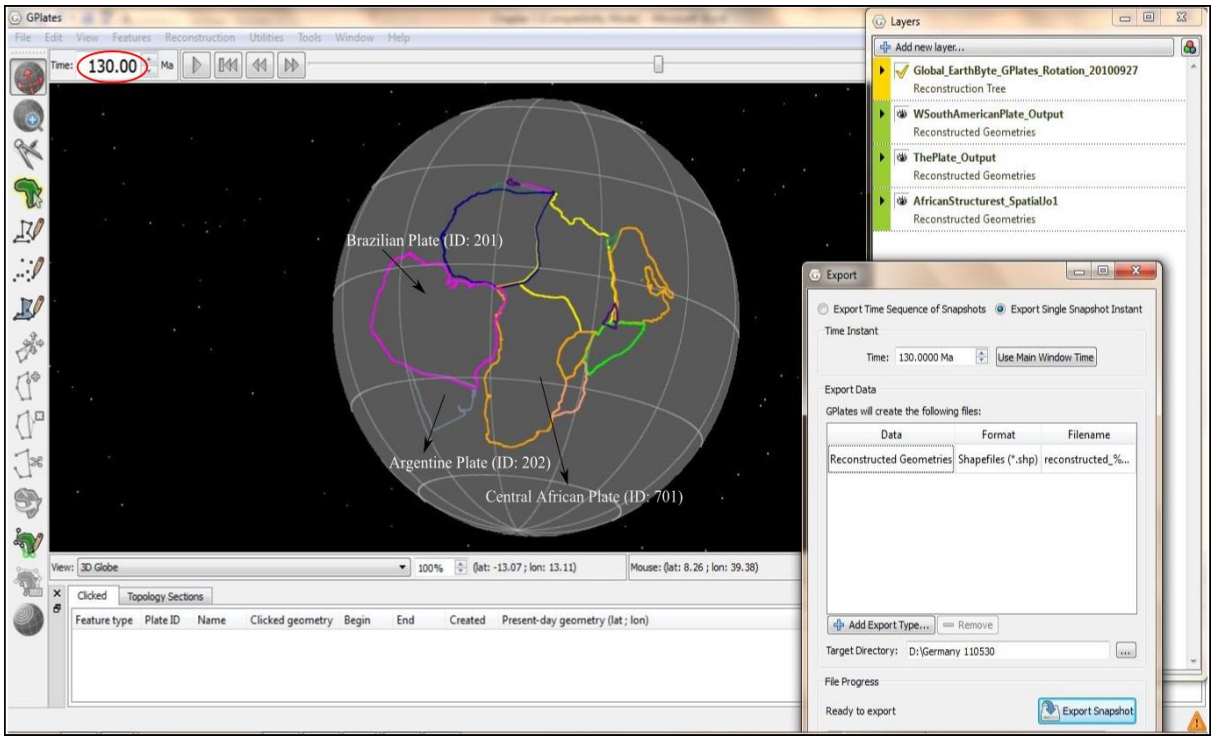

Figure 3.3: Main window of Gplates showing reconstruction of Africa and South America during Gondwana break-up at 130 Ma (Modified from: Müller *et al*., 2007).

3.5 Identifying the HOD dykes using Aeromagnetic data

Determining the HOD by aeromagnetic data is hindered by the occurrence of linear structures on the ground related to lava flows or sills, which have similar magmatic characteristics as the dykes. Integration of aeromagnetic maps with remotely sensed imagery provides high resolution data and an opportunity to visualise deep seated structures (Lord *et al*., 1996; Anderson and Nash, 1997) and the database I created and used in this research allows for better understanding of the dykes elongations and the lateral extent of crustal extension in the study area (see Figure 3.4).

Aeromagnetic and satellite images were used to map the dykes in order to interpret their geometry and distributions. Orthophotos, when integrated with aeromagnetic images and

Google Earth maps, were used to map the lateral extent of dykes, particularly in the coastal region.

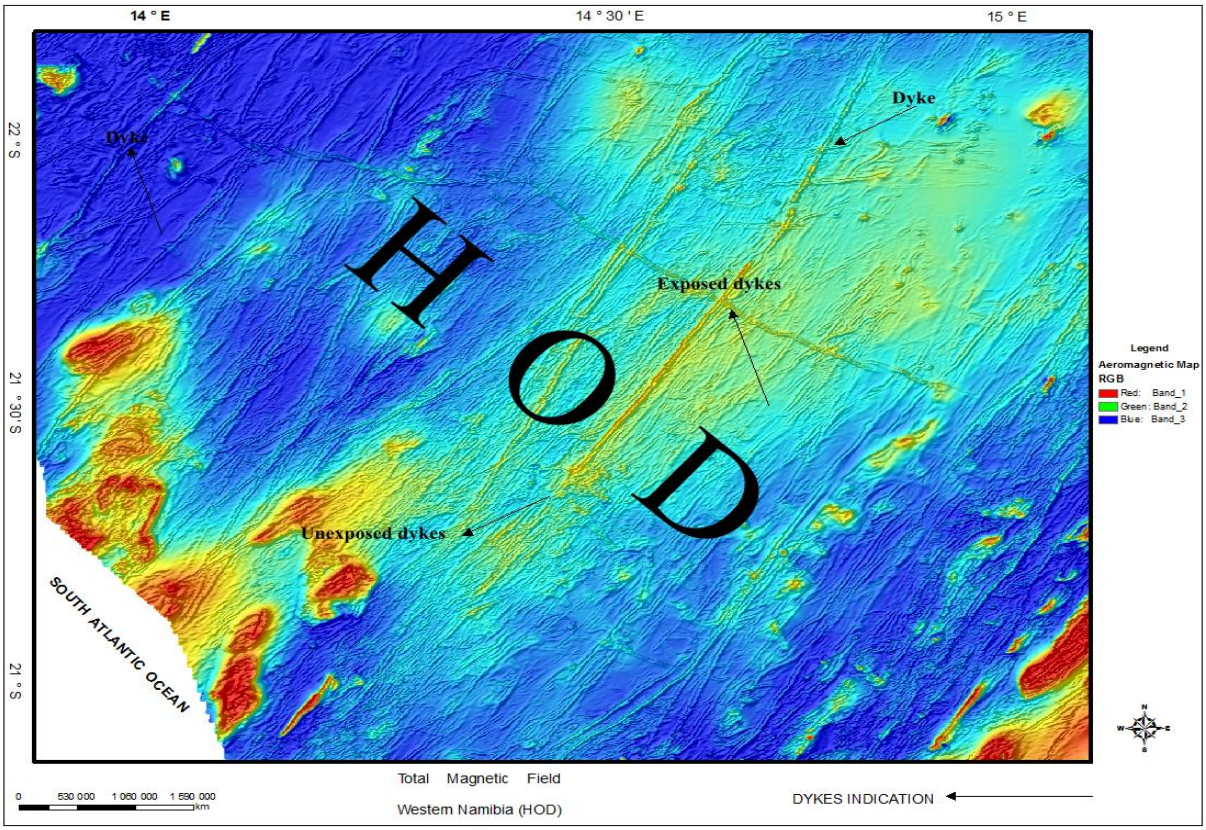

Figure 3.4: Aeromagnetic map indicating the distribution of the dykes, as well as dyke orientations, within the HOD (Modified after: Hahne, 2004).

3.6. Fractal analysis on macro to micro-scale dykes

Fractal geometry is a branch of mathematics that can identify and quantify how the geometry of patterns vary from one scale to another and test if they are scale invariant e.g. similar; (Mandelbrot, 1967). Fractal analysis is a powerful tool that may be used eventually to help predict future events in geosciences such as earthquakes (Barton and La Ponte, 1995; Schewe and Riordon, 2002; Jiangdong and Guoqing, 2011; Park *et al.*, 2010). The fractal dimension is the only statistical distribution that is scale invariant (Mandelbrot, 1978; Mandelbrot, 1979; Hirata, 1989; Dunlop, 2006). The fractal dimension (D_f) is derived as the slope of the straight line on a log-log plot of dykes within specified box sizes (see Figure 3.5). Mandelbrot was the first to introduce the concept of fractals (Mandelbrot, 1967), and since then fractals have been used in a variety of fields of Earth sciences, engineering and biology:

E.g. Fractal dimensions = $\frac{\text{Log (number of self-similar pieces)}}{\text{Log (number of magnification factors)}}$

$\frac{\text{Log N}^1}{\text{Log N}}$

$1 * \frac{\text{Log N}}{\text{Log N}}$

$D_f = 1$ Equation……....1

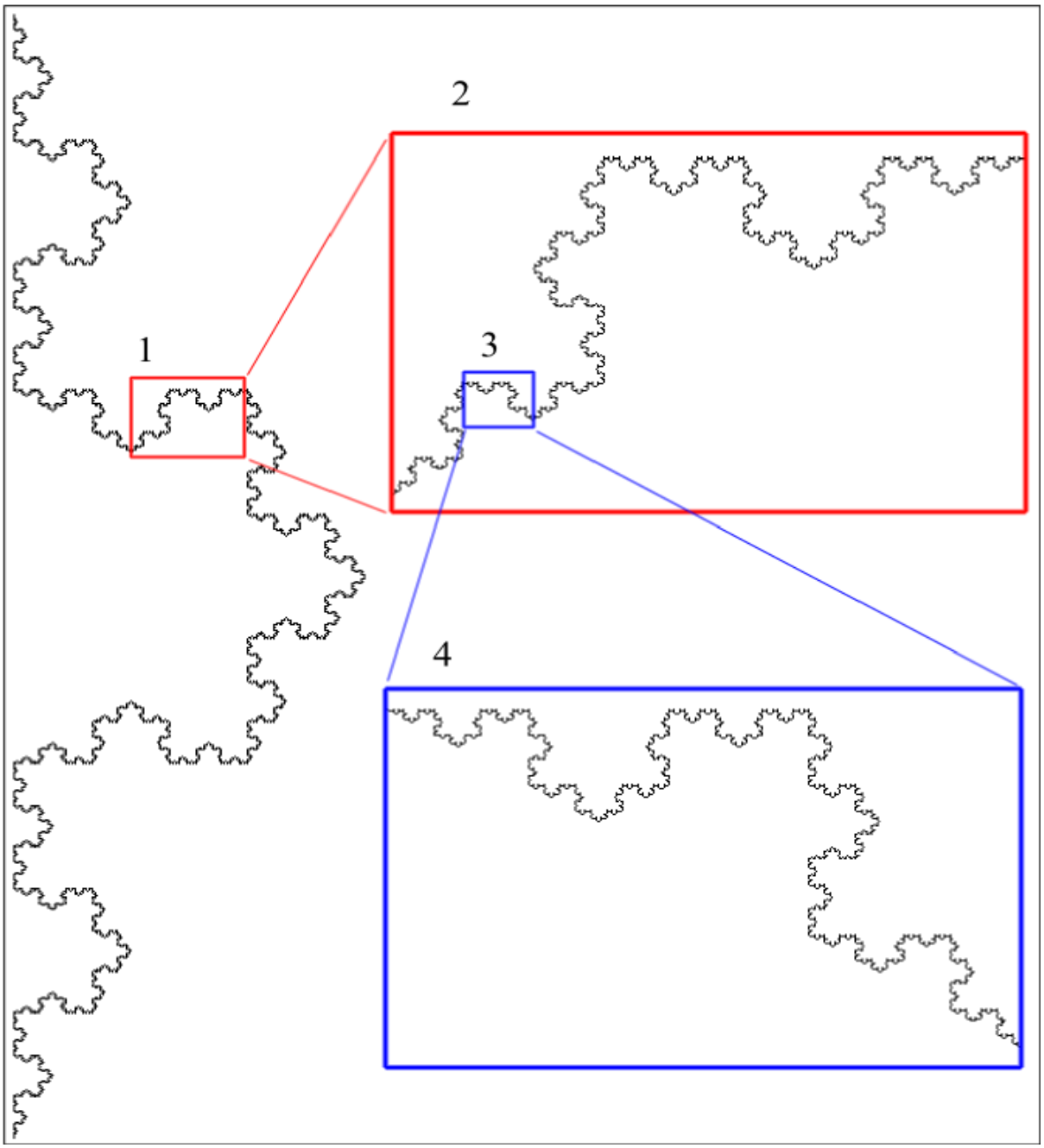

Figure 3.5: The Koch snowflakes showing the self-similarity patterns at four different scales (Mandelbrot, 1983).

In geosciences, fractals can be used to analyse the mechanical processes of fracturing. The observed self-similarities indicate that the mechanisms involved are scale independent (Turcotte, 1989; Charkaluk *et al.*, 1998; Stankiewicz, 2004). The rock structures are relative to small-scale rock structures that are contained within large-scale rock structures. Even seemingly large structures may be part of even larger structures (James Madison University, 2000). For dykes and joints, for example, self-similarity across various scales indicates that the geological structures likely formed by processes that took place under the same stress regime (Zhou *et al.*, 2003; Kruhl, 2013). A box counting method is often used for fractal analysis as described below.

3.6.1 Box counting method to determine fractal geometry of dykes and joints

The fractal geometry of dykes and joints is quantified using a box counting method freeware program (Abramoff *et al*., 2004). The box counting method within ImageJ was used for the image analysis and processing (Barnett, 2004; Rasband and Ferreira, 2010). The box counting method is a common technique used to analyse fractures on images to test for fractal patterns (Dathe and Thullner, 2005; Mandal *et al*., 2006). The box counting depends on the image resolution, as precision of the method increases with an increase in image resolution (Bėrubė and Jėbrak, 1999).

The box counting method of joints and dykes provides information about the general fracture patterns (Volland and Kruhl, 2004; Barnett, 2004). It works by covering joints and dykes with boxes of specified size, and then counting how many boxes are needed to cover the geometric patterns. The number of box length (*r*) in the box counting method covers and count all areas that contains fractures and the numbers of boxes (*N*) but empty boxes are excluded from the analyses (Melniciuc-Puica *et al*., 2006). This method has been widely used to determine many natural phenomena such as fractures to test stress regimes and of natural fractured reservoirs and to predict earthquakes of specific sizes (Odling *et al*., 1999; Babadagli, 2001).

$$N = \frac{C}{R^{D}} \qquad \text{Equation}\ldots\ldots\ldots\ldots\ldots\ldots\ 2$$

Where D is the fractal dimension, N, is number of full boxes, C is constant and R is the size of the box (Stankiewicz, 2004). The box counting method is also called box dimension (D_B). The box counting technique is simple and thus can easily be automated and used to compare different fracture pattern results. Fracture networks with similar fractal dimension may look very different to each other and they are highly controlled by change of scale (Blenkinsop, 1994; Blenkinsop, 1999). A fractal dimension does not define a geometrical pattern nor geometrical attributes such as density, orientation, length, width and roughness of fracture surfaces (Bonnet *et al.*, 2001). The box counting method is suitable to provide a quantitative measure of the geometry, length and spatial distribution of fracture patterns in order of multiple magnifications (Falconer, 1997).

In this study the box counting method was applied to images within the ImageJ software (Version 1.47d) to test fractal geometry of dykes. It was applied across a wide range of scales from satellite imagery to photographs from thin sections, covering a range of 9 scales of magnitudes (e.g. 100 km to 1 mm). The fractal dimension (D_f) is expected to be within the range of >1 or <2. If at dimensions >2 analysis becomes more complex as found by many workers (Hirata, 1989; Bonnet *et al*., 2001; Volland and Kruhl, 2004; Isabelle *et al*., 2010).

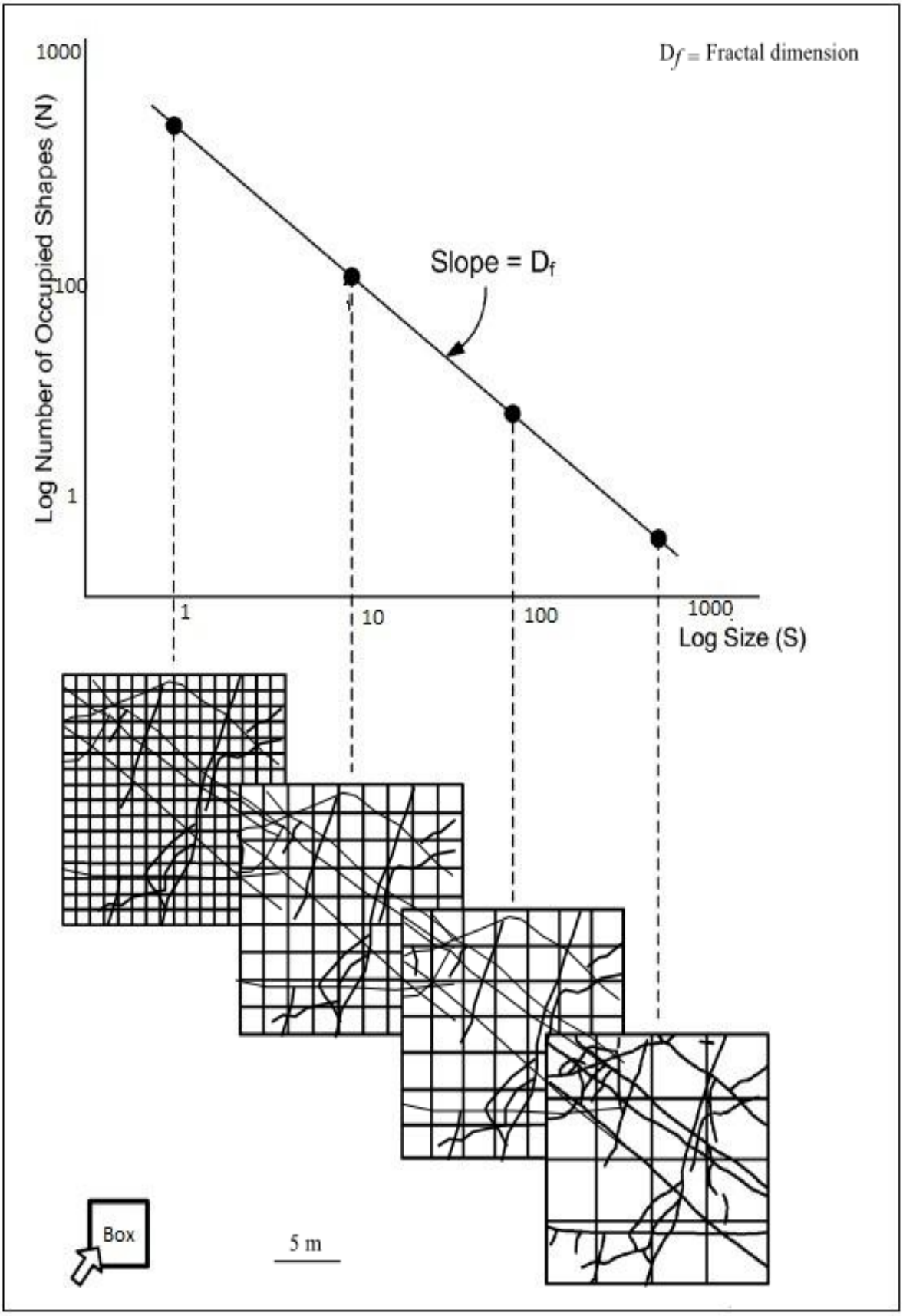

Figure 3.6: Application of the box counting method showing grid cell sizes that are superimposed onto fractures. The slope corresponds to the fractal dimension D_f (Modified after: Peternell, 2002).

3.6.2 Image analysis of fractal geometry at petrographic scale

Images of 3 different rock samples were chosen for investigations using the microscopic scales: one from the dyke fractures (HOD), one from quartzite fractures (TMG) and one sill fracture (GVS). The original RBG images taken from the thin sections were converted to 8 bit grayscale images using ImageJ, so that it could be opened in black and white and easily analysed in the ImageJ platform. In order to avoid confusing rock surface fractures and grain boundaries during image processing, specific measurements are set to analyse fractures and the threshold is also adjusted for the cracks to stand out. First of all I convert the RBG image to grayscale: Open ImageJ-File-Open and Load image-Image-Type-8bit-click Grayscale to convert and Save as Jpeg.

The grayscale image was loaded in the ImageJ platform: Open ImageJ-Load image-Image-Adjust-Threshold and Apply. The features on the image appear red and after conversion appear black and white. Analyses-Tools-Fractal box count and results show up in a separate window.

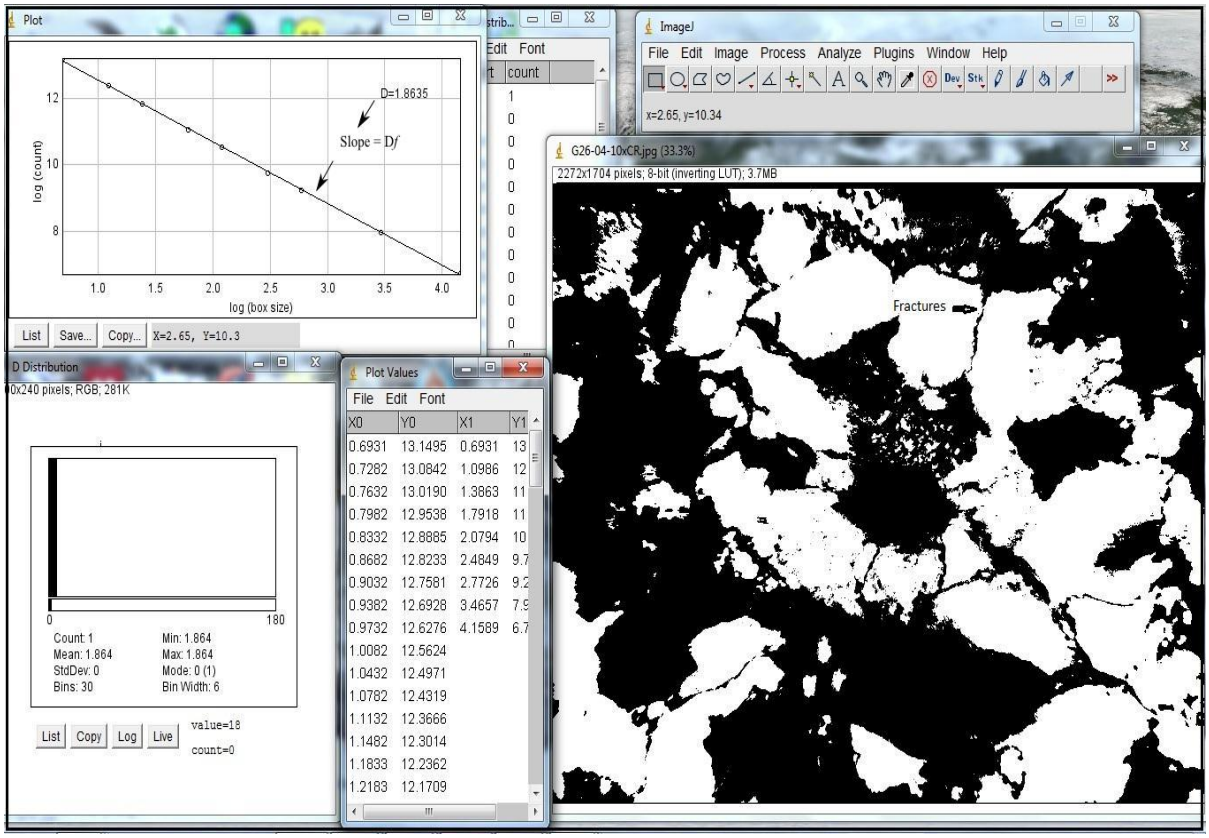

Figure 3.7: Screenshot example showing the image analysis and fractal box count and fractal dimensions (D_f).

3.7 Determining the thicknesses of dykes

Python software was used to determine the length and width of the mapped HOD dykes represented on XY graph. Python is a programming language that is used for processing scientific data and images (www.python.org). Python was used to indicate the maximum length and width of the HOD dykes. The data were imported from the source to python and the script was written to calculate the average of dyke length and width in the HOD. The procedure applied is shown in box 1 below,

```
Import numpy, pylab - Wavelength=numpy.arrange (350, 2500, 1)
 From  numpy import * Import pylab def kde (z, w, xv):
 return (sum (exp (0.5*((z - xv)/w) **2)/sqrt (2*pi*w**2)))
 d=loadtxt ("D:   \Finaletextdata.txt", usecols= (1,))
     w=0.05
     bloeh= []
    doeh= []

 For x in linspace (min (d) - w, max (d) +w, 100):
              phi=x
              omega=kde(x, w, d)
              bloeh.append (phi)
           doeh. append (omega)
 pylab.plot (bloeh, doeh)
 pylab.xlim (0, 1)
 pylab.show
```

Figure 3.8: Box 1, represents the written script in python software that determines the width and length of dykes (Figure 4.5).

3.7.1 Coefficient variation (CV) and measurements of dyke spacing

The coefficient of variation of dyke-spacing (CV): CV = Std (S)/S^{-1} was examined. Where S^{-1} is the standard deviation of dyke intervals, and S is the mean spacing between the dykes. If CV = 0 the fractures are found to be perfectly evenly spaced whilst CV = 1 indicates that fractures are random spaced. At CV<1, fractures display some regularities and are anti-clustered. If CV>1, the fractures are clustered.

A Microsoft© excel based macro, named Blocks (Hansen and Bollian, 2008), was used to measure the spacing of the dykes. This macro measures the average space between the dykes. This spacing can help calculate total crustal extension. Profiles were placed across the dykes to calculate the spacing between them. The data on dyke spacing was captured to a prepared

excel sheet. The excel sheet was prepared so that every next distance has to sum up until the end of the profile.

Data required:

- Distance between the dykes that cross the profile.
- Orientation of each dyke.

Data is imported in the excel sheet, the first column shows overall distance and second column shows distance between dykes. Blocks programme display the start button that is pressed to start processing data. Before pressing Start, the macro has to be modified to the actual column number. After pressing the start button, the spacing, dyke distribution and corrected spacing is automatically calculated.

3.7.2 Measurements of Joint in the field and dyke azimuth angles on imageJ software

The original TIFF-format map must first be converted to 8-bit grayscale image, in order to make dykes visible on the processed image. This is done using Corel photo paint. Open imageJ—adjust—threshold—dark background—apply. Analyse—analyses particles; analyse box and pixel size of 30-infinity was selected, in show ellipses. This analysis is done to determine the angles that describe the dyke orientations. Edit—Distribution box opens—angle is chosen in parameters— specifies bins 180° and ranges from 0°—180° and ok. These settings are selected to determine the distribution of the dominant dykes orientations in the study area between 0°—180°. The resulting data show angles plotted as a histogram and can be saved by clicking File —save.

Field clinometer*:* The data presented in Table Mountain Group section of this research was collected together with Roberto Almanza. Roberto used the identified joints system to analyse the geomorphological evolutions of the Bobbbejaan and Groot River Canyons (Almanza, 2012), while I focused on understanding the joint, fractal patterns.

A field clinometer performs basic tasks such as measuring orientations and angles**.** In the field, a compass was used to measure joint orientations and dip directions. Appropriate adjustments were made for magnetic declination. The purpose of accounting for magnetic declination when collecting field data is to know the trends of joints in relation to true north. Steps followed are as follows:

- Hold the compass level and steady, parallel to the joint trend, so that the needle swings freely in the azimuth directions.
- The features recorded with the compass were the azimuth and dip angles of the joints.

Chapter 4. Results of the HOD, GVS and TMG

4.1: Results of the Henties Bay-Outjo dyke swarms (HOD).

4.1.1 Geometries and cross-cutting relations of the HOD dykes

A total number of 399 dykes that cut across each other were measured, analysed and compared. There are 136 NE-SW striking dykes that dominate the NW-SE trending dykes of 101 (see Figure 4.1). About 32% of 399 dykes trend NE-SW and 26% dykes trends NW-SE. The result of the interpretation of the cross-cutting relationship shows that the dominant NE-SW orientated dykes might have been intruded later than the NW-SE HOD dykes but both occurred in Early Cretaceous time (Figure 4.1). The change of directions within the HOD dykes is not common.

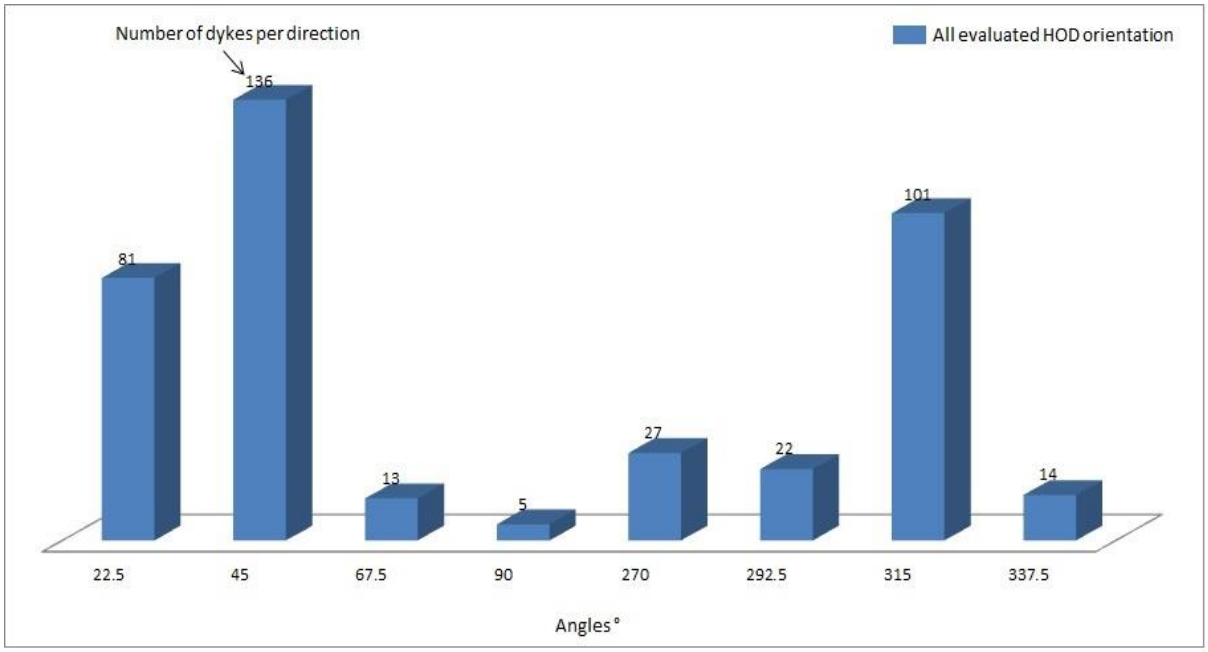

Figure 4.1: Histogram showing orientations and cross-cutting relationships of the HOD dykes. The dykes trend NE-SW (45°) interact with the NW-SE (315°) coast-parallel dykes.

Angle distribution of the HOD dykes

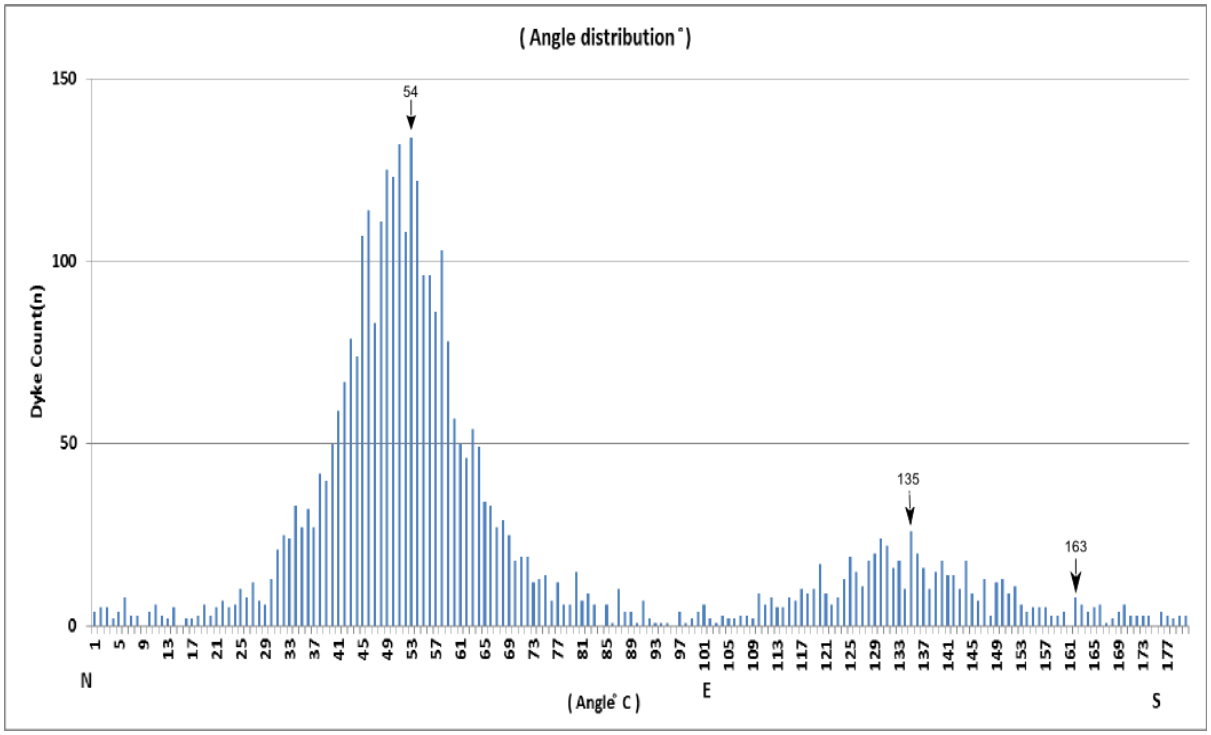

Figure 4.2: Diagram displaying the HOD dyke orientations and distributions related to Gondwana break-up.

ImageJ was used to calculate preferred orientation of the dykes. Mafic dykes in the study area tend to be clustered. A distribution of angles was measured and plotted. The greatest numbers of dykes have an angle of 54° (e.g. NE-SW trend). A second maximum occurs at 135°, indicating NW-SE trending dykes (Figure 4.2). I find that dykes trending 54° were dominant than those trending 135°. In decreasing order, the most common mafic dyke trends are 54°, 135° and 163° and the other angles are less dominant (Figure 4.2).

4.1.2 Crustal extensions and coefficient variation of the HOD dykes

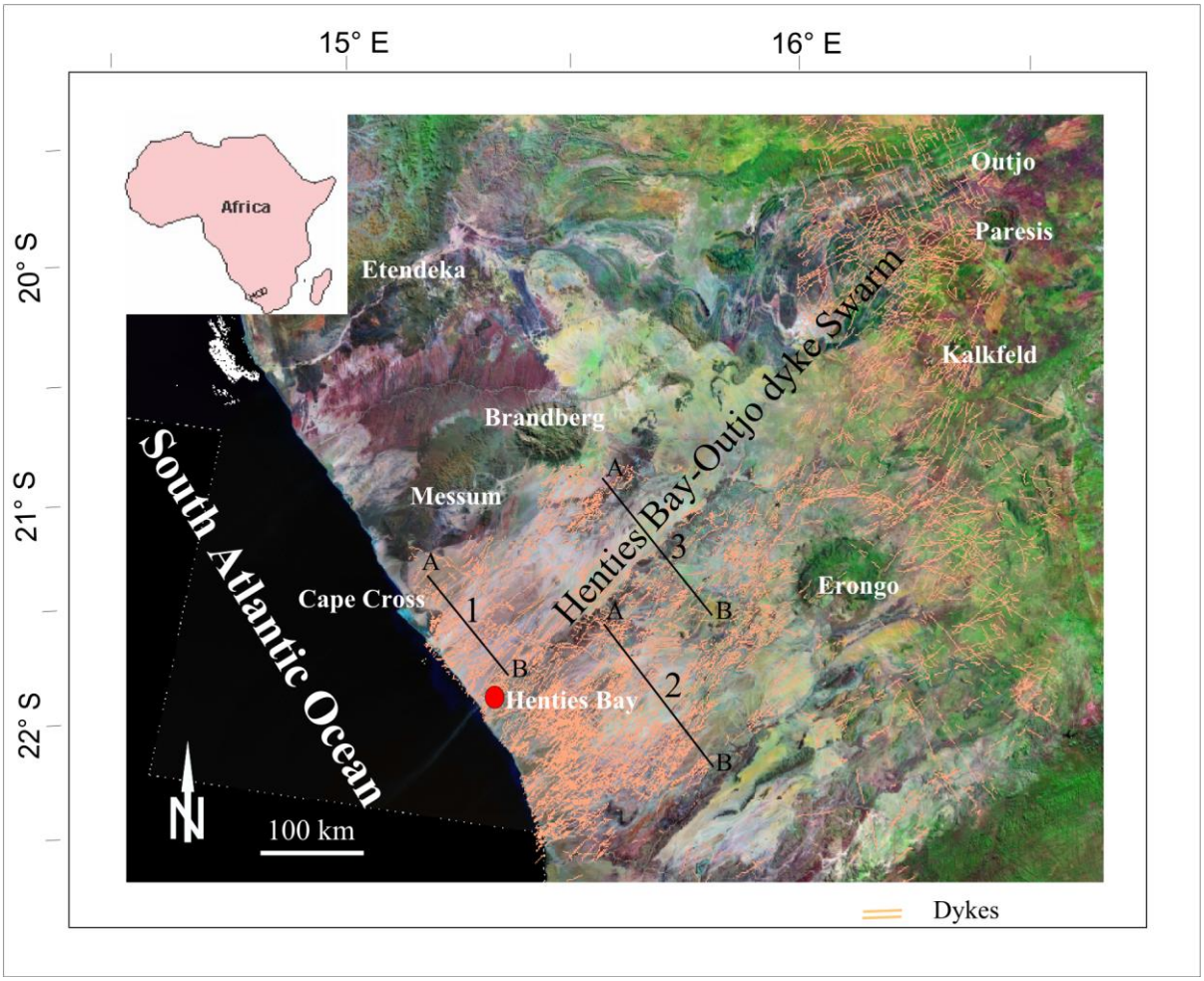

Figure 4.3: Satellite image displaying the mapped dykes of the HOD (Orange). Also shown are profiles 1-3 along which spacing variation were determined (Image: National Aeronautics and Space Administration (NASA), 2005).

Profiles were constructed perpendicular to dyke trends to calculate total crustal extension, and to determine dyke density distribution (see Figure 4.3). Only dykes within the profiles were considered. Profile 1 was placed between dyke 134 and 106, a distance of 12 km, profile 2 between dykes 564 and 14054 and profile 3 between dykes number 18566 and 18516 (see Table 4.1.). The distance across profile (2) is about 38 km and contains about 140 dykes perpendicular to the profile. Profile (3) is about 21 km long, perpendicular to dyke trends. Crustal extension was calculated within the HOD area and estimated to be approximately 3.87 %, and this result indicates that the HOD dyke intrusions have played a small role in the crustal extension of the area.

Table 4.1: Profiles perpendicular to dyke trends with their coordinates to determine crustal extension and dyke distributions.

Dyke Number	Profiles	GPS coordinates		Distance across profiles
134	1	14.409700	-22.225521	
106		14.344283	-22.150349	12 km
564	2	14.726778	-22.244064	
14054		14.500420	-22.076591	38 km
18566	3	14.733505	-21.962607	
18516		14.571301	-21.848605	21 km

Coefficient variation of dyke spacing

In our test case the dykes appear to be evenly clustered, as indicated by the deduced value of CV = 1. 17 across profile 2 as indicated in Figure 4.4. Profile 1 provided a coefficient of variation of 0.37, and profile 3 a coefficient of variation of 0.42. Since the values of profile 1 and 3 were deduced to be smaller than that of profile 2. Profile 2 was chosen for coefficient of v
ariation analysis because of interesting results compared to profile 1 and 3, which have similar results. The spacing between the dykes in profile 1 and 3 is very small, yet in some areas the dykes were very apart each other. The solid lines on Figure 4.4C indicate the concentrations of mapped dykes in profile 2, while elsewhere empty spaces indicate that dykes were very far apart (Figure 4.4). Dykes outside the profile range are not considered in the calculations.

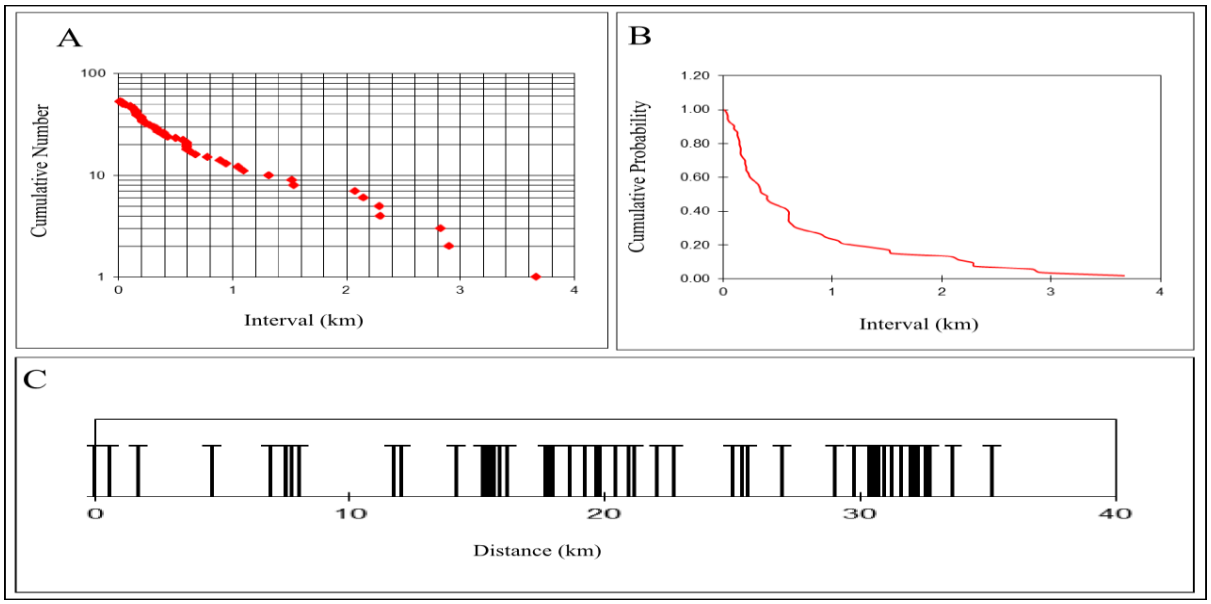

Figure 4.4: Diagram of profile 2 showing the spacing/intervals between dykes where thick lines shown on the diagram indicates clustered dykes, empty space in the spacing diagram likely represents dykes covered with Quaternary sediments and unidentified.

4.1.3 Width and length of the HOD dykes

Dykes are often represented as solid lines on geological maps and their uniform thickness determined by the diameter of the pen or a minimum-width digitized line rather than the scaled thickness of the exposed dyke. Since dyke thickness plays a crucial role in the mechanical formation of dykes, this kind of representation is not appropriate for structural investigations (Nicholson and Pollard, 1985). In this study the dyke length and width were measured using satellite images and Google Earth.

About 18605 dykes were mapped in the HOD. Their width range from 1- 3 m is about 90%, and 10% of dykes >3 m width (see Figure 4.5A), and rarely reaches 6 m. This finding shows that the width of dykes is not scale dependant as previous authors have claimed (e.g. Suryanarayana and Anjanappa, 1975). Dykes with a width of about 4-6 m show consistency in the HOD (see Figure 4.5A).

Dyke length varies from place to place within the HOD. Segmented pieces of dykes that form part of the same dyke were measured as one dyke for orientations and for partly buried dykes only the ones clearly seen using aeromagnetic method were considered. The most widely distributed dykes (60%) in the HOD vary between 100-200 m length (Figure 4.5B). There are areas where 30% of dyke lengths reach 300-400 m and 10% of the dykes are 500-550 m long. Few dykes reach lengths of 1000 m and dykes of about 600-1000 m length were measured in the central part of the HOD, close to the Namibian coast line.

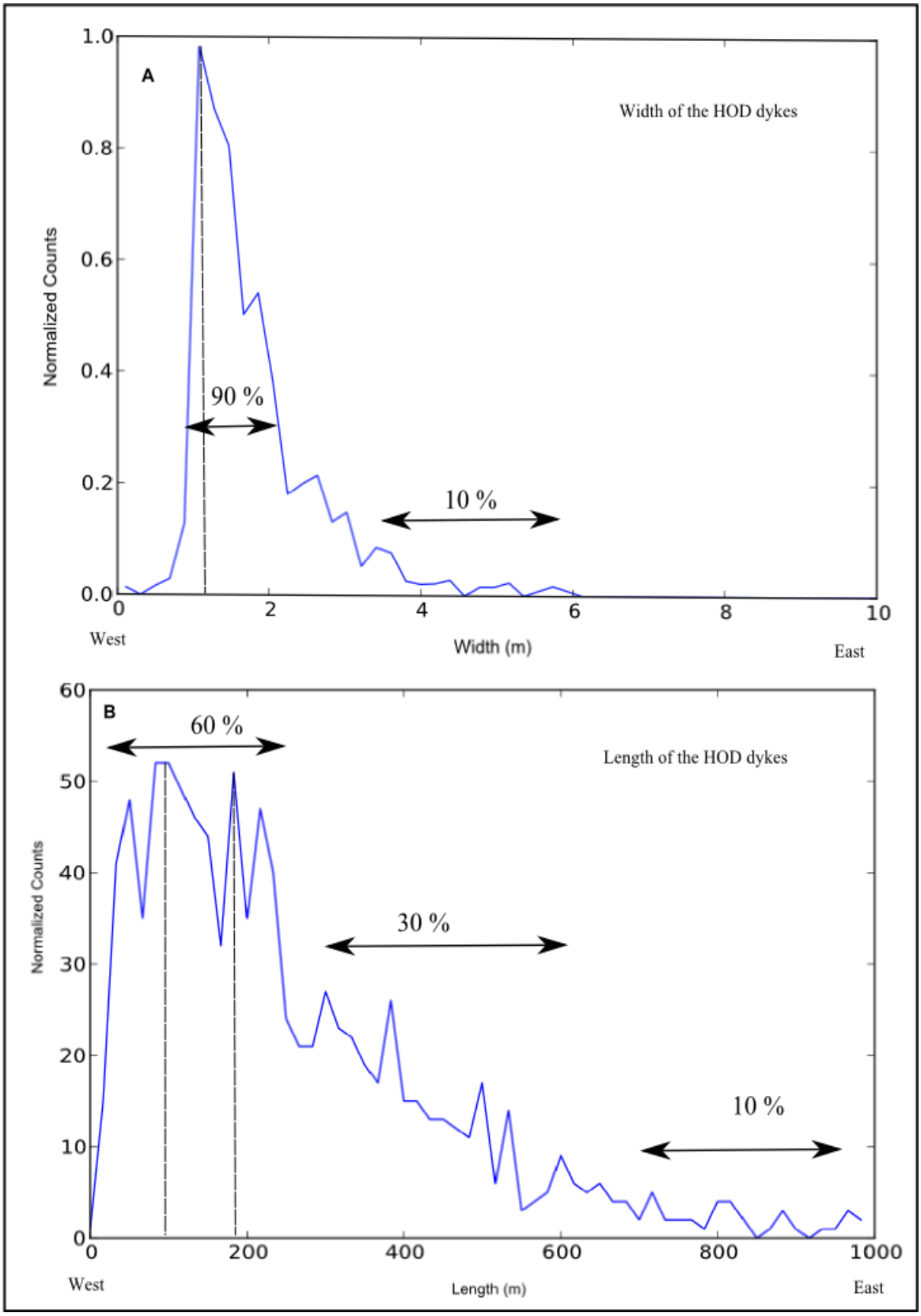

Figure 4.5: (A) Example of average dyke widths and variations, and (B) the average length and variations of the HOD dykes.

4.1.4. Testing for fractal (geometry) patterns in the HOD dykes

Fractal tests were carried out in the HOD to test if dykes display fractal geometry. The common features considered in the analysis are size, orientation, aspect ratio, shape and arrangement of features in relation to each other. Box counting also depends on the image resolution, the higher the resolution the higher the precision (Bėrubė and Jėbrak, 1999). In this study dyke images were computed with the box counting method within the ImageJ software (Version 1.47d) and the fractal dimension (D_f) ranged at >1 and 2 (e.g. $1<D_f<2$). The fractal dimension values changes with scale but still show self-similarity (Figure 4.6).

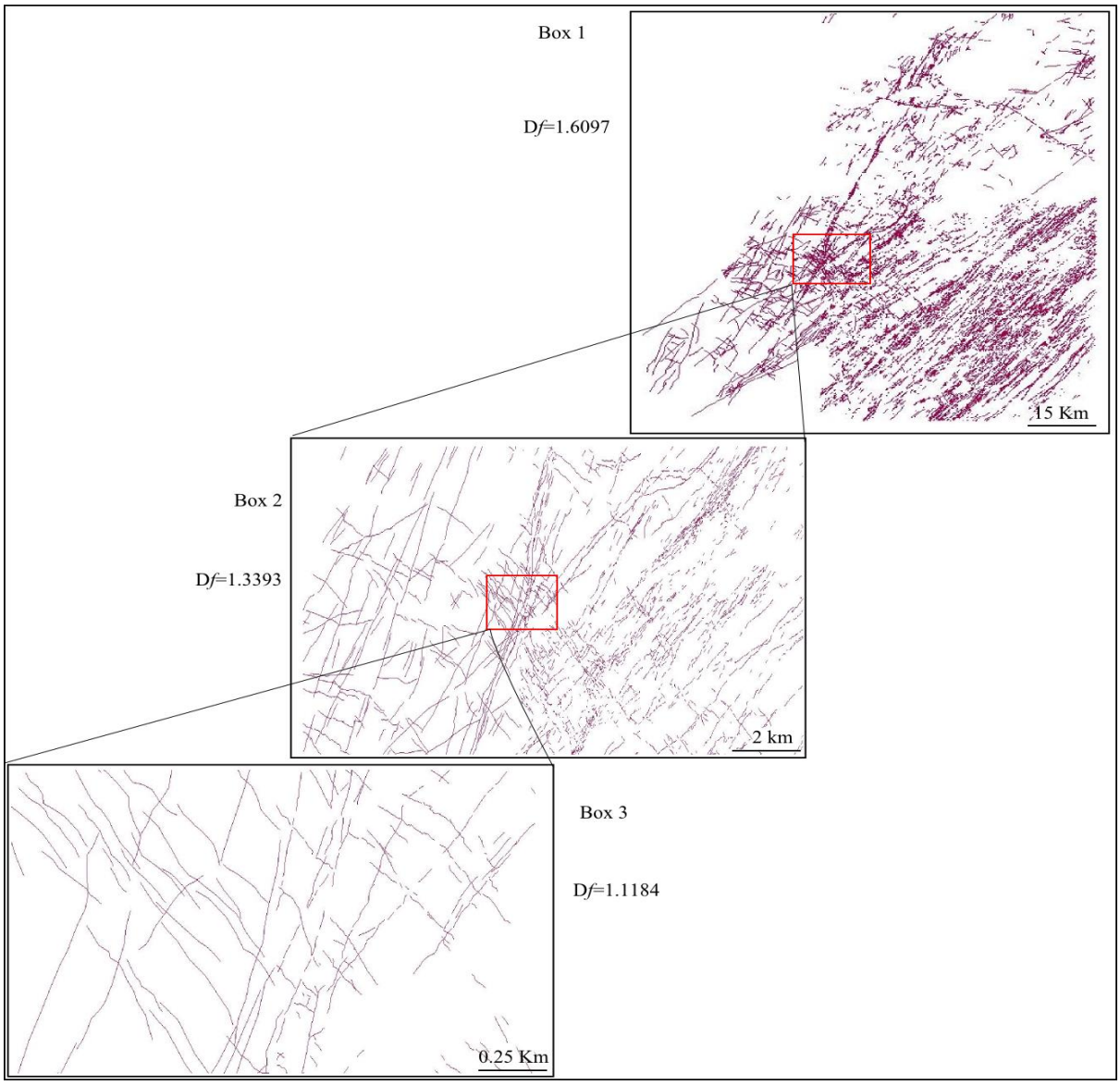

Figure 4.6: Simplified schematic illustrations of the 3 different scales at which fractal analyses of the HOD dykes were completed.

A small number of tests were performed to determine if fractures have a fractal distribution. This was done at 3 different spatial scales. When the scale decreases, features are seen clearly and the area becomes less cluttered (Figure 4.6; boxes and the fractal dimensions documented).

Rock samples (dykes) were collected in the field from the HOD by Miriam Wiegand a PhD candidate and thin sections were prepared by Stephan Unrein both from Karlsruhe Institute of Technology (KIT). Fractals in the HOD were also documented at the microscopic scale using thin section images. The fractal results found on a big scale are: 1.6097, 1.3393 and 1.1184; while at the microscope scale they are: 1.9214 and 1.7658. The results from the field and on a large regional scale are similar (see Figure 4.6 and Figure 4.7).

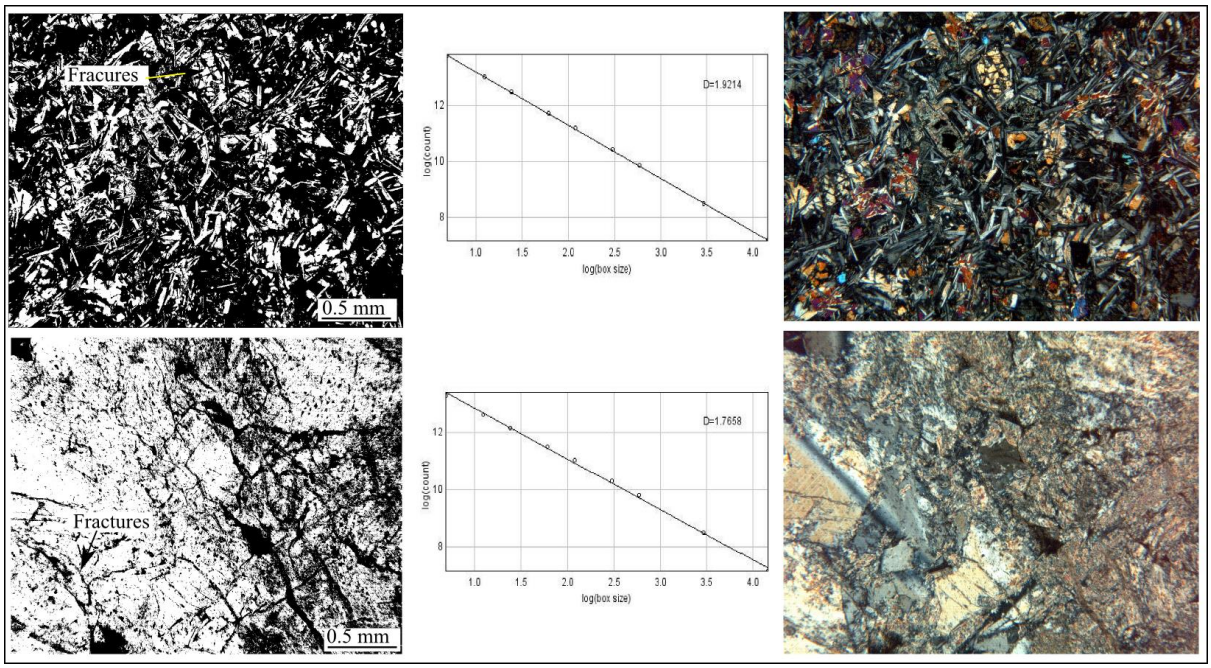

Figure 4.7: Log-Log plot showing fractal dimensions derived from polished thin sections of the HOD using imageJ software.

In summary, the rock types of the HOD have influenced the emplacement of the dykes as dykes display various orientations. They show closer spacing parallel to each other as they approach quartzite, schist and conglomerate, and discontinuous as they approach sand and gravel. The orientation of the dykes favoured a NE/NNE direction, the same direction as that of the lineaments and faults trend in the HOD. Cross-cutting relationships reveal that young dykes also trend in NNE/NE directions. The crustal extension due to intrusion of HOD dykes is small, about 4%, and shows that the width of intrusive rocks had minor influence on the extension of the crust.

4.2 Results of the Golden Valley Sills (GVS), Tarkastad area

About 1026 GVS joints were measured and plotted on a stereonet. Results in different locations of the GVS joints show various directions. The orientation distributions show that about 35% of the GVS joints are trending NNE-SSW, 40% joints trend WNW-ESE and 25% to other orientations.

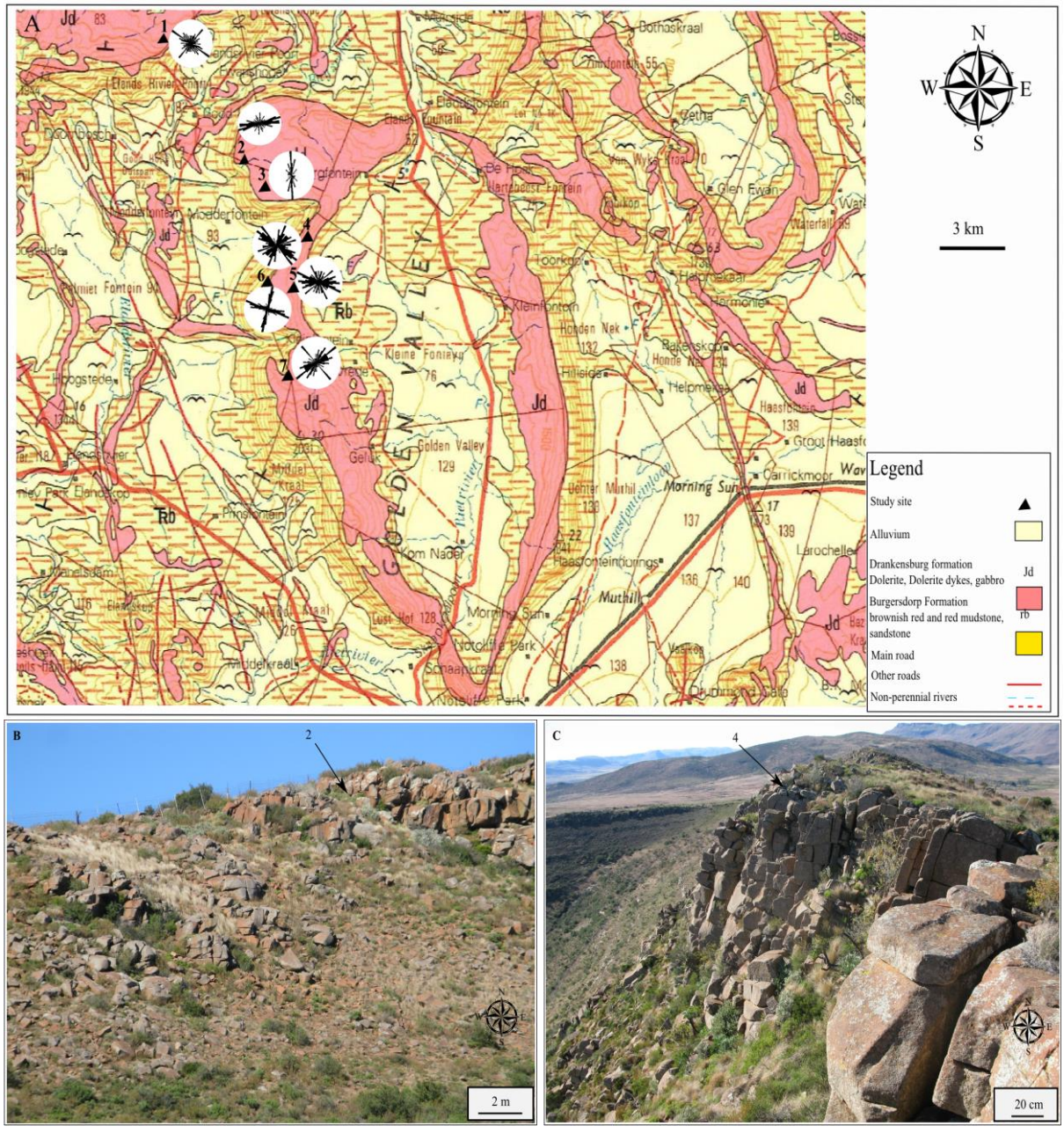

Figure 4.8: (A) Simplified locality map of the GVS showing mapped joint locations and sampled sites (Map: Republic of South Africa Geological Survey, 1982), (B) Karoo dolerite sill showing mapped and sampled site 2 on map A, (C) joints and rock blocks mapped at site 4, as shown on map A.

Table 4.2: Field data of measured joint coordinates from the compass reading of the GVS, Tarkastad area.

Locations	GPS Coordinates Golden Valley Sills (GVS)	Trends of Joints sets
1	32^0 00 09.0 S 26^0 15 31.6 E	ESE-WNW/N
2	31^0 51 59.0 S 26^0 12 51.9 E	NNE-SSW/ESE-WNW
3	31^0 53 13.6 S 26^0 12 28.1 E	NE-SW/ESE-WNW
4	31^0 52 31.3 S 26^0 12 51.1 E	NNE-SSW/ ESE-WNW
5	31^0 52 27.7 S 26^0 12 32.7 E	NNE-SSW/ESE-WNW
6	31^0 00 09.0 S 26^0 15 31.6 E	NNE-SSW/NW/N
7	31^0 52 49.2 S 26^0 12 36.9 E	NNE-SSW/ESE-WNW
8	31^0 53 00.3 S 26^0 12 43.2 E	NW-SE/ESE-WNW
9	31^0 52 57.1 S 26^0 12 43.4 E	NNE-SSW/ESE-WNW
10	31^0 53 07.3 S 26^0 12 57.6 E	ESE-WNW
11	31^0 53 08.0 S 26^0 13 02.3 E	ESE-WNW/N
12	31^0 53 00.5 S 26^0 12 16.6 E	NNE-SSW/N
13	31^0 52 57.1 S 26^0 12 23.2 E	NNE-SSW/ ESE-WNW
14	31^0 53 08.8 S 26^0 12 29.5 E	NNE-SSW/ESE-WNE

4.2.1 Block size and Fractal patterns of joints in the GVS

The blocks of rock were analysed to test for fractals in the GVS. The size and dimension of the blocks of rocks are determined by the joint set spacing. Joints divide rocks into blocks and these occur at different sizes. The shapes of blocks observed in the GVS show different sizes and the block sizes in the GVS differ in volume, although the block patterns are similar. About 120 blocks in the GVS were measured in three-dimensions and they produced an average volume of 0.2 m^3 (73.9 cm by 40.7 cm by 60.5 cm) and the average area calculated by two-dimensional blocks was found to be about 0.4 m^2 (72.5 cm by 67.4 cm). The most dominant joints at the first location in the GVS are NW-SE and NE-SW (Figure 4.9).

Figure 4.9: Photo of joints and blocks of dolerite sill from site 1 of GVS (Persons used as a scale ± 1.70 m). The rose diagram on the bottom left shows strikes of 105 mapped joints from site 1.

4.2.2. Fractal analysis of the GVS blocks and joint systems

The GVS block sizes were analysed and the fractal dimension results were found to be D_f = 1.6595. The strength of the dolerite rock controls the sizes of the rock blocks (Palmström, 1995; Palmström, 2001). Two polished dolerite sill thin section photographs from the GVS were selected to statistically analyse for fractal nature. The dolerite sill sample particle sizes

and textures were considered in the analysis. The fractal analyses were performed using box counting in ImageJ software after the image was converted to grayscale. Fractal geometry was analysed to statistically describe the fracture length and spatial distribution of the fracturing. The smaller the fracture distribution, the lower the fractal dimensions. The fractal dimension was found to range from D_f =1.8815 and D_f =1.8966 (Figure 4.10).

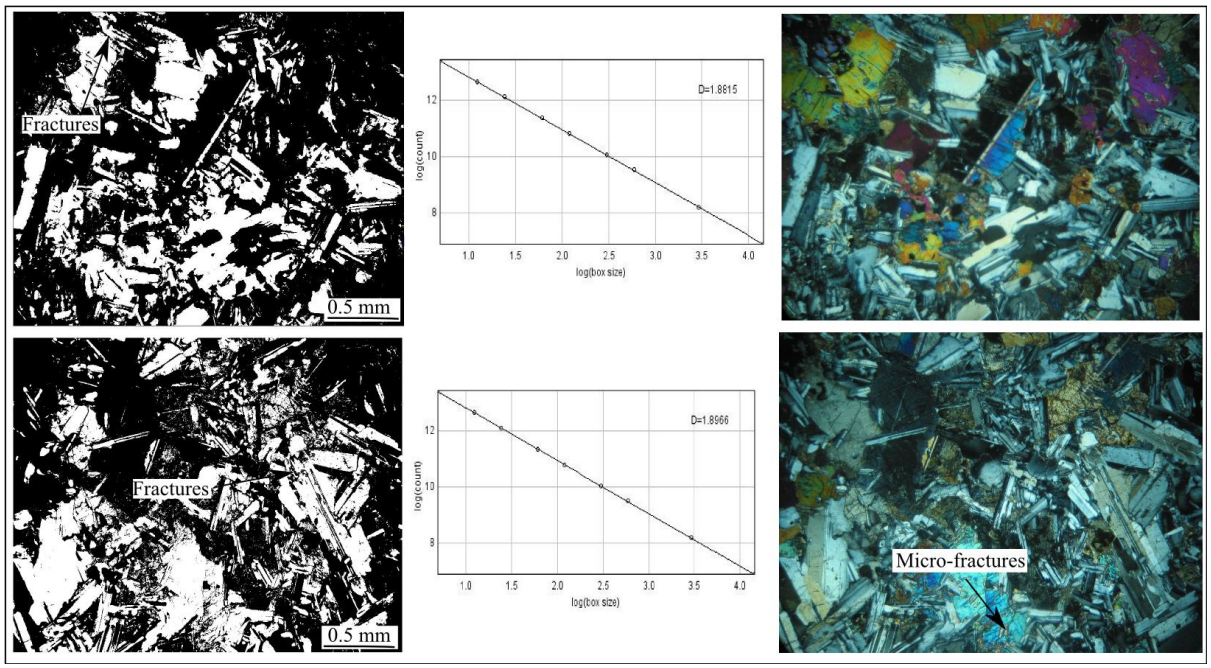

Figure 4.10: Log-Log plot showing fractal dimensions derived from polished thin sections of the GVS using imageJ software.

In summary, the orientation of the joints in the GVS shows various directions that might have been influenced by the uplifts of the margins and magma intrusions in the Karoo basin. The ESE and WNW trending joints in the GVS have mean azimuth of 105° and 283°, collectively. And the set of NNE and SSW have a mean of 30° and 190°. Analysed joints from thin section photography show fractal dimension in the form of log-log graph (Figure 4.10). The results of the GVS fractal dimensions show fractal patterns.

4.3 Results of the Table Mountain Group quartzites (TMG)

The joint orientations and lengths are the most common geometrical properties considered in the joint analysis. About 1716 joint were measured in the Tsitsikamma area and the results show that they orientate in specific directions but they show a strong and preferred joint orientation of N 347° W. A SSE joint orientation with a mean azimuth of 176° is also present in the area. Both sets are perpendicular to the bedding surface (Condon, 2003). The longest joint observed in the TMG quartzite was 1.47 m.

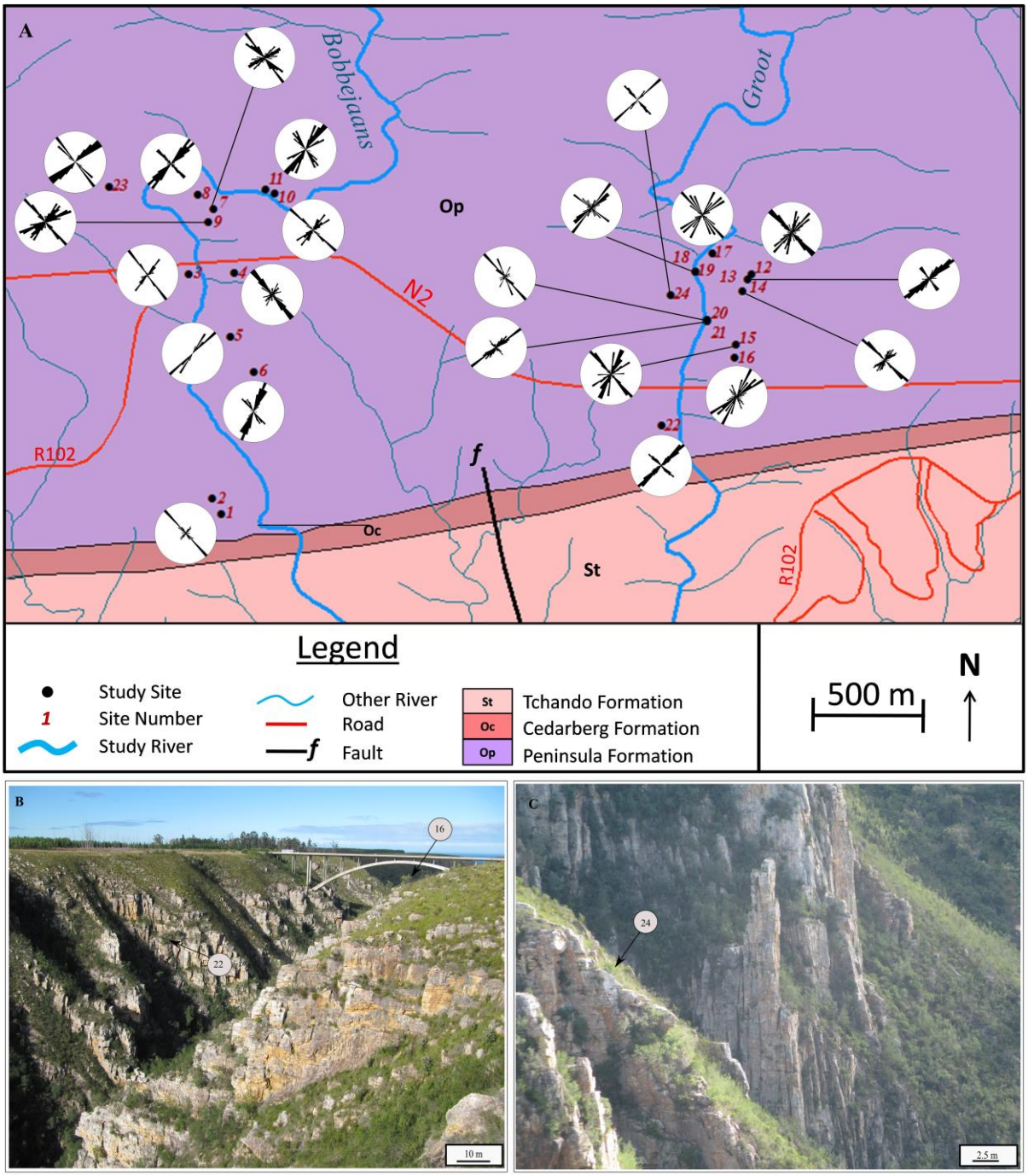

Figure 4.11: (A) Geological map of the Table Mountain Group quartzite in the Bobbejaans and Groot Rivers indicating the sites where joint data were collected, (B) surface with the rose diagrams of joints from the North (mapped site 16) and South (mapped site 24) of the bridge and (C) remnant tower of resistant quartzite blocks of rocks shaped by vertical, similarly spaced joints on the Groot river seen (From: Almanza, 2012).

Table 4.3: Tabulation of the joint coordinates of the Tsitsikamma area (From: Almanza, 2012 and Almanza and Muedi, 2012).

Locations	Eastern part of the Cape Fold Belt (TMG)	Trends of Joints sets
1	33^0 56 42.324 S 23^0 32 6.54 E	ESE-WNW/N
2	33^0 56 39.804 S 23^0 32 4.956 E	NNE-SSW/ESE-WNW
3	33^0 56 1.392 S 23^0 32 0.996 E	NE-SW/ESE-WNW
4	33^0 56 1.32 S 23^0 32 8.628 E	NNE-SSW/ ESE-WNW
5	33^0 56 12.12 S 23^0 32 7.944 E	NNE-SSW/ESE-WNW
6	33^0 56 18.06 S 23^0 32 12.084 E	NNE-SSW/NW/N
7	33^0 55 50.304 S 23^0 32 5.172 E	NNE-SSW/ESE-WNW
8	33^0 55 47.82 S 23^0 32 2.4 E	NW-SE/ESE-WNW
9	S 33^0 55 52.57 S 23^0 32 4.272 E	NNE-SSW/ESE-WNW
10	33^0 55 47.604 S 23^0 32 15.648 E	ESE-WNW
11	33^0 55 47.028 S 23^0 32 15.648 E	ESE-WNW/N
12	33^0 55 50.304 S 23^0 32 5.172 E	NNE-SSW/N
13	33^0 55 47.82 S 23^0 32 2.4 E	NNE-SSW/ ESE-WNW
14	33^0 55 52.572 S 23^0 32 4.272 E	NNE-SSW/ESE-WNE
15	33^0 56 15.648 S 23^0 33 34.092 E	NNE-SSW/NW/N
16	33^0 55 57.864 S 23^0 33 30.132 E	NNE-SSW
17	33^0 56 0.996 S 23^0 33 27.288 E	ESE-WNW/N
18	33^0 56 0.996 S 23^0 33 27.288 E	NNW-SSE
19	33^0 56 9.312 S 23^0 33 29.448 E	NE-SW/ESE-WNW
20	33^0 56 9.528 S 23^0 33 29.376 E	NNW-SSE
21	33^0 56 27.312 S 23^0 33 21.528 E	NE-SW/ESE-WNW
22	33^0 55 46.56 S 23^0 31 47.28 E	NE-SW/ESE-WNW
23	33^0 56 4.92 S 23^0 33 23.04 E	NNW-SSE/N

4.3.1 Block size and Fractal patterns of joints in the TMG

The block photo was loaded into ImageJ software and converted to grayscale to analyse for fractal pattern. The fractal dimension of blocks analysed was found to be D_f = 1.6888. The block sizes in the Tsitsikamma area were also analysed to determine the average block size. About 131 blocks in Tsitsikamma were measured in three-dimensions and they produced average volume of 0.3 m^3 (84.9 cm by 67.3 cm by 60.9 cm) and the average area was calculated by two-dimensional blocks was found to be about 0.6 m^2 (82.7 cm by 79.4 cm).

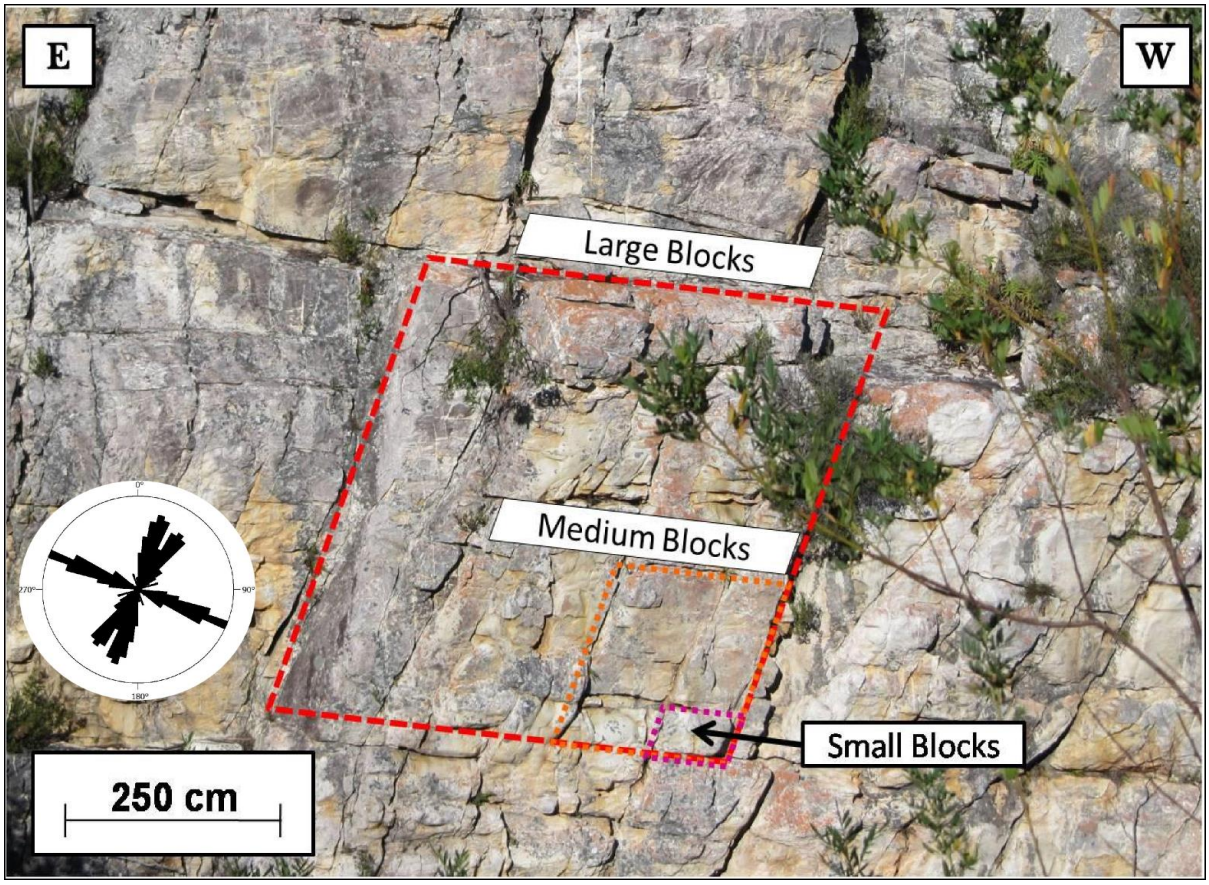

Figure 4.12: Field photograph showing fracture strikes and rock block sizes in the TMG, Tsitsikamma study site (From: Almanza, 2012).

4.3.2. Fractal analysis of joint systems in the TMG quartzites

During this investigation I used the box counting method to establish the nature and length distribution of the micro-cracks. The polished thin section contains micro-cracks which can be seen as randomly orientated, unorganized fractures. The fractal dimensions on the two microscopic samples of TMG quartzites resulted to D_f = 1.8966 and D_f = 1.8832.

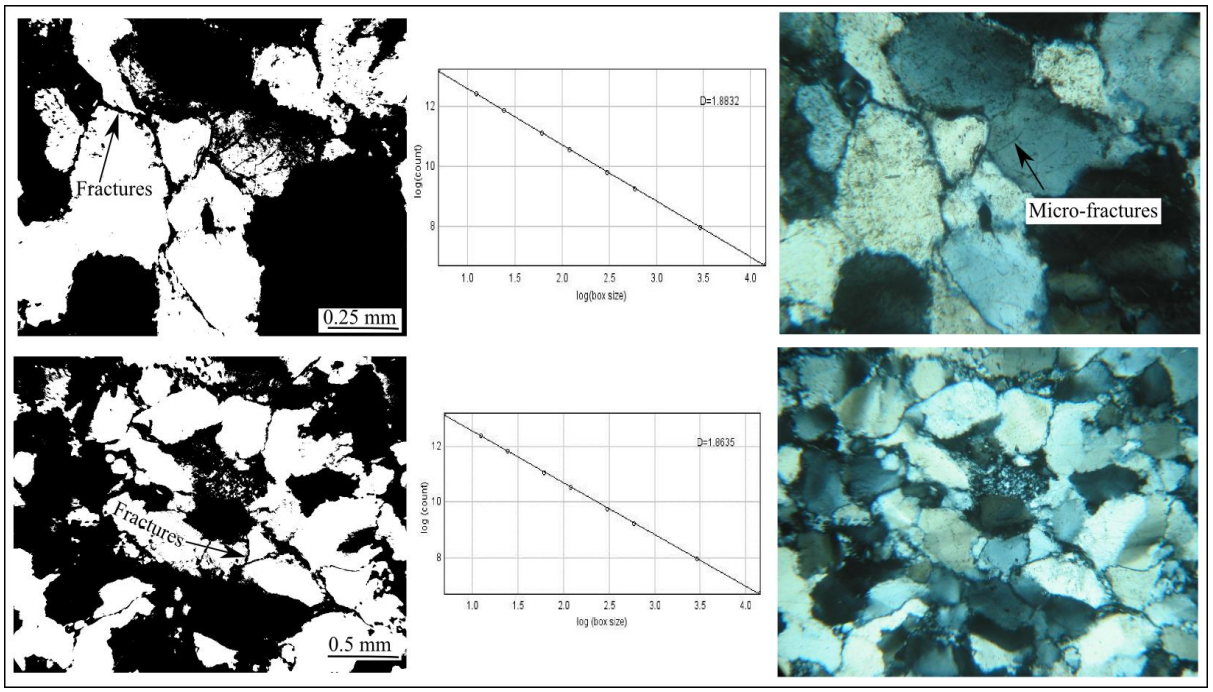

Figure 4.13: Log-Log plot showing fractal dimensions derived from polished thin sections of the TMG using imageJ software.

In summary, the Tsitsikamma joints data were obtained by plotting mapped joint data using stereonet and the plotted data showed orientation of NNW-SSE and ESE-WSW. The Tsitsikamma joints and blocks were tested for fractals and the investigations show that the Tsitsikamma joints and blocks have fractal patterns across a wide range of scales.

4.4 Patterns of brittle structures

The HOD dykes cut across all the Damara Belt lithologies within the study area. The HOD display a wide range of dyke widths, most likely as a result of alteration in the magma pressure exerted and magma supplied as the dykes intruded to the surface. The HOD dykes are longer close to the coast as compared to inland dykes. Perhaps long dykes might be related to their close proximity of the magma chamber. The HOD shows a consistent orientation in the Damara sequence rocks and they diminish in number as they approach the Kalahari Group sediments.

Joints system in the TMG traverse for a long distance compared to the GVS joints and the size of TMG block sizes are about 0.45 m^2 with the average volume of 0.40 $m^{3.}$ The GVS block sizes are about 0.77 m^2 with the average volume of 0.62 m^3. Even though the blocks have been fractured and form in different mechanical processes in the GVS and TMG their fractal geometry appear to be have similarities.

4.4.1 Fractals patterns of joints along the southern Africa margins

I have analysed fractal patterns along the southern African margins from macro to micro scales (Table 4.4). Fractures such as joints and dykes were analysed, compared and the results found shows that they have fractal geometry. The fractals dimension analysed in the southern Africa are similar to ones documented in other areas such as in Japan, Sardinia, Italy and India (Hirata, 1989; Volland and Kruhl, 2004; Mamtani and Greiling, 2010).

Table 4.4: Fractal dimensions results collected from macro-micro scale of southern African studied areas and they show differences fractal dimensions in various scales.

Macro-scale			Micro-scale		Field macro-micro scale		Field macro-micro scale	
Fractals Analysis	HOD Fractal dimensions	Scale mm	HOD Thin sections	Scale mm	TMG Thin Sections	Scale mm	GVS Thin sections	Scale mm
1	D_f=1.6097	15000000	D_f=1.9214	5.64	Rock blocks, D_f=1.6888	2.50	Rock blocks, D_f= 1.6595	1.70
2	D_f=1.3393	2000000	D_f=1.7658	2.22	D_f=1.8635	2.22	D_f=1.8815	2.22
3	D_f=1.1184	250000			D_f=1.8832	2.22	D_f=1.8966	2.22

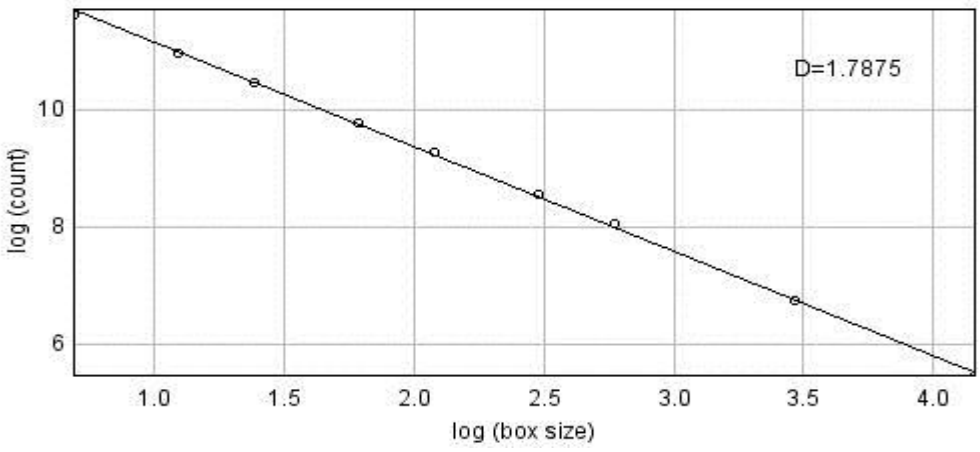

Figure 4.14: Log-Log plot showing fractal dimension of three events including the TMG, GVS and HOD using the ImageJ software.

4.4.2 Comparing geometry of the HOD dykes, GVS and TMG joints

About 18605 HOD dykes were located and mapped using GIS, About 70% of the dykes are obtained from 54° (NE-SW) orientation; 20% dykes trend NW-SE; and 10% to other orientations (Figure 4.15). The HOD shows weak orientation relationship with the TMG and close orientation relationship with the GVS joints. The TMG quartzite joints is assumed to post-date uplift (100 Ma or less); GVS joints at Jurassic to late time in basalts and HOD dykes formed in Cretaceous time.

About 1026 GVS joints were mapped and analysed in the stereonet. I found that about 35% of the GVS joints trend NNE-SSW, 40% joints trend WNW-ESE and 25% to other orientations. The TMG quartzites joints of about 1716 were measured and analysed using stereonet. I found that 50% of the joints within the TMG trend NNW-SSE, 40% joints trend WSW-ESE and 10% to other orientations (Figure 4.15). The distributions of the GVS and TMG joints were analysed in stereoplot and compared for dipping angles. The stereoplot presented shows that the GVS and TMG joint dips vertically to sub-vertical (Figure 4.15). Studies suggest that the HOD dykes, faults and lineaments dips steeply at approximately 65° (Ritter *et al*., 2003).

GVS = WNW > NNE > Other
TMG = NNW > NSW > Other
HOD = NE > NW > Other (see Figure 4.15)

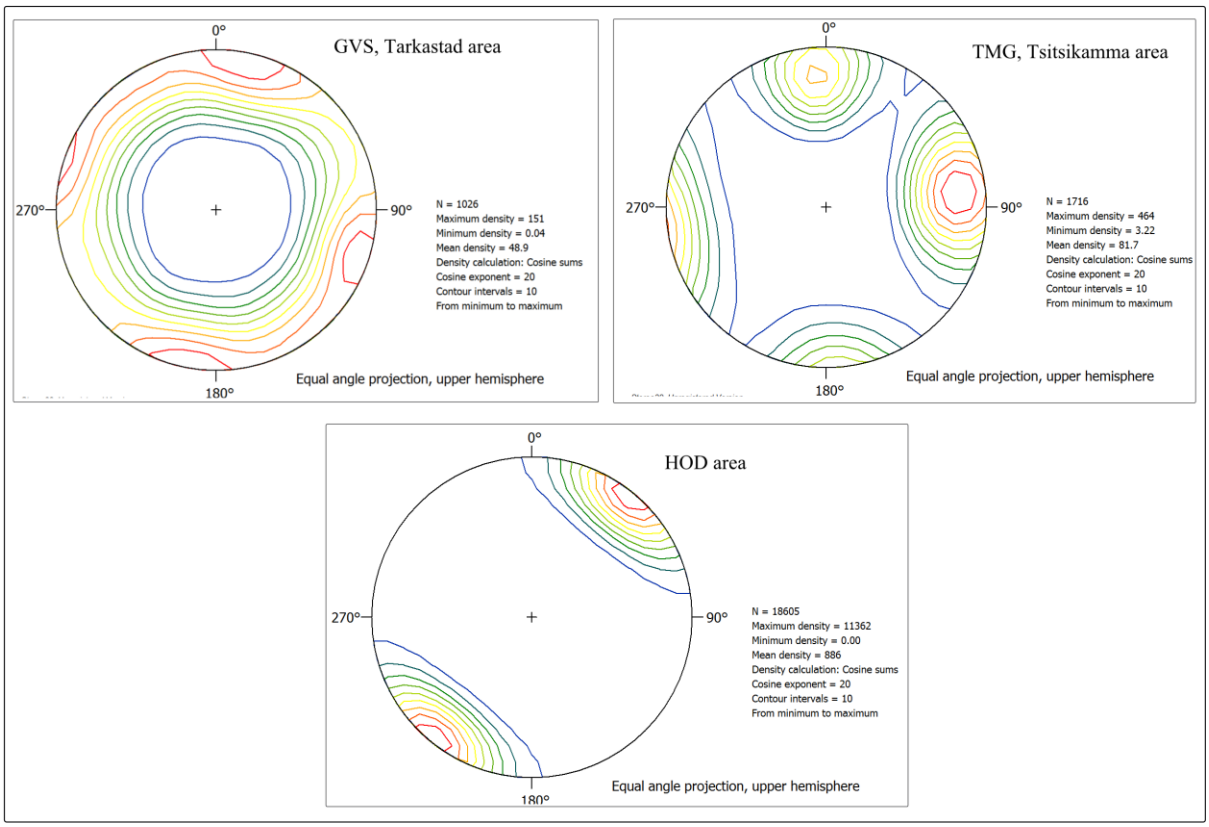

Figure 4.15: Stereoplot of the GVS, TMG joints direction and HOD, dyke orientations plotted.

Chapter 5. Discussion of brittle structures related to Gondwana break-up

While other aspects related to Gondwana break-up such as Large Igneous Provinces (LIP), mantle plumes and hotspots are well studied, this thesis examined the brittle fractures and selected dyke swarms of southern Africa in their Gondwana setting, including geometry and reconstructions of the Ponta Grossa dyke swarms (PG) and Henties Bay-Outjo dyke Swarm dyke (HOD) and the interpretation of the laboratory and field results.

5.1. Geometry and reconstruction of Ponta Grossa Dyke Swarm and Henties Bay-Outjo Dyke Swarm

The E-W extensional directions during South Atlantic rifting has influenced the orientations of geological structures such dykes (Austin and Uchupi, 1982; Moulin *et al*., 2010). The precise reconstructions of Gondwana is different from one author's model to another (e.g. Torsvik *et al*., 2004; de Wit *et al*., 2008; Reeves, 2009). The HOD and PG were reconstructed using plate reconstruction techniques to track their movements during Gondwana break-up, with aim to test details of various reconstructions.

I added African-South American plates, HOD and PG layers in the Gplates. I reconstructed the plates at 130 Ma in ArcGIS, and arranged legends, scale and geometry of dykes (Figure 5.1). Rotated dykes from continental margins on both sides of the South Atlantic Ocean show that the PG dyke swarm and HOD dyke swarm have rotated anti-clockwise.

The HOD was rotated anti-clockwise from 35° to 60° (e.g. by N 25° E (Figure 5.1) with the African plate when it separated from the South American plate, rotating anti-clockwise to its present day position. At 130 Ma, HOD is approximately parallel to the Dom Feliciano belt (Piccirillo *et al.*, 1990). The PG was back rotated from present day to 130 Ma and results show that dykes only rotated from 275° to 290° (e.g. N 15° E) (Figure 5.1).

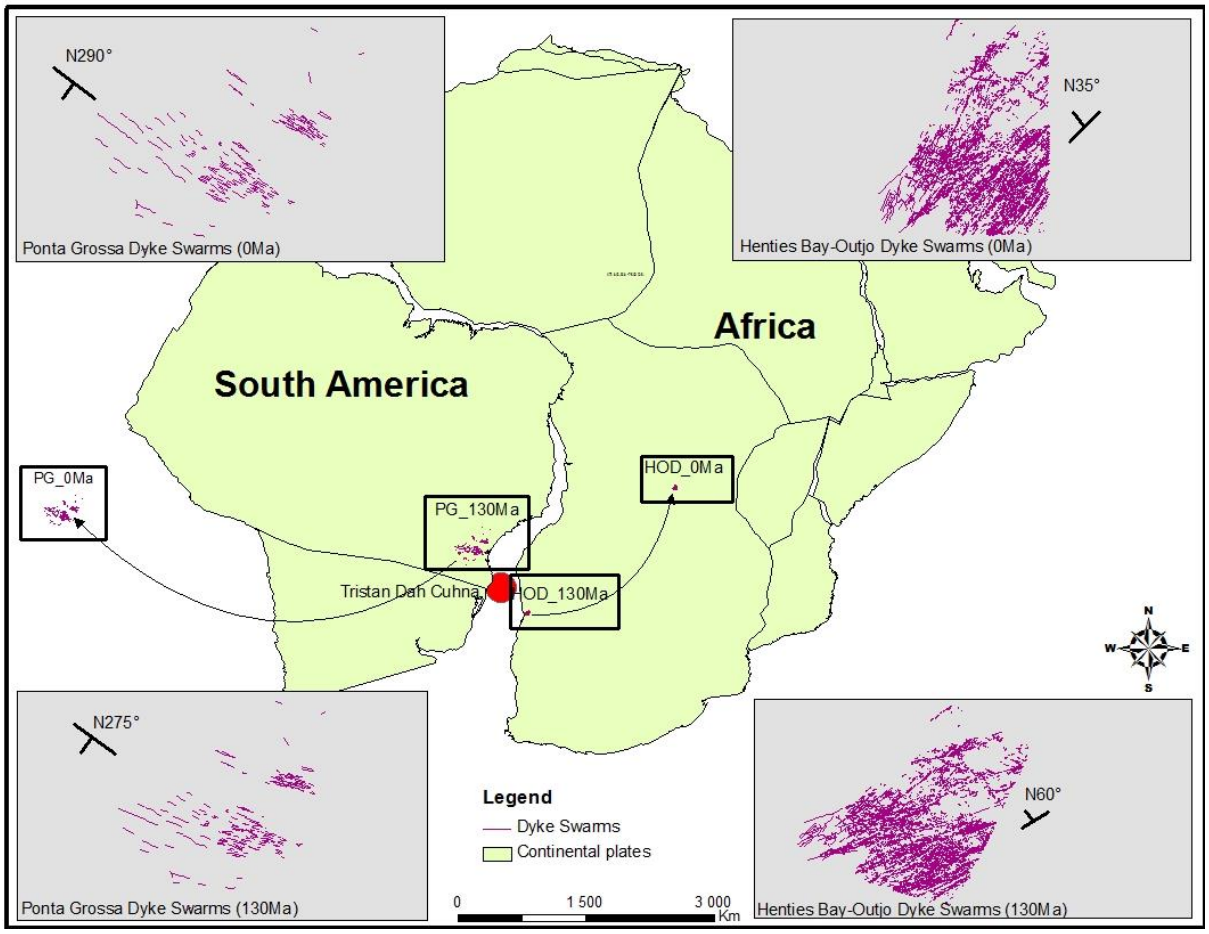

Figure 5.1: A map showing reconstructed Cretaceous coastal dyke swarms ca.130Ma, Ponta Grossa Dyke Swarms (PG) rotated clockwise and Henties Bay-Outjo Dyke Swarms (HOD) rotated anticlockwise (de Wit *et al*., 2008; reconstruction based on gplates: Torsvik *et al*., 2009).

Geometry and reconstruction of the GVS and TMG joints

The uplift in southern Africa is speculated to have contributed to the formation of the TMG and GVS joints and the orientation of joints has changed with time during subsequent Africa rotations (Figure 5.2). The TMG and GVS joints were reconstructed to see their geometry during Gondwana break-up.

The orientation results of the joints at about 100 Ma, shows that TMG joints orientation found to be dominantly NE-SW and measured joint orientation of the current TMG location is dominate by N-S/E-W (Figure 5.2), while the GVS joints orientation trends in various directions at about 100 Ma and at the current location.

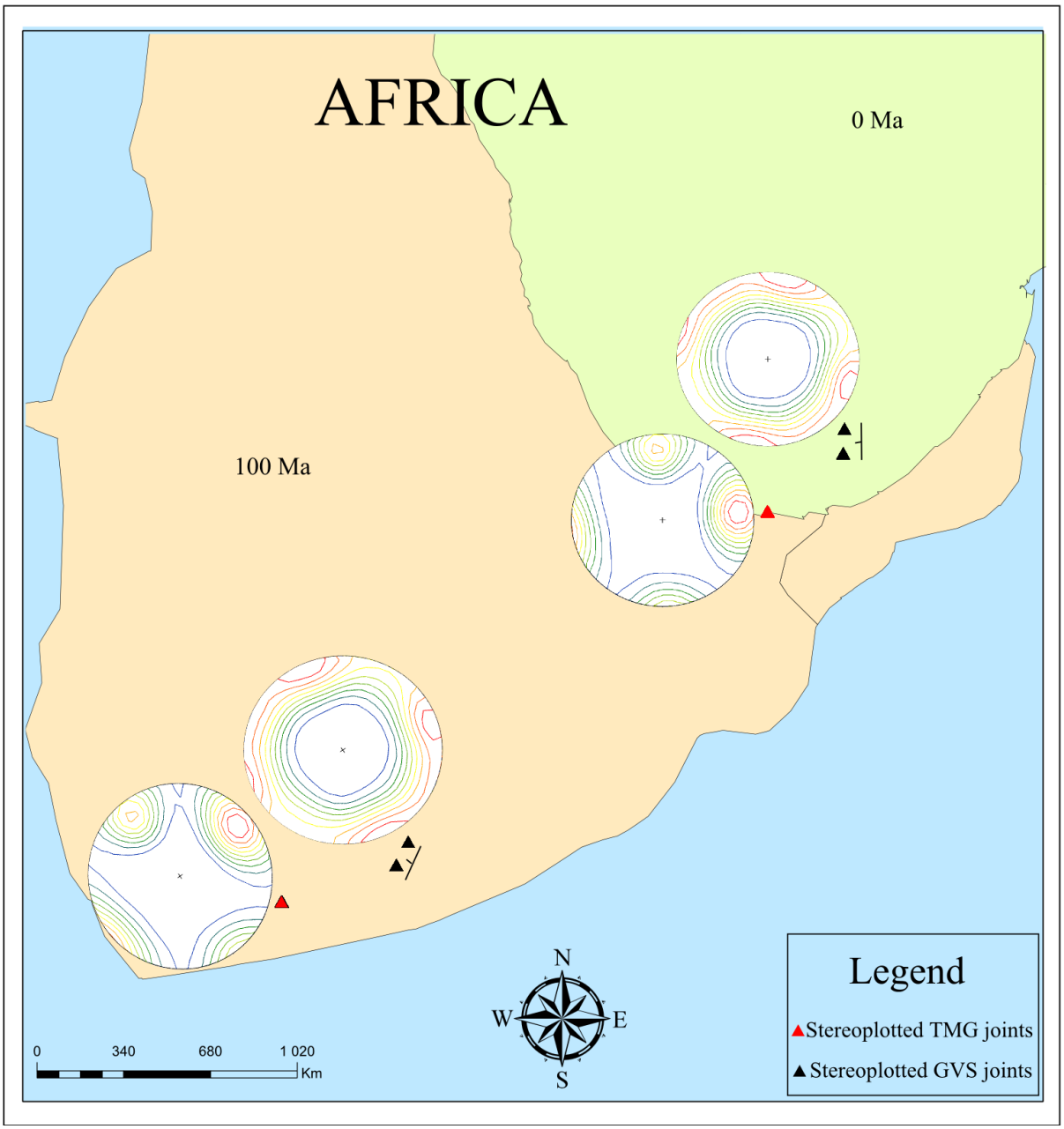

Figure 5.2: The African map at 0 Ma (Green) and at 100 Ma (Orange) showing stereoplots of TMG and GVS during Gondwana break-up.

Chapter 6. Concluding remarks and recommendations

This thesis has attempted to document and analyse brittle deformation and geometry of the HOD, Namibia, the Golden Valley Sill (GVS) joints within the Karoo dolerite intrusions and the Tsitsikamma joints in the Table Mountain Group quartzites. This was accomplished by field observations and image interpretations.

The orientations of the HOD dykes and GVS and TMG joints do not show strong correlations which means the orientations relationship between joints and dykes is not always possible and this is still a debate (see Figure 4.15). However, the different events and processes during Gondwana break-up could be the controlling factors of geometry of the joints, faults, lineaments and dykes.

The differences in the angles of rotations indicate that Africa rotated anticlockwise, South America rotated clockwise. Since joints in the southern African margins were speculated to have initiated at about 100 Ma or later during continental margins uplift, their dominant orientations may indicate that they cut through pre-existing weak zones of dykes formed as a results of the thinning of crust (Viola *et al*, 2006). I suggest that fractal dimension of fractures which could have resulted from uplift of southern African margins varies in response to high to low fractured zones; this can be inferred from different rock types and strength of the rocks (e.g. Peninsula quartzites and Karoo sill).

Fracture systems of Southern Africa may be related to Gondwana break-up processes since results indicate that they rotate anticlockwise from 15° to 25° during Gondwana break-up. The differences in rotational angles of dykes during Gondwana break-up may indicate that South America plate rotated less while Africa rotated greater than South America during the break-up.

Fractal patterns of brittle structures close to D_F = 1.6-1.7, on the southern African margins show fractal dimensions analysed from one scale to another. When a fractal dimension (D) value is closer to 1 it reflects a high degree of fragmentation of the studies rocks and different quantity of particles of different sizes, while D closer to 2 reflect less fractured surface. The change of fracture network behaviour may be fracture scale independent. I speculate that the fractal dimension in the studied areas may reflect the geological history. Fractures are fractal which means they are scale invariant from microscopic-megascopic. And fractal dimensions indicate that fracture systems in the southern Africa have fractal geometry.

Studies on the uplift of southern Africa margins remain uncertain, about which force caused surface uplift between dynamic uplift and isostatic rebound. To improve our understanding more studies need to be done on the fracture development in response to horizontal movement of the tectonic plates and mantle upwelling.

Recommendations: from the results of this research it is recommended that the following may be taken into account as future research projects:

Mapping joints of the HOD and comparing them with joints along the entire coastal region of southern Africa is required. My database for dykes and joints should be integrated with the geometry of faults, lineaments across the whole southern Africa. The data should be integrated with on-going thermo-chronology leg-(Flowers and Stanley, 2013) to test for differential uplift during plate motion.

Much work on ground geological field observations on joints and dykes still need to be completed and integrated with the Gondwana database for Gondwana reconstruction to test their fractal geometry during Gondwana break-up at continental scales.

APPENDIX A

Table 1: Interval and distances between dykes in the **HOD** along **profile 1**

Locality: **Henties Bay-Outjo Dyke Swarm (HOD)**, **Namibia**

Sharper angle between line profile and fractures: 91.5555556
1.59794589 **Cv....** 0.36768617

Distances		Correct Spacing	Assorted Spacing	Cumulative Number	Assorted interval	Cumulative Probability	Distances	
0	1.86	1.86522236	2.97890179	1	2.97890179	0.14285714	0	1
1.86591	1.35	1.34950249	1.86522236	2	1.86522236	0.28571429	1.86591	1
3.21591	1.50	1.5070714	1.5070714	3	1.5070714	0.42857143	3.21591	1
4.723537	1.11	1.10959094	1.34950249	4	1.34950249	0.57142857	4.723537	1
5.833537	2.98	2.97890179	1.27934535	5	1.27934535	0.71428571	5.833537	1
8.813537	1.27	1.27934535	1.26953197	6	1.26953197	0.85714286	8.813537	1
10.093354	1.27	1.26953197	1.10959094	7	1.10959094	1	10.093354	1
11.363354								

Table 2: Interval and distances between dykes in the **HOD** along **profile 2**

Sharper angle between line profile and fractures:				91.5555556	**Number of distances**		53	
				1.59794589	**Cv....**		1.17438775	
Distance	**Interval**	**Correct Interval**	**Assorted Interval**	**Cumulative Number**	**Assorted Interval**	**Cumulative Probability**	**Distance**	
0	0.6	0.59977888	3.66864751	1	3.66864751	0.01886792	0	1
0.6	1.1	1.09959462	2.89893127	2	2.89893127	0.03773585	0.6	1
1.7	2.9	2.89893127	2.82895707	3	2.82895707	0.05660377	1.7	1
4.6	2.3	2.29915239	2.29915239	4	2.29915239	0.0754717	4.6	1
6.9	0.57	0.56978994	2.28915607	5	2.28915607	0.09433962	6.9	1
7.47	0.2	0.19992629	2.14920767	6	2.14920767	0.11320755	7.47	1
7.67	0.34	0.3398747	2.07923346	7	2.07923346	0.13207547	7.67	1
8.01	3.67	3.66864751	1.53943247	8	1.53943247	0.1509434	8.01	1
11.68	0.33	0.32987839	1.51943984	9	1.51943984	0.16981132	11.68	1
12.01	2.15	2.14920767	1.31951354	10	1.31951354	0.18867925	12.01	1
14.16	1.05	1.04961305	1.09959462	11	1.09959462	0.20754717	14.16	1
15.21	0.13	0.12995209	1.04961305	12	1.04961305	0.22641509	15.21	1
15.34	0.14	0.13994841	0.93965358	13	0.93965358	0.24528302	15.34	1
15.48	0.15	0.14994472	0.88967201	14	0.88967201	0.26415094	15.48	1
15.63	0.21	0.20992261	0.77971255	15	0.77971255	0.28301887	15.63	1
15.84	0.31	0.30988576	0.66975309	16	0.66975309	0.30188679	15.84	1
16.15	1.52	1.51943984	0.62976783	17	0.62976783	0.32075472	16.15	1
17.67	0.16	0.15994104	0.59977888	18	0.59977888	0.33962264	17.67	1
17.83	0.1	0.09996315	0.59977888	19	0.59977888	0.35849057	17.83	1
17.93	0.03	0.02998894	0.59977888	20	0.59977888	0.37735849	17.93	1
17.96	0.67	0.66975309	0.59977888	21	0.59977888	0.39622642	17.96	1
18.63	0.6	0.59977888	0.56978994	22	0.56978994	0.41509434	18.63	1
19.23	0.4	0.39985259	0.49981574	23	0.49981574	0.43396226	19.23	1
19.63	0.1	0.09996315	0.42984153	24	0.42984153	0.45283019	19.63	1
19.73	0.06	0.05997789	0.39985259	25	0.39985259	0.47169811	19.73	1
19.79	0.6	0.59977888	0.39985259	26	0.39985259	0.49056604	19.79	1

20.39	0.5	0.49981574	0.34987102	27	0.34987102	0.50943396	20.39	1
20.89	0.23	0.22991524	0.3398747	28	0.3398747	0.52830189	20.89	1
21.12	0.94	0.93965358	0.32987839	29	0.32987839	0.54716981	21.12	1
22.06	0.63	0.62976783	0.30988576	30	0.30988576	0.56603774	22.06	1
22.69	2.29	2.28915607	0.2699005	31	0.2699005	0.58490566	22.69	1
24.98	0.4	0.39985259	0.23991155	32	0.23991155	0.60377358	24.98	1
25.38	0.21	0.20992261	0.22991524	33	0.22991524	0.62264151	25.38	1
25.59	1.32	1.31951354	0.20992261	34	0.20992261	0.64150943	25.59	1
26.91	2.08	2.07923346	0.20992261	35	0.20992261	0.66037736	26.91	1
28.99	0.78	0.77971255	0.19992629	36	0.19992629	0.67924528	28.99	1
29.77	0.6	0.59977888	0.19992629	37	0.19992629	0.69811321	29.77	1
30.37	0.04	0.03998526	0.17993367	38	0.17993367	0.71698113	30.37	1
30.41	0.15	0.14994472	0.15994104	39	0.15994104	0.73584906	30.41	1
30.56	0.16	0.15994104	0.15994104	40	0.15994104	0.75471698	30.56	1
30.72	0.2	0.19992629	0.15994104	41	0.15994104	0.77358491	30.72	1
30.92	0.04	0.03998526	0.14994472	42	0.14994472	0.79245283	30.92	1
30.96	0.24	0.23991155	0.14994472	43	0.14994472	0.81132075	30.96	1
31.2	0.43	0.42984153	0.13994841	44	0.13994841	0.83018868	31.2	1
31.63	0.35	0.34987102	0.12995209	45	0.12995209	0.8490566	31.63	1
31.98	0.01	0.00999631	0.12995209	46	0.12995209	0.86792453	31.98	1
31.99	0.13	0.12995209	0.09996315	47	0.09996315	0.88679245	31.99	1
32.12	0.16	0.15994104	0.09996315	48	0.09996315	0.90566038	32.12	1
32.28	0.27	0.2699005	0.05997789	49	0.05997789	0.9245283	32.28	1
32.55	0.18	0.17993367	0.03998526	50	0.03998526	0.94339623	32.55	1
32.73	0.89	0.88967201	0.03998526	51	0.03998526	0.96226415	32.73	1
33.62	1.54	1.53943247	0.02998894	52	0.02998894	0.98113208	33.62	1
35.16	2.83	2.82895707	0.00999631	53	0.00999631	1	35.16	1
37.99								

Table 3: Interval and distances between **HOD** dykes along **profile 3**

Sharpener angle between line profile and fractures:				91.5555556 1.59794589		**Number of distances** **Cv....**	9 0.4169253	
Distance	**Interval**	**Correct Interval**	**Assorted Interval**	**Cumulative Number**		**Assorted Interval**	**Cumulative Probability**	**Distance**
0	3.16941	3.16824199	4.45201271	1		4.45201271	0.11111111	0 1
3.16941	1.698234	1.69760816	3.16824199	2		3.16824199	0.22222222	3.16941 1
4.867644	2.230442	2.22962002	2.55008688	3		2.55008688	0.33333333	4.867644 1
7.098086	2.551027	2.55008688	2.32221489	4		2.32221489	0.44444444	7.098086 1
9.649113	4.453654	4.45201271	2.22962002	5		2.22962002	0.55555556	9.649113 1
14.102767	1.253118	1.25265619	2.2207313	6		2.2207313	0.66666667	14.102767 1
15.355885	1.05144	1.05105252	1.69760816	7		1.69760816	0.77777778	15.355885 1
16.407325	2.323071	2.32221489	1.25265619	8		1.25265619	0.88888889	16.407325 1
18.730396	2.22155	2.2207313	1.05105252	9		1.05105252	1	18.730396 1
20.951946								

BIBLIOGRAPHY

Abramoff, M.D., Magalhães, P.J., and Ram, S.J., 2004. Image processing with ImageJ. *Biophotonics International*, 11, pp.36–42.

Almanza, R.D., 2012. Joint control on the geomorphic evolution of the Groot and Bobbejaan River Canyons in the Western Province, South Africa. In Port Elizabeth: Unpublished dissertation. In *Honors dissertation*. Port Elizabeth: Unpublished, pp. 1–92.

Almeida, J., Valeriano, C.M., Heilbron, M.,and Geraldes, M., 2005. Triple junctions during break-up of Western Gondwana along south Atlantic Ocean. *3 International Gondwana Symposium*, p.39.

Anderson, H., and Nash, C., 1997. Intergratated Lithostructural Mapping of the Rossing Area, Namibia using high resolution Aeromagnetic, Radiometric, Landsat Data and Aerial Photographs. *Exploration Geophysics*, 28, pp.185–191.

Annen, C., Provost, A., and Lenat, J-F., 2001. The long-term growth of volcanic edifices : numerical modelling of the role of dyke intrusion and lava-flow emplacement. *Journal of Volcanology and Geothermal Research*, 105, pp.263–289.

Austin, J.A., and Uchupi, E., 1982. Continental-Oceanic crustal transition off Southwest of Africa. *American Association of Petroleum Geologist Bulletin*, 66, pp.1328–1347.

Babadagli, T., 2001. Fractal analysis of 2-D fracture networks of geothermal reservoirs in south-western Turkey. *Journal of Volcanology and Geothermal Research*, 112, pp.83–103.

Bachtadse, V., Van der Voo, R., and Balbich, W.I., 1987. Paleomagnetism of the Western Cape Fold Belt, South Africa, and its bearing on the Paleozoic apparent polar wander path for Gondwana. *Earth and Planetary Science Letters*, 84, pp.487–499.

Bahat, D., 1991. Tectonofractography. In Bahat, D, *Springer-Verlag*. Berlin, Heidelberg, p.354.

Bahat, D., and Engelder, T., 1984. Surface morphology on cross-fold joints of the Appalachian plateau, New York and Pennyslvania. *Tectonophysics*, 104, pp.299–313.

Bahat, D., Frid, V., and Avinoam, R., 2005. Tensile Fracturing in Rocks. In R. Bahat, D., Frid, V., and Avinoam, ed. *Tectonofractographic and Elecromagnetic Radiation Method*. Heidelberg, Germany: *Springer Berlin Heidelberg*, p. 81.

Bai, T., Maerten, L., Gross, M.R, and Aydin, A., 2002. Orthogonal cross joints: do they imply a regional stress rotation? *Journal of Structural Geology*, 24, pp.77–88.

Barnett, W., 2004. Subsidence breccias in kimberlite pipes—an application of fractal analysis. *Lithos*, 76, pp.299–316.

Barton, C.C., and La Ponte, P.R., 1995. Fractal Analysis of scaling and spatial clustering of fractures. In: Barton, C. C., and La Pointe, P.R (eds.), Fractal in the Earth Science. , pp.141–178.

Behn, M.D., Buck, R.W., and Selwyn, S.I., 2006. Topographic controls on dike injection in volcanic rift zones. *Earth and Planetary Science Letters*, 246, pp.188–196.

Behn, M.D., Conrad, C,P., and Silver, P.G., 2004. Detection of upper mantle flow associated with the African Superplume. *Earth and Planetary Science Letters*, 224, pp.259–274.

Bench, B.M., Diamond, W.P., and McCulloch, C.M., 1977. Methods of determining the orientations of bedrock fracture systems in Southwestern Pennsylvania and Northern West Virginia. , pp.27–30.

Bėrubė, D. and Jėbrak, M., 1999. High precision boundary fractal analysis for shape characterization. *Computers & Geosciences*, 25, pp.1059–1071.

Bird, P., Ben-Avraham, Z., Schubert, G., Andreoli, M., and Viola, G., 2006. Patterns of stress and strain rate in southern Africa. *Journal of Geophysical Research*, 111, pp.1–14.

Blenkinsop, T.G., 1999. Are gold deposits in the crust fractals? A study of gold mines in the Zimbabwe craton. In J. J. MCcaffrey, K.J.W., Lonergan, L., and Wilkingson, ed. *Geological Society Special Publications, 155*. Fractures, fluid flow and mineralization, pp. 141–151.

Blenkinsop, T.G., 1994. The fractals distribution of gold deposits. In J. H. Kruhl, ed. *Fractals and Dynamic systems in Geosciences*. *Springer, Berlin Heidelberg*, pp. 247–258.

Bonnet, E., Bour, O., Odling, N.E., Davy, P., Main, I., Cowie, P., and Berkowitz, B., 2001. Scaling of fracture systems in geological media. *Reviews of Geophysics*, 39, pp.347–383.

Bonnet, S., and Crave, A., 2003. Landscape response to climate change: Insights from experimental modeling and implications for tectonic versus climatic uplift of topography. *Geology*, 31, p.123.

Booth, P.W.K., 2009. A review of the structural geology of the Cape Fold Belt and challenges towards future research. *11th SAGA Biennial Technical Meeting and Exhibition Swaziland*, (September), pp.481–485.

Bordy, E.M., and Prevec, R., 2008. Sedimentology, palaeontology and palaeo-environments of the Middle (?) to Upper Permian Emakwezini Formation (Karoo Supergroup, South Africa). *South African Journal of Geology*, 111, pp.429–458.

Bordy, E.M., Hancox, P.J., and Rubidge, B.S., 2005. Turner, B.R and Thomson, K., Discussion on " Basin development during deposition of the Elliot Formation (Late Triassic – Early Jurassic), Karoo Supergroup , South Africa " (South African Journal of Geology, 107, 397-412) – A Reply. *Geological Society of South Africa*, 108, pp.454–461.

Botha, J.F., Verwey, J.P., Van Der Voort, Vivier, J.J.P., Buys, J., Colliston, W.P., and Loock, J.C., 1998. Karoo Aquifers. In Botha, J.F., Verwey, J.P., Van Der Voort, Vivier, J.J.P., Buys, J., Colliston, W.P., and Loock, J.C., 1998. *Their Geology, Geometry and Physical Properties*. Free State: *Water Research Commission*, pp. 13–35.

Bouldier, F., and Nicolas, A., 1985. Earth Planet. *Science Letters*, 76, pp.84–92.

Brandt, D., Andreoli M.A.G., and McCarthy, T.S., 2003. Mesozoic fluvial deposits on a rifted continental margin near Vaalputs, Namaqualand, South Africa. *South African Journal of Geology*, 106, pp.11–16.

Buck, R.W., 1986. Small-scale convection induced by passive rifting: the cause for uplift shoulders. *Earth and Planetary Science Letters*, 77, pp.362–372.

Burke, K., 1996. The African plate. *South African Journal of Geology*, 99, pp.341–409.

Burke, K., 1977. Aulacogens and Continental break-up. *Ann. Rev. Earth Planet. Sci.*, 5(c), pp.371–396.

Burov, E., and Guillou-Frottier, L., 2005. The plume head-continental lithosphere interaction using a tectonically realistic formulation for the lithosphere. *Geophysical Journal International*, 161(2), pp.469–490.

Catuneanu, O., Wopfner, H., Eriksson, P.G., Cairncross, B., Rubidge, B.S.. Smith, R.M.H., and Hancox, P.J., 2005. The Karoo basins of south-central Africa. *Journal of African Earth Sciences*, 43(1-3), pp.211–253.

Chapman, C.A., and Wingard, P.S., 1958. Physical control and age of dike formations in the Maine coastal region. *Bulletin of the Geological Society of America*, 69, pp.1193–1196.

Charkaluk, E., Bigerelle, M., and Iost, A., 1998. Fractals and fracture. *Engineering Fracture Mechanics*, 61(1), pp.119–139.

Clemente, C.S, Amorós, E. B., and Crespo, M.G., 2007. Dike intrusion under shear stress: Effects on magnetic and vesicle fabrics in dikes from rift zones of Tenerife (Canary Islands). *Journal of Structural Geology*, 29, pp.1931–1942.

Clemson, J., Cartwright, J., and Booth, J., 1997. Structural segmentation and the influence of basement structure on the Namibian passive margin. *Journal of the Geological Society of London*, 154(3), pp.477–482.

Clemson, J., Cartwright, J., and Swart, R., 1999. The Namib Rift: a rift system of possible Karoo age, offshore Namibia. *Geological society of london, special publications*, 153, pp.381–402.

Coffin, F.M., and Eldholm, O., 1994. Large Igneous Provinces: Crustal Structures, Dimensions, and External Consequences. *Reviews of Geophysics*, 32, pp.1–36.

Compton, J.S., 2004. The Rocks and Mountain of Cape Town. In H. Laurenson, ed. *Understanding the Landscape. Double Storey Books*. Cape Town, South Africa, pp. 16–23.

Condon, S.M., 2003. Fracture network of the Ferron Sandstone Member of the Mancos Shale, east-central Utah, USA. *International Journal of Coal Geology*, 56, pp.111–139.

Conrad, C.P., 2003. Seismic tomography, surface uplift, and the breakup of Gondwanaland: Integrating mantle convection backwards in time. *American Geophysical Union*, 4, pp.1–16.

Conrad, C.P., and Gurnis, M., 2003. Seismic tomography, surface uplift, and the breakup of Gondwanaland: Integrating mantle convection backwards in time. *Geochemistry Geophysics Geosystems*, 4, p.1031.

Cook, J., and Gordon, J.E., 1964. A Mechanism for the Control of Crack Propagation in All-Brittle Systems. *Proceedings of the Royal Society of London*, 282, pp.508–520.

Cooke, M., and Pollard, D., 1996. Fracture propagation paths under mixed mode loading within rectangular blocks of polymethyl methacrylate. *Journal of Geophysical Research*, 101, pp.3387–3400.

Corner, B., 2000. Crustal framework of Namibia derived from magnetic and gravity data. In Miller, R, McG, ed. *Communications of the Geological Survey of Namibia*. Windhoek, 12, pp.13–19.

Cox ,K.G., 1989. The role of mantle plumes in the development of continental drainage patterns. *Nature*, 342, pp.873–877.

Cox, K.G., 1992. Karoo igneous activity, and the early stages of the break-up of Gondwanaland. *Geological Society of London*, 68, pp.137–148.

Cox, K.G., 1988. The karoo Province. In J. D. MacDougall, ed. *Continental flood basalts*. Dordrecht: Kluwer Academic publishers, pp. 239–271.

Crider, J.G., and Peacock, D.C.P., 2004. Initiation of brittle faults in the upper crust: a review of field observations. *Journal of Structural Geology*, 26, pp.691–707.

Cruikshank, K.M., and Aydin, A., 1995. Unweaving the joints in Entrada sandstone, Arches National Park, Utah, USA. *Journal of Structural Geology*, 17, pp.409–421.

Currie, K.L., and Ferguson, J., 1970. The mechanism of intrusion of lamphrophyre dikes indicated by "offsetting" of dikes. *Tectonophysics*, 9, pp.525–535.

Dangermond, J., and Dangermond, L., 1969. *Environmental System Research Institute (Esri)-Geographical Information System*, New York, Redlands: Environmental System Research Institute (Esri).

Dathe, A., and Thullner, M., 2005. The relationship between fractal properties of solid matrix and pore space in porous media. *Geoderma*, 129, pp.279–290.

Decker, J.E., Niedermann, S., and de Wit, M.J., 2013. Climatically influenced denudation rates of the southern African plateau: Clues to solving a geomorphic paradox. *Geomorphology*, 190, pp.48–60.

Delaney, P.T, Pollard D.D., Ziony, J.I., and Mckee, E.H., 1986. Field relations between dikes and joints: Emplacement processes and paleostress Analysis. *Journal of Geophysical Research*, 91, pp.4920–4938.

Delaney, P.T., and Gartner, A.E., 1997. Physical processes of shallow mafic dike emplacement near the San Rafael Swell , Utah. *Geological Society of American Bulletin*, 109, pp.1177–1192.

Delaney, P.T., and McTigue, D.F., 1994. Volume of magma accumulation or withdrawal estimated from surface uplift or subsidence , with application to the 1960 collapse of Kilauea Volcano. *Bulletin of Volcanology*, 56, pp.417–424.

Delaney, P.T., and Pollard, D.D., 1981. Deformation of Host Rocks and flow of magma during growth of Minette Dikes and breccia-Bearing Intrusions near ship rock, New Mexico. *Geological Survey Professional Paper*, 1202, pp.59–61.

Dershowitz, W.S, LaPointe, P.R., Einstein, H.B., and Ivanova, V., 1997. Fracture Reservoir Discreet Feature Network Technologies. *Golder Associates report*.

Dershowitz, W.S., and Einstein, H.H., 1988. characterizing rock joint geometry with joint system models. *Rock Mechanics and Rock Engineering*, 21, pp.21–51.

Dewey, J.F., and Burke, K., 1974. Hot Spots and Continental Break-up : Implications for Collisional Orogeny. *Geology*, 2, pp.57–60.

de Wit, M.J., 2007. The Kalahari Epeirogeny and climate change : differentiating cause and effect from core to space. *South African Journal of Geology*, 110, pp.367–392.

de Wit, M.J., Stankiewicz, J., and Reeves, C., 2008. Restoring Pan-African-Brasiliano connections: more Gondwana control, less Trans-Atlantic corruption. *Geological Society, London, Special Publications*, 294, pp.399–412.

Dominique, C., Jean-Louis G., Anicet B., and Delphine, R., 2013. Cenozoic dynamics of the West African transform margin: Drainage evolution, denudation patterns, sediment budget and vertical mobility (TopoAFRICA abstract, Saasveld, South Africa, January 21-25.

Duncan, A.R., and Marsh, J.S., 2006. The Karoo Large Igneous Province. In R. J. Johnson, M R., Anhausser, C R., and Thomas, ed. *Geology of South Africa*. Pretoria: Geological Society of South Africa, pp. 501–510.

Dunlop, H., 2006. *Automatic rock detection and classification in natural scenes*. Pennsylvania: Msc thesis, Robotic Institute Carnegie Mellon University, Pittsburgh, Pennyslvania., pp.8-9.

Emerman, S.H., and Marrett, R., 1990. Why dikes ? *Geology*, 18, pp.231–233.

Encarnación, J., Fleming, T.H., Elliot, D.H., and Eales, H.V., 1996. Synchronous emplacement of Ferrar and Karoo dolerites and the early breakup of Gondwana. *The Geological Society of America*, 24, pp.535–538.

Engelder, T., 1987. Joints and shear fractures in rock. *Academic Press, London, UK*, 27, pp.27–69.

Engelder, T., and Geiser, P., 1980. On the use of regional joint sets as trajectories of paleostress fields during development of the Appalachian Plateau. *Journal of Geophysical Research*, 85, pp.6319–6340.

England, P., and Molnar, P., 1990. Surface uplift, uplift of rocks, and exhumation of rocks. *Geology*, 18, pp.1173–1177.

Ernst, R.E., and Buchan, K.L., 1997. Giant radiating dyke swarms: their use in identifying pre-Mesozoic large igneous provinces and mantle plumes. In: Mahoney J., Coffin M. (Eds.) Large Igneous Provinces: Continental, Oceanic, and Planetary Volcanism,. *AGU Geophys. Monogr. Ser.*, 100, pp.297–333.

Ernst, R.E., Grosfils, E.B., and Mege, D., 2001. Giant Dike Swarms: Earth, Venus and Mars. *Ann. Rev. Earth Planet. Sci.*,, 29, pp.489–534.

Esedo, R., van Wijk, J., Coblentz, D., and Meyer, R., 2012. Uplift prior to continental breakup: Indication for removal of mantle lithosphere? *Geosphere*, 8, pp.1078–1085.

Fairhead, J.D., and Wilson, M., 2002. Sea-floor spreading and deformation processes in the South Atlantic Ocean: Are hot spots needed? *www.MantlePlumes.org*, pp.1–12.

Falconer, K., 1997. Fractal Geometry. *Biometrics*, 53, p.1183.

Fender, M.L., Lechenault, F., and Daniels, K.E., 2010. Universal Shapes Formed by Two Interacting Cracks. *Physical Review Letters*, 105, pp.1–4.

Flament., N., Gurnis, M., and Muller, D.R., 2013. Evolution of the subduction-driven, long-wavelength topography of Africa ,TopoAfrica abstract, Saasveld, South Africa, January 21-25.

Flint, S.S., Hodgson, D.M., Sprague, A.R., Brunt, R.L., Van der Merwe, W.C., Figueiredo, J., Prélat, A., Box, D., Di Celma, C., and Kavanagh, J.P., 2011. Depositional architecture and sequence stratigraphy of the Karoo basin floor to shelf edge succession, Laingsburg depocentre, South Africa. *Marine and Petroleum Geology*, 28, pp.658–674.

Flowers, R.M., and Schoene, B., 2010. (U-Th)/He thermochronometry constraints on unroofing of the eastern Kaapvaal craton and significance for uplift of the southern African Plateau. *Geology*, 38, pp.827–830.

Flowers, R.M., and Stanley, J.R., 2013. Apatite (U-TH)/He thermocronology of the southern African plateau (TopoAfrica abstract, Saasveld, South Africa, Januray 21-25).

Fossen, H., 2010. Structural Geology R.C. McDowell, ed. *Geology*, 22, pp.119–126.

Fourie, P., Naidoo, T., and Zimmerman, U., 2008. Provenace of the Cape Supergroup in the Cape Fold Belt of South Africa-Preriliminary results. In *33rd, International Geological Congress*. Oslo.

Frindt, S., Trumbull, R.B., and Romer, R.L., 2004. Petrogenesis of the Gross Spitzkoppe topaz granite, central western Namibia: a geochemical and Nd–Sr–Pb isotope study. *Chemical Geology*, 206, pp.43–71.

Furnes, H., Rosing, M., Dilek, Y., and de Wit, M.J., 2009. Isua supracrustal belt (Greenland)—A vestige of a 3.8 Ga suprasubduction zone ophiolite, and the implications for Archean geology. *Lithos*, 113, pp.115–132.

Gates, A.E., 2003. A to Z of Earth Scientists. In Gates, A.E., ed. New York: Notable scientist, p. 55.

Gehle, C., and Kutter, H K., 2003. Breakage and shear behaviour of intermittent rock joints. *International Journal of Rock Mechanics and Mining Sciences*, 40, pp.687–700.

Gentle, R.I., Hooker, P.J., Fitch, F.J and Miller, J.A., 1978. Evidence for Cape Fold Belt overprinting of the Groot Haelkraal granite during the Upper Permian. *Transactions of the Geological Society of South Africa*, 81, pp.105–107.

Geological Survey of Namibia, 1997. Geological Survey of Namibia. In *sheet 2114-Omaruru, 1:250 000 Geological Series*. Windhoek Namibia.

Germs, G.J.B., 1995. The Neoproterozoic of southwestern Africa , with emphasis on platform stratigraphy and paleontology. *Precambrian Research*, 73, pp.137–151.

Germs, G.J.B., and Gresse, P.G., 1991. The foreland basin of the Damara and Gariep orogens in Namaqualand and southern Namibia : stratigraphic correlations and basin dynamics. *South African Journal of Geology*, 94(2-3), pp.159–169.

Gibson, S.A., Thompson, R.N. & and Day, J.A., 2006. Timescales and mechanisms of plume–lithosphere interactions: 40Ar/39Ar geochronology and geochemistry of alkaline igneous rocks from the Paraná–Etendeka large igneous province. *Earth and Planetary Science Letters*, 251, pp.1–17.

Girty, G.H., 2009. *Case study from Perilous Earth: Understanding processes behind natural disaster, Version 1.0*, United States of America: San Diego State University.

Gohl, K., Uenzelmann-Neben, G., and Grobys, N., 2012. Growth and Dispersal of a Southeast African Large Igneous Province. *South African Journal of Geology*, 114(3-4), pp.379–386.

Gray, D.R., Foster, D.A., Meert, J.D. & Goscombe, B.D., Armstrong, R., Trouw, R.A.J., and Passchier, C.W., 2008. A Damara orogen perspective on the assembly of southwestern Gondwana. *Geological Society, London, Special Publications*, 294, pp.257–278.

Griffith, A.A., 1924. The theory of rapture. In Burgers, C.B., and Biezeno, J.M., ed. *First International Congress on Applied Mechanics*. J. Waltman, pp. 55–63.

Gross, M.R., Fischer, M.P., Engelder, T., and Greenfield, Roy, J., 1995. Factors controlling joint spacing in interbedded sedimentary rocks: intergrating numerical models with field observation from the Monterey Formation, USA. *Fractography*, 92, pp.215–233.

Grout, M.A., and Verbeek, E.R., 1998. Relation Between Middle Tertiary dike Intrusion, Regional Joint Formation, and Crustal Extension in the Southeastern Paradox Basin, Colorado. *United State of America Geological Survey Bulletin*, pp.101–110.

Hahne, K., 2004. Detection of a Mesozoic response swarms in NW Namibia and reconstruction of regional voltage states during the opening of the South Atlantic. *Diagnostica*, 50(1), pp.18–110.

Hälbich, I.W., Fitch, F.J., and Miller, J.A., 1983. Dating the Cape orogeny, In Söhnge, A.P.G., and Hälbich, I.W., eds., Geodynamics of the Cape Fold Belt. *Geological Society of South Africa Special Publication*, 12, pp.149–164.

Hald, N., and Tegner, C., 2000. Composition and age of tertiary sills and dykes, Jameson Land Basin, East Greenland: relation to regional flood volcanism. *Lithos*, 54, pp.207–233.

Halls, H.C., and Fahrig, W.F., 1987. Mafic Dyke Swarms. *Geological Association of Canada Special Paper*, 34, pp.331–348.

Hancock, P.L., and Engelder, T., 1989. Neotectonic joints. *Geological Society of America, Bulletin*, 101, pp.1197–1208.

Hansen, J., and Bollian, A., 2008. BLOCKS programme. *Universität Karsuhe - Geologisches Institut*, (September).

Heine, C., Zoethout, J., and Muller, D.R., 2013. Kinematics of the South Atlantic rift. *Copernicus Publications*, 4, pp.215–253.

Helgeson, D.E., and Aydin, A., 1991. Characteristics of joint propagation across layer interfaces in sedimentary rocks. *Journal of Structural Geology*, 13, pp.897–911.

Hirata, T., 1989. Fractal Dimension of Fault systems in Japan: Fractal Structure in rock Fracture Geometry at Various Scales. *PAGEOPH*, 131, pp.157–169.

Hoek, J.D., 1991. A classification of dyke-fracture geometry with examples from PrecambHan dyke swarms in the Vestfold Hills , Antarctica. *Geologische Rundschau*, 80/2, pp.233–248.

Hou, G., 2012. Mechanism for three types of mafic dyke swarms. *Geoscience Frontiers*, 3, pp.217–223.

Hung, L.Q., Batelaan, O., and De Smedt, F., 2005. Lineament extraction and analysis, comparison of LANDSAT ETM and ASTER imagery. *Proceedings of SPIE*, 5983,59830.

Hutton, D.H.W., 2009. Insights into magmatism in volcanic margins: bridge structures and a new mechanism of basic sill emplacement - Theron Mountains, Antarctica. *Petroleum Geoscience*, 15, pp.269–278.

Isabelle, T., Pierre, F., and Badariotti, D, ., 2010. Comparing the fractality of European urban neighbourhoods: do national contexts matter? *Journal of Geographical Systems*, 14, pp.189–208.

James Madison University, 2000. The fractal nature of structural geology during the late Paleozoic Alleghanian Orogeny in the Mid-Atlantic region of the United States of America., Report. pp.1–6.

Johnson, M.R., Van Vuuren, C.J., and Hegenberger, W.F., Rey, R., and Shoko, U., 1996. Stratigraphy of the Karoo Supergroup in southern Africa: an overview. *Journal of Earth Sciences*, 23, pp.3–15.

Johnston, S.T., 2000. The Cape Fold Belt and Syntaxis and the rotated Falkland Islands: dextral transpressional tectonics along the southwest margin of Gondwana. *Journal of African Earth Sciences*, 31, pp.51–63.

Jolly, R.J.H., and Lonergan, L., 2002. Mechanisms and controls on the formation of sand intrusions. *Journal of the Geological Society of London*, 159, pp.605–617.

Jourdan, F., Féraud, G., Bertrand, H., Kampunzu, A B., Tshoso, G., Le Gall, B., Tiercelin, J J., and Capiez, P., 2004. The Karoo triple junction questioned: evidence from Jurassic and Proterozoic 40Ar/39Ar ages and geochemistry of the giant Okavango dyke swarm (Botswana). *Earth and Planetary Science Letters*, 222, pp.989–1006.

Jourdan, F., Féraud, G., Bertrand, H., Watkeys, M.K., Kampunzu, A.B., and Le Gall, B., 2006. Basement control on dyke distribution in Large Igneous Provinces: Case study of the Karoo triple junction. *Earth and Planetary Science Letters*, 241, pp.307–322.

Kiinkenberg, B., 1994. A review of Methods Used to Determine the Fractal Dimension of Linear Features. *Mathematical Geology*, 26, pp.23–46.

Kirstein, L.A., Kelley, S., Hawkesworth, C., Turner, S., Mantovani, M., and Wijbrans, J., 2001. Protracted felsic magmatic activity associated with the opening of the South Atlantic. *Journal of the Geological Society of London*, 158, pp.583–592.

Koppers, A.A.P., 2011. Mantle plumes persevere. *Nature Geoscience*, 4, pp.816–817.

Kröner, A., and Stern, R.J., 2005. Pan-African Orogeny. *Encyclopedia of Geology*, 1, pp.1–11.

Kruhl, J.H., 2013. Fractal-geometry techniques in the quantification of complex rock structures: A special view on scaling regimes, inhomogeneity and anisotropy. *Journal of Structural Geology*, 46, pp.2–21.

Lacazzete, A., and Engelder, T., 1992. Fluid-driven cyclic propagtion of a joint in the Ithasa siltstone, Appalachian Basin, New York. In Evans, B., and Wong, T.F., ed. *Faults mechanism and transport properties of rocks*. London: Academic press, pp. 297–323.

Ladeira, F.L., and Price, N.J., 1981. Relationship between fracture spacing and bed thickness. *Journal of Structural Geology*, 3, pp.179–183.

Lawver, L.A., Gahagan, L.M., and Dalziel, W.D., 1998. A tight fit-early Mesozoic Gondwana, A plate reconstruction perspective. *Memoirs of National Institute of Polar Research, Special*, 53, pp.214–229.

Leech, D.P., Treloar, P.J., Lucas, N.S., and Grocott, J., 2003. Landsat TM analysis of fracture patterns: a case study from the Coastal Cordillera of northern Chile. *International Journal of Remote Sensing*, 24, pp.3709–3726.

Le Gall, B., Tshoso, G., Jourdan, F., Feraud, G., Bertrand, H., Tiercelin, J J., Kampunzu, A. B., Modisi, M. P., Dyment, J and Maia, M., 2002. $^{40}Ar/^{39}Ar$ geochronology and structural data from the giant Okavango and related mafic dyke swarms, Karoo igneous province, northern Botswana. *Earth and Planetary Science Letters*, 202, pp.595–606.

Lithgow-Bertelloni, C., and Silver, P.G., 1998. Dynamic topography, plate driving forces and the African superswell. *Nature*, 395, pp.345–348.

Lord, J., Oliver, G. J., and Soulby, J. A., 1996. Landsat MSS imagery of a Lower Cretaceous regional dyke swarm, Damaraland, Namibia: a precursor to the splitting of Western Gondwana. *International Journal of Remote Sensing*, 17, pp.2945–2954.

Mahoney, J., and Coffin, M., 1997. Large igneous provinces: continental, oceanic, and planetary flood volcanism. In Coffin, M.F., and Mahoney, J.J., ed. *Large Igneous Provinces Continental Oceanic and Planetary Flood Volcanism*. American Geophysical Union, p. 280.

Mamtani, M.A., and Greiling, R.O., 2010. Serrated quartz grain boundaries , temperature and strain rate: testing fractal techniques in a syntectonic granite. *Geological Society of London*, 332, pp.35–48.

Mamtani, M.A., Ghosh, A., Chaudhuri, A.K., and Sengupta, D., 2004. Joint Pattern in Precambrian Rocks Around Galudih (India): Implications for Fold Mechanism. *Gondwana Research*, 7, pp.579–583.

Mandal, N., Mitra, A.K., Misra, S., and Chakraborty, C., 2006. Is the outcrop topology of dolerite dikes of the Precambrian Singhbhum Craton fractal? *Journal of Earth System Science*, 115(6), pp.643–660.

Mandelbrot, B.B., 1979. Fractals: Form, Chance and Dimension. *Journal of Statistical Physics*, 20, pp.725–729.

Mandelbrot, B.B., 1978. Getting snowflakes into shapes. *Fractals-Curbing unruly nature, New Science*, pp.808–810.

Mandelbrot, B.B., 1983. *The Fractal Geometry of Nature*. San Francisco: W.H. Freeman.

Mandelbrot, B.B., 1967. How Long is the Coast of Great Britain? Statistical Self-Similarity and Fractional Dimension. *Science*, 156, pp.636–638.

Mandl, G., 2005. Rock Joints. In G. Mandl, ed. *The Mechanical Genesis*. Springer Berlin Heidelberg, New York, p. 221.

Manninen, T., Eerola, T., Hannu, M., and Saku, V., 2008. The Karoo volcanic rocks and related intrusions in Southern and Central Mozambique. *Geological survey of Finland, Special Paper*, 48, pp.211–250.

Marinoni, L.B., 2001. Crustal extension from exposed sheet intrusions: review and method proposal. *Journal of Volcanology and Geothermal Research*, 107, pp.27–46.

Mason, T.R., and Christie, A.D.M., 1986. Palaeoevironmental significance of ichnogenus Diplocraterion torell from the Permian vryheid formation of the Karoo Supergroup, South Africa. *Palaeogeography, Palaeoclimatology and Palaeocology*, 52, pp.249–265.

Mcloughlin, S., 2001. The breakup history of Gondwana and its impact on pre-Cenozoic floristic provincialism. *Australian Journal of Botany*, 49, pp.271–300.

Melniciuc-Puica, N., Oancea, S., and Dorohoi, D., 2006. Fractal analysis as investigation method in old organic support. *Romanian Journal of Biophysics*, 16, pp.135–140.

Miller, R. McG, 2008. The Geology of Namibia. In Miller, R. McG., and Becker, T., ed. *Ministry of Mines and Energy, in three volumes, Namibia, Windhoek*. Windhoek, Namibia: Ministry of Mines and Energy, National Government publication, pp. 16–43/16–44.

Miller, R. McG., 2008. The geology of Namibia. Ministry of Mines and Energy of Namibia, Windhoek (Paleozoic to Cenozoic). In *Etendeka Group, Kalahari Group, Namib Group, Volume 3*. Windhoek Namibia: Ministry of Mines and Energy Geological Survey, pp. 17–1/24–1/25–1.

Milner, S.N., Le Roex, A.P., and O'Connor, J.M., 2004. Age of Mesozoic igneous rocks in northwesternNamibia, and their relationship to continental breakup. *Journal of Geological Society of London*, 152, pp.97–104.

Mogi, K., 1958. Relations between the eruption of various volcanoes and deformation of the ground surface around them. *Bulletin Earthquakes Research Institute*. University of Tokyo, pp. 99–134.

Moore, A., and Blenkinsop, T.B., 2002. The role of mantle plumes in the development of continental-scale drainage patterns: The southern African example revisited. *South African Journal of Geology*, 105, pp.353–360.

Morgan, J., 2004. Dike propagation to a surface load. *ERS 416 Structural Geology proceedings*. *United State of America Geological Surevy*, United States of America pp. 1–5.

Moulin, M., Aslanian, Da., and Unternehr, P., 2010. A new starting point for the South and Equatorial Atlantic Ocean. *Earth-Science Reviews*, 98, pp.1–37.

Mountain, E.D., 1968. Karoo. In *Geology of Southern Africa*. Cape Town, South Africa: Books of Africa, pp. 65–75.

Mubu, S.M., 1995. Aeromagnetic Mapping and Interpretation of Mafic dyke swarms in Southern Africa, Msc thesis., p.36.

National Aeronautics and Space Administration (NASA), 2005. Orthorectified Landsat Enhanced Thematic Mapper (ETM+) Compressed Mosaics for 2000.

Newton, A.R., Shone, W.R., and Booth, P.W.K., 2006. The Cape Fold Belt. In Johnson, M.R., Anhaeusser, C.R., And Thomas, R.J., ed. *Geology of South Africa*. Pretoria, South Africa.

Nicholson, R., and Ejiofor, I.B., 1987. The three-dimensional morphology of arrays of echelon and sigmoidal, mineral-filled fractures: data from north Cornwall. *Journal of the Geological Society*, 144, pp.79–83.

Nürnberg, D., and Müller, R.D., 1991. The tectonic evolution of the South Atlantic from Late Jurassic to present. *Tectonophysics*, 191(1-2), pp.27–53.

O'Connor, J.M., and Duncan, R.A., 1990. Evolution of the Walvis Ridge-Rio Grande Rise Hot Spot System: Implications for African and South American Plate Motions Over Plumes. *Journal of Geophysical Research*, 95, pp.17475–17502.

Odling, N.E., Gillespie, P., Bourgine, B., and Castaing, C., 1999. Variations in fracture system geometry and their implications for fluid flow in fractured hydrocarbon reservoirs. *Petroleum Geoscience*, 5, pp.373–384.

Olson, J.E., and Pollard, D.D., 1991. The initiation and growth of en enchelon veins. *Journal of Structural Geology*, 13, pp.595–608.

Palmström, A., 1995. *A rock mass characterization system for engineering purposes*. Norway: PhD thesis, Oslo University, Norway.

Palmström, A., 2001. In-Situ Characterization of rocks. In V.M, Sharma and Saxena, K.R., *Measurement and characterization of rock jointing*. Norway: A.A Balkema Publishers, pp. 1–40.

Parsiegla, N., Gohl, K., and Uenzelmann-Neben, G., 2007. Deep crustal structure of the sheared South African continental margin: first results of the Agulhas-Karoo Geoscience Transect. *South African Journal of Geology*, 110, pp.393–406.

Partiff, E.A., and Wilson, L., 2008. Fundamentals of physical volcanology. In L. Partiff, E.A., and Wilson, ed. *Magama migration*. United Kingdom: Blackwell Science Ltd, p. 36.

Partridge, T.C., and Maud, R.R., 1987. Geomorphic evolution of southern Africa since the Mesozoic. *South African Journal of Geology*, 90, pp.179– 208.

Passchier, C.W., 2002. Tectonic evolution of the southern Kaoko belt , Namibia. *Journal of African Earth Sciences*, 35, pp.61–75.

Peate, D.W., 1997. The Parana-Etendeka province, large igneous province: continental,oceanic and planetary flood Volcanism. *Geophysical Monograph, American Geological Union*, 100, pp.217–245.

Peternell, M., 2002. *Geology of syntectonic granite in the Itapama region (SE Brazil)-magmatic structures of Rio Pequeno granite (SE Brazil) and analysis with method of fractal geometry*. Msc thesis, Technique Universitat munchen, pp.98.

Petters, S.W., 1978. Stratigraphic Evolution of the Benue Trough and Its Implications for the Upper Cretaceous Paleogeography of West Africa. *Journal of Geology*, 86, pp.311–322.

Piccirillo, E.M., Bellieni, G., Cavazzini, G., Comin-Chiaramonti, P., Petrini, R., Melfi, A.J., Pinese, J.P.P., Zantadeschi, P., and De Min, A., 1990. Lower Cretaceous tholeiitic dyke

swarms from the Ponta Grossa Arch (southeast Brazil)" Petrology , Sr-Nd isotopes and genetic relationships with the Parana flood volcanics. *Chemical Geology*, 89, pp.19–48.

Pinkerton, H., Wilson, L., and Mcdonald, R., 2002. The transport and eruption of magma from volcanoes : a review. *Contemporary Physics*, 43, pp.197–210.

Poland, M. P., Moats, W.P., and Fink, J.H., 2007. A model for radial dike emplacement in composite cones based on observations from Summer Coon volcano, Colorado, USA. *Bulletin of Volcanology*, 70, pp.861–875.

Pollard, D.D., 1987. Elementary fracture mechanics applied to the structural interpretation of dykes. In W. F. Halls, H.C., and Fahrig, ed. *Mafic Dyke Swarms*. Canada: Geological Association of Canada Special Paper 34, pp. 5–24.

Pollard, D.D., and Aydin, A., 1988. Progress in understanding jointing over the past century. *Geological Society of America Bulletin*, 100, pp.1181–1204.

Pollard, D.D., and Nicholson, R., 1985. Dilation and linkage of echelon cracks. *Journal of Structural Geology*, 7, pp.583–590.

Pollard, D.D., and Raymond, C.F., 2005. Fundamental of structural geology. In *Brittle Behaviour*. United Kingdom: Cambridge University Press, pp. 333–383.

Polteau, S., Ferré, E.C., Planke, S., Neumann, E.-R., and Chevallier, L., 2008. How are saucer-shaped sills emplaced? Constraints from the Golden Valley Sill, South Africa. *Journal of Geophysical Research*, 113, pp.1–13.

Prave, A.R., 1996. Tale of three cratons : Tectonostratigraphic anatomy of the Damara orogen in northwestern Namibia and the assembly of Gondwana. *Geology*, 24, pp.1115–1118.

Price, N.J., and Cosgrove, J.W., 1990. Analysis of Geological Structures. In Price, N.J., and Cosgrove, J.W., ed. *Discordant and concordant intrusions*. United Kingdom: Cambridge University Press, pp. 60–76.

Qin, X., Cannon, J., Landgrebe, T. C. W., Heine, C., Watson, R.J., and Turner, M., 2012. The GPlates Geological Information Model and Markup Language. *European Geoscience Union*, 2, pp.365–428.

Raab, M.J., 2001. *The Geomorphic Response of the Passive Continental Margin of Northern Namibia to Gondwana Break-Up*. PhD thesis, Universitat zu Gottingen.

Ramsay, J.G., and Buber, M.I., 1983. The techniques of modern structutal geology. In Ramsay, J.G., and Buber, M.I., ed. *Measurement of progressive deformation*. London: Academic Press Limited, 1, pp. 235–237.

Ransome, I.G.D., 1992. *The geochemistry,kinematics and geodynamics of the Gannakouriep dyke swarm*. Msc thesis, University of Cape Town, South Africa.

Rao, J.M., Poornachandra, G.V.S., Widdowson, M., and Kelley, S.P., 2005. Evolution of Proterozoic mafic dyke swarms of the Bundelkhand Granite Massif, Central India. *Current Science*, 88, pp.502–506.

Raposo, M.I.B., and Ernesto, M., 1995. An Early Cretaceous paleomagnetic pole from Ponta Grossa dikes (Brazil): Implications for the South American Mesozoic apparent polar wander path. *Journal of Geophysical Research*, 100, pp.20095–20109.

Rasband, W., and Ferreira, T.A., 2010. The Image Analysis and measurements with ImageJ. , (March), pp.124–128.

Reeves, C. V., 1999. Aeromagnetic and gravity features of Gondwana and their relation to continental break-up " more pieces , less puzzle. *Journal of Earth Sciences*, 28, pp.263–277.

Reeves, C.V., 2000. The geophysical mapping of Mesozoic dyke swarms in southern Africa and their origin in the disruption of Gondwana. *Journal of African Earth Sciences*, 30, pp.499–513.

Reeves, C.V., 1978. A failed Gondwana spreading axis in southern Africa. *Nature 273*, pp.222 – 223.

Reeves, C.V., 2009. Re-examining the evidence from plate-tectonics for the initiation of Africa' s passive margins. *Geological Society of Houston/Petroleum Exploration Society of Great Britain, London*, pp.1–4.

Reid, D. L., Erlank, A. J., and Rex, D.C., 1991. Age and correlation of the False Bay dolerite dyke swarm, south-western Cape, Cape Province. *South African Journal of Geology*, 94, pp.155–158.

Renne, P.R., Deckart, K., Ernest, M., Fraud, G., and Piccirillo, E.M., 1996. Age of the Ponta Grossa dike swarm (Brazil), and implications to Parana flood volcanism. *Earth and Planetary Science Letters*, 144, pp.199–211.

Renne, P.R., Ernesto, M., Pacca, I.G., Coe, R.S., Glen J.M., Prévot, M., and Perrin, M., 1992. The age of Parana flood volcanism, rifting of Gondwanaland, and the Jurassic-Cretaceous boundary. *Science*, 258, pp.975–979.

Renne, P.R., Glen, J.M., Milner, S.C., and Duncan, A.R., 1996. Age of Etendeka flood volcanism and associated intrusions in southwestern Africa. *Geology*, 24, pp.659–662.

Republic of South Africa Geological Survey, 1982. Republic of South Africa Geological Survey, Department of Mineral and Energy Affairs (1:50 000 Map).

Richards, J.P., 2000. Lineament revisited. *SEG newsletter*, 42, pp.14–21.

Ritter, O., Weckmann, U., Vietor, T., and Haak, V., 2003. A magnetotelluric study of the Damara Belt in Namibia. *Physics of the Earth and Planetary Interiors*, 138, pp.71–90.

Rives, T., Rawnsley, K. D., and Petit, -P. J., 1994. Analogue simulation of natural orthogonal joint set formation in brittle varnish. *Journal of Structural Geology*, 16, pp.419–429.

Roberts, J.C., 1995. Fracture surface markings in Liassic limestone at Lavernock point. *Geological Society of London, Special Publications*, 92, pp.175–186.

Robinson, P. T., Malpas, J., Dilek, Y., and Zhou, M.F., 2008. The significance of sheeted dike complexes in ophiolites. *GSA Today*, 18, p.4.

Rowberry, M., McCarthy, T., and Tooth, S., 2010. The late Mesozoic and Cenozoic development of southern Africa : geological and geomorphological evidence for widespread denudation and epeirogenic uplift. *Geophysical Research Abstracts*, 12, p.9165.

Rubin, A.M., 1995. Propagation of Magma-Filled Cracks. *Earth Planet Science Letters*, 23, pp.287–336.

Rymer, H., and Williams-jones, G., 2000. Volcanic eruption prediction : Magma chamber physics from gravity and deformation measurements. *Geophysical Research Letters*, 27, pp.2389–2392.

Sahagian, D., 1988. Epeirogenic motions of Africa as inferred from Cretaceous shoreline deposits. *American Geophysical Union*, 7, pp.125–138.

Saunders, A.D., Jones, S.M., Morgan, L.A., Pierce, K.L., Widdowson, M., and Xu, Y.G., 2007. Regional uplift associated with continental large igneous provinces: The roles of mantle plumes and the lithosphere. *Chemical Geology*, 241, pp.282–318.

Scharf, T., 2012. *Denudation rates and geomorphic evolution of the Cape Mountain, determined by the analysis of in-situ produced cosmogenic ^{10}Be.* Msc thesis, University of Cape Town, South Africa.

Schofield, N., Stevenson, C., and Reston, T., 2010. Magma fingers and host rock fluidization in the emplacement of sills. *Geology*, 38, pp.63–66.

Scholz, C.H., 2002. The Mechanics of Earthquakes and Faulting. In Scholz, C.H., ed. *Brittle fracture of rock*. Cambridge University Press, pp. 1–52.

Secor, D.T., 1965. Role of fluids pressure in jointing. *American Journal of Science*, 263, pp.633–646.

Segwade, T., 2008. *The Geological Framework and Depositional Environments of the Coal-Bearing Karoo Strata in the Central Kalahari Karoo Basin , Botswana*. Msc thesis, Rhodes University, South Africa, pp.28-30.

Séranne, M., and Zahie, A., 2005. South Atlantic continental margins of Africa: a comparison of the tectonic vs climate interplay on the evolution of equatorial west Africa and SW Africa margins. *Journal of African Earth Sciences*, 43, pp.283–300.

Shake, S.N., and McHone, J.G., 1987. Topographic lineaments and their Geologic significance in central new England and adjacent New York. *Northeastern Geology*, 9, pp.120–128.

Skameta, J., 1983. *The structural geology of Sierra Moreno, Northern Chile*. Chile: PhD thesis, University of London, pp.299.

Srivastava, R.K., and Oliveira, E.P., 2011. Dyke Swarms: Keys for Geodynamic Interpretation. In Oliveira, E.P., ed. *The Late Archaean Uaua mafic dyke swarms. Sao*

Franscisco Craton, Brazil, and Implications for Paleoproteozoic Extrusion Tectonics and Orogen Recontruction. Springer, Berlin Heidelberg, pp. 19–32.

Stankiewicz, J., 2004. *African River Basins: Their Present Geometry and recent past as a framework for their evolution*. PhD thesis, University of Cape Town, South Africa, pp.9-13.

Stanley, J.R., and Flowers, R.M., 2011. Using apatite (U-Th)/He thermochronometry to resolve regional unroofing patterns across the interior of the southern African Plateau and implications for mantle dynamics. *American Geophysical Union, Fall meeting, Abstract (T33D-2439)*.

Stecker, M.R., George, H.E., Blisniuk, P.M., and Reuther, C.D., 2005. Neotectonics. *Geology*, 1, pp.425–428.

Storey, C.B., 1995. The role of mantle plumes in continental breakup: case histories from Gondwanaland. *Nature*, 377, pp.301–308.

Suryanarayana, K.V., and Anjanappa, K., 1975. Joint pattern and dyke trends in the Tirupati area, Andhra Pradesh, India. *Proceedings of Indian National Science Academy*, 41, pp.386–402.

Taisne, B., and Tait, S., 2011. Effect of solidification on a propagating dike. *Journal of Geophysical Research*, 116, p.14.

Thamm, A.G, and Johnson, M.R., 2006. The Cape Supergroup. In R. J. Johnson, M.R.Anhaeusser, C.R., and Thomas, ed. *Geology of South Africa*. Pretoria, South Africa, pp. 443–460.

Thompson, R.N., Riches, A.J.V., Antoshechkina, P.M., Pearson, D.G., Nowell, G.M., Ottley, C.J., Dickin, A.P., Hards, V.L., Nguno, A.-K., and N.-P. V., 2007. Origin of CFB Magmatism: Multi-tiered Intracrustal Picrite-Rhyolite Magmatic Plumbing at Spitzkoppe, Western Namibia, during Early Cretaceous Etendeka Magmatism. *Journal of Petrology*, 48, pp.1119–1154.

Tinker, J., de Wit, M.J., and Brown, R., 2008. Mesozoic exhumation of the southern Cape , South Africa , quantified using apatite fission track thermochronology. *Tectonophysics*, 455, pp.77–93.

Toramaru, A., and Matsumoto, M., 2004. Columnar joint morphology and cooling rate: A starch-water mixture experiment. *Journal of Geophysical Research*, 109, p.B02205.

Torsvik, T.H., and Cocks, L.R.M., 2011. The Palaeozoic palaeogeography of central Gondwana. *Geological Society, London, Special Publications*, 357, pp.137–166.

Torsvik, T.H., Burke, K., Steinberger, B., Webb, S.J., and Ashwal, L.D., 2010. Diamonds sampled by plumes from the core-mantle boundary. *Nature*, 466, pp.352–355.

Torsvik, T.H., Redfield, T.F., Lundin, E., Smethurst, M.A., Ebbing, J., and Eide, E.A., 2004. *South Atlantic plate reconstructions: A self-consistent model*, NGU Report No: 2004.024., pp.1-90, Norway.

Torsvik, T.H., Rousse, S., Labails, C., and Smethurst, M.A., 2009. A new scheme for the opening of the South Atlantic Ocean and the dissection of an Aptian salt basin. *Geophysical Journal International*, 177, pp.1315–1333.

Traversa, P., and Grasso, J.-R., 2009. Brittle Creep Damage as the Seismic Signature of Dyke Propagations within Basaltic Volcanoes. *Bulletin of the Seismological Society of America*, 99, pp.2035–2043.

Trumbull, R.B., Reid, D.L., de Beer, C.H., and Romer, R.L., 2007. Magmatism and continental breakup at the west margin of southern Africa: A geochemical comparison of dolerite dikes from northwestern Namibia and the Western Cape. *South African Journal of Geology*, 110, pp.477–502.

Trumbull, R.B., Vietor, T., Hahne, K., Wackerle, R., and Ledru, P., 2004a. Aeromagnetic mapping and reconnaissance geochemistry of the Early Cretaceous Henties Bay-Outjo dike swarm, Etendeka Igneous Province, Namibia. *Journal of African Earth Sciences*, 40, pp.17–29.

Turcotte, L., 1989. Fractals in Geology and Geophysics. *Pure and Applied Geophysics*, 131, pp.171–194.

Twiss, R.J., and Moore, E.M., 1992. Structural geology. In Twiss, R.J., and Moore, E.M., ed. *Brittle deformation*. New York: W.H. Freeman and company, pp. 35–50.

University of Cape Town, 2012. Geology of the Peninsula. In *Department of Geoscienes, University of Cape Town*. Cape Town, Western Cape. Available at: http://web.uct.ac.za/depts/geolsci/cape.htm.

Valente, S.C., Corval, A., Duarte, B.P., Ellam, R.L., Fallick, Anthony, A.E., Meighan, I.G., and D.T., 2007. Tectonic boundaries, crustal weakness zones and plume-subcontinental lithospheric mantle interactions in the Serra do Mar dyke swarm, SE Brazil. *Revista Brasileira Geociencias*, 37, pp.194–201.

Van Balen, R. T., Van Beek, P.A ., and Cloetingh, S.A.P.L., 1995. The effect of rift shoulder erosion on strata1 patterns at passive margins: Implications for sequence stratigraphy. *Earth and Planetary Science Letters*, 134, pp.527–544.

Van der Pluijm, B., and Marshak, S., 2004. Brittle Deformation. In Van der Pluijm, B., and Marshak, S., ed. *Earth Structures: An Introduction to Structural Geology and Tectonics*. New York: WW. Norton, pp. 1–27.

Van Zyl, J.A., 1982. The Age and origin of the Prinspoort in the Little Karoo. *The South African Geographers*, 10, pp.135–143.

Viola, G., Andreoli, M., Ben-Abraham, Z., Stengel, I., and Moshe, R., 2005. Offshore mud volcanoes and onland faulting in southwestern Africa: neotectonic implications and constraints on the regional stress field. *Earth and Planetary Science Letters*, 231, pp.147–160.

Viola, G., Kounov, A., Andreoli, M.A.G., and Mattila, J., 2012. Brittle tectonic evolution along the western margin of South Africa: More than 500Myr of continued reactivation. *Tectonophysics*, 514-517, pp.93–114.

Viola, G., Kounov, A., Andreoli, M.a.G., and Mattila, J., 2012. Brittle tectonic evolution along the western margin of South Africa: More than 500Myr of continued reactivation. *Tectonophysics*, 514-517, pp.93–114.

Viola, G., Mancktelow, N.S., and Miller, J.A., 2006. Cyclic frictional-viscous slip oscillations along the base of an advancing nappe complex , Naukluft Nappe Complex, Central Namibia. *Geophysical Research Abstracts*, 8.

Volland, S., and Kruhl, J.H., 2004. Anisotropy quantification: the application of fractal geometry methods on tectonic fracture patterns of a Hercynian fault zone in NW Sardinia. *Journal of Structural Geology*, 26, pp.1499–1510.

Walker, F., and Poldervaart, A., 1949. Karoo dolerite of the union of South Africa. *Geological Society of America Bulletin*, 60, pp.591–706.

Wanke, A., 2000. *Karoo-Etendeka Unconformities in NW Namibia and their Tectonic Implications*. Dissertation zur Erlangung des naturwissenschaftlichen Doktorgrades der Bayerischen Julius-Maximilians-Universität Würzburg, pp.3-58.

Watkeys, M.K., 2006. The Geological Society of South Africa. In R. J. Johnson, M.R., Anhaeusser, C.R., and Thomas, ed. Johannesburg/Council for Geosciences: Council for Geoscience.

Watkeys, M.K., and Kattenhorn, S.A., 1995. Blunt-ended dyke segments. *Journal of Structural Geology*, 17, pp.1535–1542.

Weinberger, R., 2001. Joint nucleation in layered rocks with non-uniform distribution of cavities. *Journal of Structural Geology*, 23(8), pp.1241–1254.

Weinberger, R., Vladimir, L., Baer, G., and Agnon, A., 2000. Damage zones around en echelon dike segments in porous sandstone. *Journal of Geophysical Research*, 105, pp.3115–3133.

White, R., and Mckenzie, D., 2000. Magmatism at Rift Zones : The Generation of Volcanic Continental Margins. *Journal of Geophysical Research*, 94, pp.7685–7729.

White, R.S., Drew, J., Martens, H.R., Key, J., Soosalu, H., and Jakobsdóttir, S.S., 2011. Dynamics of dyke intrusion in the mid-crust of Iceland. *Earth and Planetary Science Letters*, 304, pp.300–312.

Wilson, J.T, 1965. A new class of faults and their bearing on continental drift. *Nature 207*, p.PP. 343–347.

Yoneyama, S., Sakaue, K., Kikuta, H., and Takashi, M., 2007. Observation of Stress Field Around an Oscillating Crack Tip in a Quenched Thin Glass Plate. *Experimental Mechanics*, 48, pp.367–374.

Zerfassl, H., Farid, C. Jr., and Ernesto, L., 2005. Tectonic Control of the Triassic Santa Maria Supersequence of the Paranii Basin, Southernmost Brazil, and its Correlation to the Waterberg Basin, Namibia. *Gondwana Research*, 8, pp.163–176.

Zhou, H.W., Yue, Z.Q., Tham, L.G., and Xie, H., 2003. The Shape of Moving Boundary of Fluid Flow in Sandstone : Video Microscopic Investigation and Stochastic Modeling Approach. *Transport in Porous Media*, 50, pp.343–370.

Websites

http://aeon.org.za/activities/kalahari_drilling_project

www.gplates.org.

www.python.org.

www.reeves.nl/gondwana